Contents

Reacting rocks deform - deforming rocks react: examples from experiment and nature

Rainer Abart

Department of Lithospheric Research, University of Vienna

It has long been recognized that mineral reactions and non-isostatic stress may interfere. On the one hand, deformation driven by a far field stress may trigger mineral reactions. On the other hand, stress heterogeneity and local deformation may be internally produced through volume changes associated with phase transformation and mineral reactions.

An example for deformation induced mineral reactions will be shown from the Glarus thrust. There the Permian Verruccano in the hangingwall and the Cretaceous limestone in the footwall of the thrust receive a marked geochemical imprint through deformation induced or deformation mediated mineral reactions (Hürzeler and Abart 2008). Another example is taken from an eclogite facies overprint on metapelites from a shear zone in the Monte Rosa area (Keller et al. 2004). There the change in reaction microstructure, texture and mineral modes across a shear zone testifies to the effect that reaction progress may largely be enhanced by deformation. In low strain rocks outside the shear zone garnet forms delicate reaction rims along plagioclase – biotite contacts, and garnet growth is stranded at very low reaction progress. In contrast the extent of reaction progress is substantially larger within then shear zone, and garnet forms idiomorphic porphyroblasts.

With respect to reaction induced deformation an example of K/Na exchange between alkali feldspar and an NaCl-KCl melt at ambient pressure is used to illustrate the effect of coherency stress induced by composition gradients that are generated during cation exchange. When the composition of an intermediate alkali feldspar is shifted towards the Na-rich side, a fracture pattern is generated with fractures opening perpendicular to the direction of largest contraction of the lattice. If an intermediate alkali feldspar is shifted towards more potassian compositions this implies a dilation of the lattice, This may lead to spallation of potassium-rich rinds due to lattice misfit between the original feldspar and the potassium rich rind.

Finally an example of orthopyroxene reaction rim formation at olivine-quartz contacts is discussed. In experiments done at 1 GPa and 900°C the reaction ol+qtz=opx has a negative volume change of about 6%. If orthopyroxene forms around olivine grains embedded in a quartz matrix or around quartz grains embedded in an olivine matrix, the volume change must be accommodated by compaction of the entire assembly. Based on a thermodynamic analyses it is shown that either diffusion of MgO/SiO2 components across the growing orthopyroxene rim, or, alternatively, creep of the matrix may be rate limiting. If the rack matrix is stiff, this may eventually quench the reaction – a phenomenon that could be referred to as mechanical-closure (Schmid et al. 2009)

Hürzeler J-P, Abart R (2008) Fluid flow and rock alteration along the Glarus thrust. Swiss Journ. Geosc. 101, 251-268.

Keller L, Abart R, Stünitz H, De Capitani C (2004) Deformation, reaction progress and mass transfer in an eclogitE FACIES shear zone in a polymetamorphic metapelite (Monte Rosa nappe, western Alps). J. Met. Geol. 22, Journ. Metam. Geol. 22 (2): 97-118.

Schmid DW, Abart R, Podladchikov YY, Milke R (2009) Matrix rheology effects on reaction rim growth II: coupled diffusion and creep model, J. Met. Geol., 27, 83-91.

Petrology of Tinguaites from the Ditrău Alkaline Massif, Romania

Anikó Batki, Elemér Pál-Molnár

Department of Mineralogy, Geochemistry and Petrology, University of Szeged, Hungary, PO Box 651, 6701 Szeged, Hungary (batki@geo.u-szeged.hu; palm@geo.u-szeged.hu)

The Ditrău Alkaline Massif [DAM] is a Mesozoic alkaline igneous complex and situated in the S-SW part of the Giurgeu Alps belonging to the Eastern Carpathians (Romania). The DAM outcrops right east of the Neogene-Quaternary Călimani-Gurghiu-Harghita calc-alkali volcanic belt by breaking through the pre-Alpine metamorphic rocks of the Alpine Bukovina Nappe (Pál-Molnár, 2000). Tinguaites are very rare in the DAM, form thin dykes and are in connection with white nepheline syenites which they are also chemically related to (Streckeisen, 1954). This paper discusses new results on petrology of tinguaites occurring at the northern part of the DAM.

Tinguaite is a pale- to dark-green, very fine-grained undersaturated igneous rock consisting of essential alkali feldspar, nepheline, and aegirine (with or without sodic amphibole or biotite) that may be considered the dike equivalent of phonolite. Tinguaite in which the amount of nepheline equals or is greater than that of feldspar has a characteristic texture: the light-coloured groundmass is equigranular and sugary, with needles of aegirine between and randomly crossing the other constituents to give a feltlike appearance (Allaby and Allaby, 1999).

Whole-rock major oxide compositions for representative samples were analysed on a Finnigan MAT Element spectrometer by HR-ICP-MS, trace and rare-earth elements were determined by ICP-AES using a Varian Vista AX spectrometer.

Tinguaite dykes occurring at the northern part of the DAM are light grey to greenish grey in colour. Their texture is fine-grained, porphyritic and hipidiomorphic to xenomorphic. The main rock-forming minerals are andradite-grossular or aluminian sodian ferroan diopside and aegirine-augite phenocrysts, groundmass eckermannite, albite (Ab_{98-99}), orthoclase and nepheline. Accessories are titanite, zircon and magnetite. Secondary minerals are phlogopite (mg#=0.57–0.76), chlorite, epidote, calcite and sericite. The Ti vs Al ratio of diopsides indicates their formation under high pressure, while aegirin-augites formed under low pressure (Pál-Molnár et al., 2010). The diopsides are anorogenic and derive from an alkaline magma based on their Ti+Cr vs Ca and Ti vs Ca+Na ratios respectively.

The DAM tinguaites are characterized by moderate SiO_2 contents (54–58 wt.%) and high concentrations of alkalies, LREE and other incompatible trace elements such as Zr, Nb, Ba, Rb, Sr up to 1301 ppm, 224 ppm, 550 ppm, 631 ppm, and 743 ppm, respectively. They are silica-undersaturated (ne = 7.1–24.8) alkaline, intermediate rocks and phonolitic in composition. Their alkaline affinity is confirmed by high Ti/V (99–108), $(La/Yb)_N$ (17–29) and low Y/Nb (0.11–0.15) ratios. Tinguaites with diopside phenocrysts have peralkaline to peraluminous character while tinguaites with garnets are metaluminous. The chondrite-normalised REE patterns of tinguaites show a strong decrease from La to Yb [$(La)_N$ = 260–400; $(Yb)_N$ = 10–19]. Such fractionation of the LREE and HREE (La/Yb = 24-40) shows that during partial melting the tinguaite magma is enriched in LREE much more than in HREE. The OIB-normalised REE patterns, the Y+Nb vs Rb and Y vs Nb distribution of the tinguaites indicate, that they are related to an intraplate magmatic activity.

Allaby A. and Allaby M., 1999. A Dictionary of Earth Sciences. Encyclopedia.com.

Pál-Molnár E., 2000. Hornblendites and diorites of the Ditrău Syenite Massif. Ed. Department of Mineralogy, Geochemistry and Petrology. University of Szeged, Szeged, 172 p.

Pál-Molnár E., Batki A. and Ódri Á., 2010. Mineralogy of nepheline syenite dykes from the Ditrău Alkaline Massif, Romania. In: Zaharia L, Kis A, Topa B, Papp G, Weiszburg TG (ed.) IMA2010 20th General Meeting of the International Mineralogical Association 21–27 August, 2010 Budapest, Hungary. (Acta Min. Petr. Abstr. Ser.; 6.) p. 529.

Streckeisen A., 1954. Das Nephelinsyenit-Massiv von Ditro (Siebenbürgen), II. Teil. Schweiz. Min. Petr. Mitt., 34, 336-409.

Paleogene to Neogene kinematics of the Outer West Carpathian fold-and-thrust belt and Miocene strike-slip faulting at the front of the Magura Superunit (Slovakia and Czech Republic)

Andreas Beidinger[1], Kurt Decker[1], Andras Zamolyi[1,2], Eun Young Lee[1]

[1]*Department of Geodynamics and Sedimentology, University of Vienna, Austria, andreas.beidinger@univie.ac.at*
[2]*Department of Geophysics and Space Sciences, Eötvös University, Budapest, Hungary*

The area of investigations covers the Outer West Carpathian (OWC) flysch units, which are referred to as the external fold and thrust belt of the West Carpathian orogen. The OWC is separated from the Central and Inner West Carpathians by the Pieniny Klippen Belt (PKB). Kinematic data obtained from brittle structural analyses of outcrops within the OWC flysch units (Silesian-, Foremagura-, Magura- and Biele Karpaty unit; see Fig. 1 for location of study area) depict a polyphase deformation history including several deformations, which could be correlated into the adjacent PKB to the South (see Beidinger et al., this volume). Four different deformations (D_{F1}, D_{F2}, D_{F3}, D_{F4}) are distinguished in the OWC- flysch units.

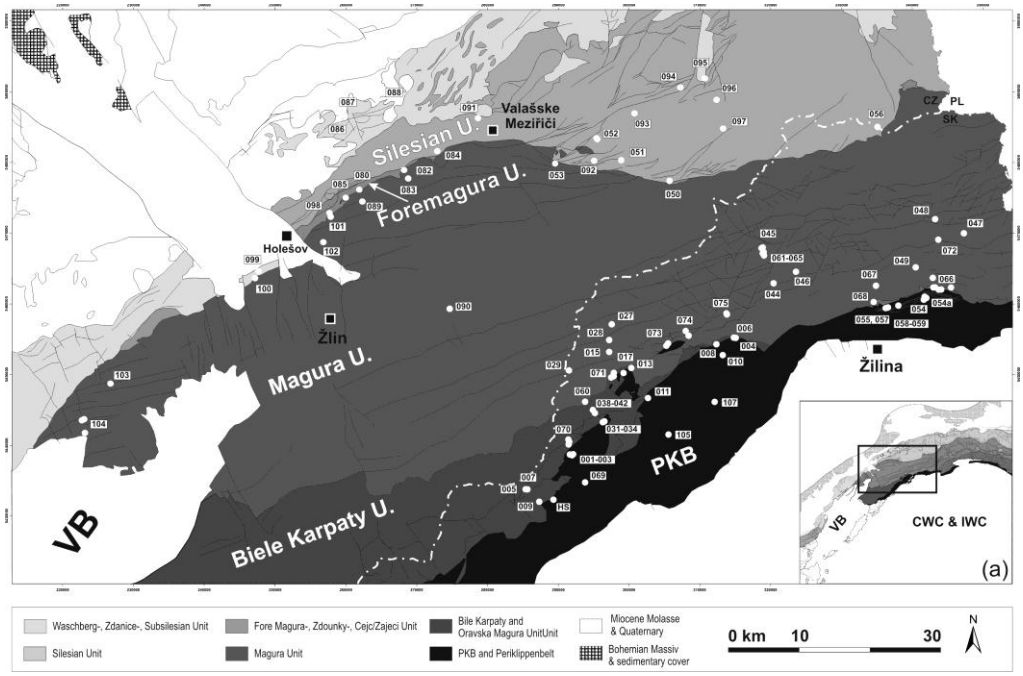

Fig.1 Geological map (redrawn after ÚÚG (1963) and ŠGUDŠ (2008)) with location of outcrops, studied for kinematic interpretation. Insert (a): Geological map with location of field study area in the Outer West Carpathians (redrawn after ŠGUDŠ 2000).

The most prominent deformation D_{F1} is characterized by NNW-directed shortening, which formed the large-scale architecture of the roughly ENE-trending fold and thrust belt. The stratigraphic record found in the different OWC flysch units indicates an in-sequence foreland-propagating thrust sequence. According to the ages of the youngest overthrust sediments (Zytko et, al., 1989; Nemcok et al., 1998), thrusting progresses from the PKB into the OWC flysch during Paleocene/Eocene times and terminates in the most external flysch units close to the Karpatian/Badenian stage boundary. We interpret foreland propagating, NNW-directed folding and thrusting to be responsible for the progressive steepening of units towards the internal parts of the orogen leading to subvertical to overturned positions in the innermost part of the fold and thrust belt. Crosscutting relationships in outcrops give evidence that NNW-directed shortening (D_{F1}) is followed by ENE-striking sinistral strike-slip faulting of D_{F2}. This deformation is concentrated within the flysch units close to the boundary with the adjacent PKB. Structures there indicate sinistral strike-slip reactivation of the floor thrusts of the Bystrica and Biele Karpaty unit. Additional ENE-striking strike-slip faults occur within the Biele Karpaty unit and in the PKB. Structures of D_{F1} and D_{F2} are further overprinted or cut by by map-scale (N)NE-striking sinistral strike-slip faults attributed to NNE-directed shortening (D_{F3}). D_{F3} strike-slip faults are linked with NNE-directed out-of-sequence thrusts. Structural data and geological maps show that NNE-directed out-of-sequence thrusts and kinematically linked strike-slip faults coincide with major bends at the fronts of the Magura and Bystrica units NNE of Žilina (SK; Fig. 1). The timing of D_{F3} is constrained by Egerian sediments, which are affected by NNE-directed shortening at the southern margin of the Silesian unit near Rožnov pod Radhoštěm (CZ). Further recordings of NNE-directed shortening around the front of the Magura unit coincide

with the bend of the Magura front from ENE-directed strike to ESE-directed strike near Valašske Meziříči (Fig. 1). Structural data from outcrops in the Magura and Foremagura unit west of the bend depict sinistral strike-slip faulting sub-parallel to the ENE-striking Magura front Structures are interpreted as due to sinistral reactivation of the front of the Magura unit. At the ESE-striking section of the Magura front, NNE-directed shortening is accomodated by NNE-directed out-of-sequence thrusting. The situation is interpreted as a restraining bend formed by the bending of the front of the Magura unit. The interpretation is corroborated by map-scale ENE-striking faults, which splay off from the ESE-striking floor thrust of the Magura unit. The strike of these faults fits the expected strike of Riedel-faults at a restraining bend of a sinistral strike-slip fault. Deformation D_{F4} within the flysch units is characterized by WNW-directed shortening and is restricted to the area around the Magura front. This deformation is related to minor strain and appears as the youngest deformation although no high-quality cross-cutting relationships could be identified in outcrops.

The outcrop-derived deformation history is compared with the tectonic evolution in the Vienna Basin area, where seismic data provide excellent constraints for deformation ages (Hölzel et al., 2010). There, studies show that Early Miocene NE-striking sinistral strike-slip faults are cut by NNE-striking Middle to Late Miocene sinistral strike-slip faults. Both types of strike-slip faults are related to distinct stages of the eastward lateral extrusion of the Eastern Alps towards the Pannonian region. The older NE-striking faults pre-date the formation of the pull-apart basin, whereas NNE-striking faults are linked to the pull-apart stage of the basin during Middle to Late Miocene times. D_{F2} and D_{F3} identified in the Outer West Carpathians are therefore correlated to Miocene extrusion kinematics. We correlate the ENE-striking strike-slip faults recorded in the OWC (D_{F2}) with the Early Miocene strike-slip faults found in the Vienna Basin. NNE-directed out-of-sequence thrusting and (N)NE striking strike-slip faults (D_{F3}) are linked to the pull-apart stage of the Vienna Basin. The sinistral strike-slip faults of D_{F3} at the Magura front are regarded as continuations of the of Middle to Upper Miocene strike-slip faults delimiting the Middle to Upper Miocene Vienna pull-apart basin towards the Northwest.

The proposed structural model suggests that structures of D_{F3} serve to accommodate the displacement of NNE-striking sinistral strike-slip faults delimiting extruding blocks to the Northwest. NNE-directed block-movement during Middle to Late Miocene lateral extrusion is compensated by NNE-directed shortening and out-of-sequence thrusting at the leading edge of the fault blocks.

Decker, K., Nescieruk, P., Reiter, F., Rubinkiewicz, J., Rylko, W. & Tokarski, A.K., 1997. Heteroaxial shortening, strike-slip faulting and displacement transfer in the Polish Carpathians, Przeglad Geologiczny, 45 (10): 1070-1071.

Decker, K., Rauch, M., Jankowski, l., Nescieruk, P., Reiter, F., Tokarski, A.K. & GALICIA T. GROUP, 1999. Kinematics and timing of thrust shortening in the Polish segment of the Western Outer Carpathians, Rom. J. Tect. Reg. Gol., 77 (1): 24.

Hölzel, M., Decker, K., Zámolyi, A., Strauss, P. & Wagreich, M., 2010. Lower Miocene structural evolution of the central Vienna Basin (Austrai). Marine and Petroleum Geology, 27: 666-681.

ŠGÚDŠ, 2000. Geological map of Western Carpathians and adjacent areas, 1:500000. Ministry of Environment of Slovak Republic (ŠGÚDŠ), Bratislava.

ŠGÚDŠ, 2008. General Geological map of the Slovak Republic, 1:200000. Ministry of Environment of Slovak Republic (ŠGÚDŠ), Bratislava.

Nemcok, M., Houghton, J. & Coward, M.P., 1998. Strain partitioning along the western margin of the Carpathians. Tectonophysics 292: 119–143.

ÚÚG (1963). Geological map of Czechoslovakia, 1:200000. Ústredny ústav geologický. Praha.

Zytko, K., Garlicka, I., Gucik, S., Oszczypko, N., Rylko, W., Zajac, R., Elias, M., Mencik, E., Nemcok, J., Stranik, Z., 1989. Columnar cross sections of the Western Outer Carpathians and their Foreland. In: Poprawa, D. & Nemcok, J. (Eds.): Geological Atlas of the Western Outer Carpathians and their Foreland. PIG Warszawa/GUDS Bratislava/UUG Praha.

Deciphering polyphase deformation in the Žilina segment of the Pieniny Klippen Belt (Steny ridge, NW Slovakia)

Andreas Beidinger[1], Kurt Decker[1], Andras Zamolyi[1,2], Eun Young Lee[1]

[1]*Department of Geodynamics and Sedimentology, University of Vienna, Austria, andreas.beidinger@univie.ac.at*
[2]*Department of Geophysics and Space Sciences, Eötvös University, Budapest, Hungary*

Brittle structural analyses of outcrops in the Outer West Carpathian (OWC) flysch units of Southern Moravia and Northwest Slovakia distinguished four different deformations (D_{F1}, D_{F2}, D_{F3}, D_{F4}; see Beidinger et al., this volume) from Paleocene to Upper Miocene times. The most prominent and oldest deformation identified there (D_{F1}) is NNW-directed shortening. This deformation lasted from Paleocene to late Early Miocene times and is interpreted as to be responsible for the large-scale architecture of the ENE-striking fold and thrust belt. Cross-cutting relationships identified in the flysch units show that structures of D_{F1} are overprinted by ENE- striking sinistral strike-slip faults (D_{F2}) with abundant faults occurring in the innermost units of the flysch belt close to the PKB. Structures of D_{F1} and D_{F2} are further overprinted by NNE-directed shortening (D_{F3}). Structures of D_{F3} are out-of-sequence thrusts and sinistral strike-slip faults striking parallel to the thrust direction.

Structures from the NW-margin of the PKB south of the flysch units prove a polyphase deformation history, which is more complicated than the deformations observed in the flysch nappes. Multiple folding events, tilting and refolding of ramp-flat structures as well as the overturning of strata complicate deciphering individual deformations and their relative chronology. However, in the region around the Middle Váh Valley structures were identified, which correlate with D_{F1} to D_{F3} within the flysch units. As in the flysch units, NNW- directed shortening is followed by NNE- directed shortening. ENE-striking sinistral strike-slip faults comparable to D_{F2} were identified in the PKB close to the border to the Biele Karpaty and Bystrica unit.

The ENE-striking section of the PKB NE of the Middle Váh Valley exhibits a distinct very complex structural inventory. Structures occur in the overturned NNW-dipping succession of the Middle Jurassic to Upper Cretaceous Kysuca unit. Kinematic analyses mainly use ramp-flat structures and related folds exposed in the strongly folded strata of the overturned succession. Four major groups of folds could be distinguished with (1) and (2) as the dominant ones:

(1) Open to tight folds with (N)NW-plunging axes and sub-vertical NNW-striking fold axial planes; (2) Folds with sub-horizontal ENE-trending fold axes; (3) folds with sub-vertical fold axes and NNW-striking sub-vertical fold axial planes linked to a ESE-striking sinistral strike slip fault; (4) folds exhibiting ~NE trending fold axes. The listed fold types are partly linked to ramp-flat structures. In order to obtain information on the chronological relationship of folding with respect to the large-scale overturning of the Kysuca sequence, the observed fold-related ramps were further subdivided into two groups. These are ramps in geometrically upright position, wich cut up into older strata in thrust direction, and ramps in overturned position, which cut into younger sediments in the inverted sedimentary succession. This classification provides information on whether ramps asscoiated with folds developed before or after large scale overturning of the sedimentary succession.

Analyses of ramp-flat structures and other structural features observed in outcrops reveal three different deformations, which occurred after the large-scale overturning of the Kysuca Sequence N of Žilina. The oldest of this three is characterized by NE-directed shortening, evident form folds of group (1) and corresponding ramps. Resulting (N)NW-plunging folds are subsequently steepened due to sinistral strike-slip faulting, which results in the development of folds of group (3). Sinistral strike slip faulting is related with E(NE)-directed shortening as evident from ramp-structures and conjugated dextral faults. Crosscutting relationships prove that E(NE)-directed shortening is overprinted by SSE-directed backthrusting. Backthrusting is evident from folds of group (2), which are related with ramps and reverse faults cutting the inverted sedimentary succession.

Comparing this deformations with kinematics in the area around the Middle Váh Valley and the adjacent flysch units NE- and E(NE)-directed shortening may be correlated with deformation D_{F2} (Beidinger et al., this volume). SSE-directed shortening is interpreted as to depict backthrusting at the latest stage of D_{F1} when the most external flysch units have reached their final position and foreland-propagating thrusting is blocked during the late Early Miocene.

D_{F1} in the flysch units is thought to cause today's subvertical to overturned position of the innermost units of the OWC fold and thrust belt due to passive rotation of upper structural units in the rear part of the fold and thrust belt (Beidinger et al., this volume). Considering this, the major mechanism for the overturning of the Kysuca sedimentary sequence may be related to D_{F1}. As no large-scale tectonic duplication of the considered Kysuca succession is evident it may depict an individual thrust sheet with a lack of large scale structures related to the early stage of deformation D_{F1} before thrusting progresses into the flysch units.

A unique volcanic field in Tharsis, Mars: monogenetic cinder cones and associated lava flows.

Petr Brož[1], Ernst Hauber[2]

[1]*Institute of Geophysics Acad. Sci. Czech Republic, Boční II/1401, 141 31 Prague 4, Czech Republic (Petr.broz@ig.cas.cz)*
[2]*Institut für Planetenforschung, DLR, Rutherfordstr. 2, Berlin, Germany (Enrst.Hauber@dlr.de)*

Mars displays a wide range of relatively young volcanic landforms (Greeley and Spudis, 1981). However most of them are related to effusive activity, like giant shield volcanoes, small and low shields, lava flows, and lava plains. Although the most common type of volcanic edifices on Earth are monogenic cinder or spatter cones (e.g. Wood, 1979), the unambiguous identification of cinder cones on Mars is rare. The previous studies discussed the existence of cinder cones on Mars on theoretical grounds (Wilson and Head, 1994; Dehn and Sheridan, 1990), or used relatively low-resolution Viking Orbiter images for putative interpretations. With the exception of morphologically similar pseudocraters (Fagents and Thordarson, 2007), however, they were not analyzed in detail yet. We report of several possible cinder cones in area situated north of Biblis Patera in the

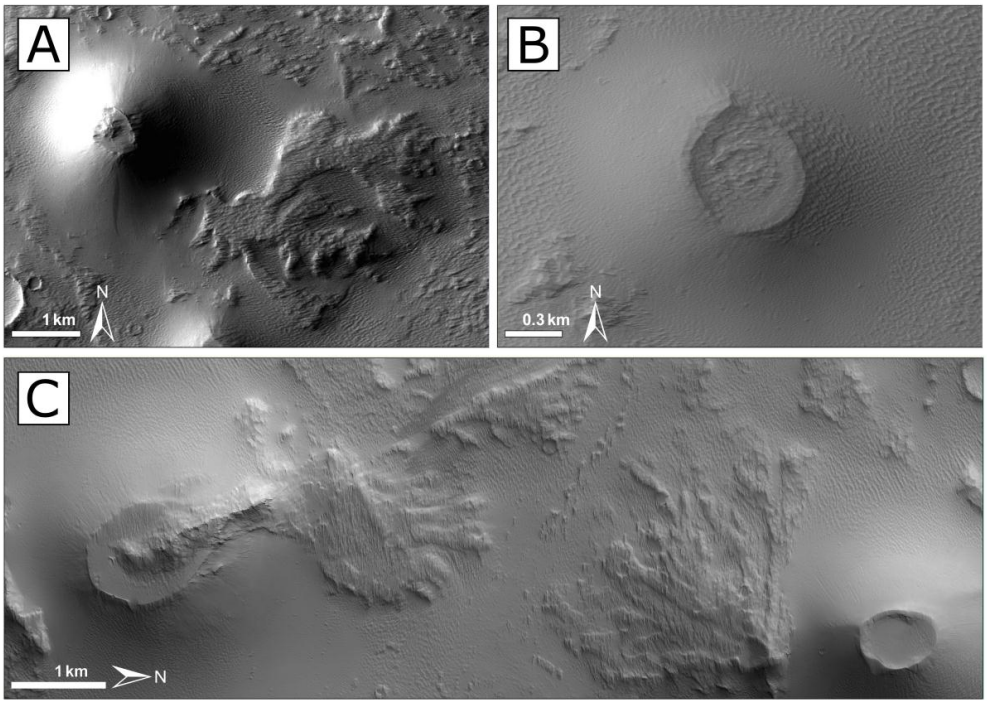

Fig. 1. Detail of parasitic lava flow starting on the side of cone (CTX, P22_009554_1858_XN_05N122W, centered 5.87°N/237.15° E), detail of summit crater of one small edifice (HiRISE, PSP_008262_1855_RED, centered 5.78°N/237.01°E) and two lava flows, one is down sloping from summit crater and second on flank of cone (HiRISE, PSP_008262_1855_RED, centered 5.65°N/237.02°E).

Tharsis region on our investigation.

This study uses imaging data from several cameras, i.e. Context Camera (CTX), High Resolution Stereo Camera (HRSC), and High Resolution Imaging Science Experiment (HiRISE). CTX images have sufficient resolution (5-6 meters/pixel) to identify possible cinder cones and associated edifices. Topographic information (e.g., heights and slope angles) were determined from single shots of the Mars Orbiter Laser Altimeter (MOLA; Zuber et al., 1992; Smith et al., 2001) in a GIS environment, and from stereo images (HRSC, CTX) and derived gridded digital elevation models (DEM).

Monogenic volcanic landforms on Earth were well described previously, and several basic ratios were established to classify them (Wood, 1979a). We calculate these ratios for the cones on Mars to test the hypothesis that there are Martian analogues to cinder cones, taking into account theoretically predicted differences in their morphology due to the specific Martian environment and its effect on eruption processes (Wood, 1979; Dehn and Sheridan, 1990). Our measurements suggest that the investigated Martian have a mean basal diameter of 2,300 m, about ~2.6 times larger than terrestrial cinder cones. The crater diameter for Martian cones range from 185 to 1,173 meters. The Wcr/Wco ratio has mean value 0.28. The edifices are also higher (from 64 to 651 meters) than terrestrial cinder cones (in average 90 meters). The Hco/Wco ratio of 0.12, which is less than that of pristine terrestrial cinder cones with a ratio of 0.18. The slope distribution of cone flanks is

between 12° and 27.5° (the steepest sections reach >30°).Based on morphological and morphometrical analyses, we interpret an assemblage of landforms in Tharsis as a cinder cone field. It is surprising that this is the only well-preserved field of this kind seen so far on Mars, given the fact that cinder cones are the most common volcanoes on Earth (Wood, 1980; Valentine and Gregg, 2008). The evidence for physiological diversity of Martian volcanism is still growing (see also Lanz et al., 2010).

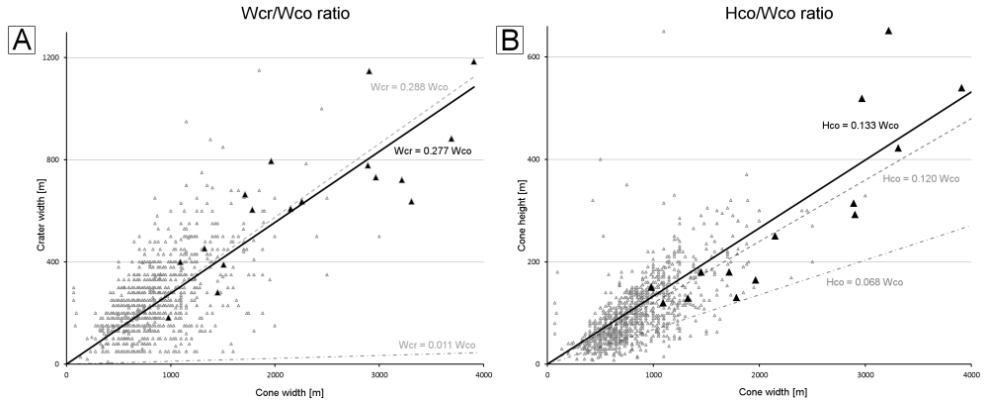

Fig. 2: Morphometry of investigated cinder cones in compare with terrestrial cinder cones and stratovolcanoes with summit craters. Full triangles correspond to investigated Martian cinder cones; empty triangles terrestrial cinder cones (~1060 edifices from Hasenaka, 1985; Inbar and Risso, 2001 and Pike, 1978). (A) Plot of summit craters width (WcR) versus basal cones width (Wco) of volcanic cones. The solid line represents the best fit using linear regression for Martian cones with value WcR/Wco = 0.277. Terrestrial cinder cones are represented by dashed line (WcR/Wco = 0.288) and for comparison dot-and-dash line represents stratovolcanoes with summit craters (WcR/Wco = 0.011). (B) Plot of the cone's height (Hco) versus basal width of cone. Lines represent same edifices as in Plot A. In both plots is visible close relationship between Martian cones and terrestrial cinder cones.

Greeley, R., and P. D. Spudis (1981), Volcanism on Mars, Rev. Geophys., 19(1), 13–41, doi:10.1029/RG019i001p00013.

Dehn J. and Sheridan, M. F. (1990), Cinder Cones on the Earth, Moon, Mars, and Venus: A Computer Model, Abstracts of the Lunar and Planetary Science Conference, volume 21, page 270.

Fagents, S.A. and Thordarson, T. (2007) in: Chapman, M. (ed.) The Geology of Mars, pp. 151-177, Cambridge University Press, Cambridge.

Hasenaka, T. and Carmichael, I.S.E., (1985). The cinder cones of Michoac~n--Guanajuato, central Mexico: their age, volume and distribution, and magma discharge rate. J. Volcanol. Geotherm. Res., 25: 104—124.

Inbar, M., Risso, C., 2001. A morphological and morphometric analysis of a high density cinder cone volcanic field — Payun Matru, south-central Andes, Argentina. Zeitschrift für Geomorphologie 45, 321–343.

Malin, M.C., Bell, J.F., Cantor, B.A., Caplinger, M.A., Calvin,W.M., Clancy, R.T., Edgett, K.S., Edwards, L., Haberle, R.M., James, P.B., Lee,S.W., Ravine, M.A., Thomas, P.C.,Wolff, M.J., (2007). Context camera investigation on board the Mars Reconnaissance Orbiter. J.Geophys.Res.112. doi:10.1029/2006JE002808. CiteIDE05S04.

Pike R. J. (1978), Volcanoes on the inner planets: some preliminary comparisons of gross topography. Proc. Lunar Planet. Sci. Conf. 9th, p. 3239 – 3273.

Smith, D.E., et al., (2001). Mars Orbiter Laser Altimeter: experiment summary after the first year of global mapping of Mars. J. Geophys. Res. 106, 23689–23722.

Valentine G.A., Gregg TKP. (2008). Continental basaltic volcanoes - processes and problems. Journal of Volcanology and Geothermal Research 177, 857-873, doi:10.1016/j.jvolgeores.2008.01.050.

Wilson, L., and Head, J., (1994), Review and analysis of volcanic eruption theory and relationships to observed landforms: Reviews of Geophysics, v. 32, no. 3, p. 221–263, doi: 10.1029/94RG01113.

Wood CA. (1979a). Monogenetic volcanoes of the terrestrial planets. In: Proceedings of the 10th lunar planetary science conference, Pergamon Press, New York, pp 2815–2840.

Wood C.A. (1980). Morphometric evolution of cinder cones. J. Volcanol Geotherm Res 7:387–413.

Zuber, M.T., Smith, D.E., Solomon, S.C., Muhleman, D.O., Head, J.W., Garvin, J.B., Abshire, J.B., Bufton, J.L., (1992). The Mars observer laser altimeter investigation. J. Geophys. Res. 97, 7781–7797.

Structural characterization of Eastern part of the separation zone between the Gemer and Vepor units in the West Carpathians

Zita Bukovská[1], Petr Jeřábek[1], Ondrej Lexa[1], Marian Janák[2]

[1]Institute of Petrology and Structural Geology, Faculty of Science, Charles University, Albertov 6, 128 43 Prague 2, Czech Republic (zita.bukovska@natur.cuni.cz)
[2]Geological Institute, Slovak Academy of Science, Dúbravská 9, P.O. BOX 106, 840 05 Bratislava 45, Slovak Republic

The Gemer Unit in the south and the Vepor and Tatra Unit in the north represent major crustal segments of the Central West Carpathians incorporated into the Alpine thrust sheet. This structure originates from Early Cretaceous convergence responsible for overthrusting of the Gemer Unit over the Vepor Unit causing overall crustal thickening and regional prograde metamorphism in the Vepor Unit (Janák et al., 2001, Jeřábek et al., 2008). Subsequent Late Cretaceous eastward lateral escape of the Gemer Unit (Lexa et al., 2003) was responsible for the development of a large-scale detachment zone obscuring primary contact of the Gemer and Vepor units (Janák et al., 2001). In this study we concentrate on detailed characterization of the Gemer-Vepor contact zone as it appears to play a major role in the evolution of the Central West Carpathians orogenic wedge.

The studied area is located in the northern part of Gemer-Vepor contact zone between Dobšiná and Štítnik. Here the Vepor Unit is formed by intensely deformed orthogneisses, crystalline schists and Permian-Triassic quartzites. Our study has revealed that some schist complexes, previously considered as Late Paleozoic cover, bear two-generations of garnet indicating its basement affinity (Korikovskij, 1990). These basement schists occur in the vicinity of the chlorite-chloritoid-kyanite schists near Hanková (Vrána, 1964; Lupták et al., 2000) thus arguing for considerable structural complexity of the Gemer-Vepor contact zone. Detailed structural mapping in the studied area revealed structural record of three main deformation events. The first deformation phase D1 is associated with the development of metamorphic foliation S1 defined by shape preferred orientation of quartz aggregates and micas. This fabric is generally subhorizontal to gently-dipping to the east and bears an E-W trending stretching lineation. This fabric is best preserved in orthogneisses to the west and rarely preserved in cover sequences to the east due to subsequent D2 overprint. The second deformation phase is associated with the formation of S2 cleavage defined by shape preferred orientation of micas and it develops subparallel to S1. The obliquity of S_1 and S_2 is well defined in orthogneiss, while in the cover sequences the S1 fabric is mostly obliterated by S_2. The S_1/S_2 geometrical relationship commonly forms SC' geometries, which however represent diachronuous structures. The deformational phase D3 is associated with the development of open folds and crenulation cleavage with steep axial planes and E-W trending fold axes.

The two main fabrics S1 and S2 have been further examined by means of microstructural and microchemical analyses. The microstructural analysis of orthogneiss and quartzite indicates distinct quartz grain size and quartz c-axis pattern within S1 and S2 fabrics. The quartz CPO`s determined by computer integrated polarization microscopy (Panozzo Heilbronner and Pauli, 1993) indicate symmetrical c-axis pattern for S1 and asymmetrical with top-to-the-east shear sense c-axis pattern for S2. In orthogneiss several generations of white mica are present with chemical composition varying from muscovite to phengite. The oldest large mica grains of probably magmatic origin have a chemical composition of muscovite 1. These grains are overgrown by smaller flakes of phengitic mica occurring in the S1 fabric, which is in turn overgrown by muscovite 2 representing the majority of measured mica and defining the S2 fabric. The chlorite-chloritoid-kyanite schists contain also muscovite, paragonite, margarite and quartz together with accessory rutile, ilmenite, apatite, allanite and zircon. The peak chlorite-chloritoid-kyanite assemblage clearly postdates the metamorphic foliation S1 as demonstrated by its transversal growth. This assemblage is subsequently affected by chlorite-muscovite cleavage S2 resulting in replacement of chloritoid and kyanite. In some places, mostly in between chloritoid grains, remnants of paragonite or margarite can be found. The peak assemblage is associated with the growth of monazite and xenotime occurring in the vicinity of chloritoid (at the rims) or separately in the matrix. Xenotime locally overgrows zircon of probable detrital origin. The EMPA dating of monazite yields the average age of 118±15Ma, that is interpreted to date the formation of S1 fabric. These new data are nicely in contrast with previously published Ar-Ar age of 77 Ma from these rocks (Janák et al., 2001). This younger age has been interpreted as exhumation age and most likely corresponds to the formation of S2 cleavage.

We conclude that the first deformation event was associated with burial of the Vepor Unit due to overthrusting by Gemer Unit at approximately 118±15Ma. The second deformational event was related to exhumation of the Vepor unit combined with eastward escape of the Gemer Unit. The third deformation phase represents late stage transpressional deformation affecting both units (Lexa et al., 2003).

AMS discrepencies in Ordovician sediments, Prague Synform, Barrandian

Jan Černý, Rostislav Melichar

Department of Geological Sciences, Faculty of Science, Masaryk University, Kotlarska 2, 611 37 Brno, Czech Republic, (176111@mail.muni.cz, 56@mail.muni.cz)

The focus of this paper is to study the magnetic fabrics within the different Ordovician sedimentary rocks of the Prague Synform, which is located in central Bohemia. The Prague Synform is located between the cities of Prague and Pilsen, Czech Republic. Eleven localities were sampled in the area and are located in (Fig 1). This work is a pilot study aimed at understanding the regional tectonic and magnetic development of the Prague synform. Field data and specimens were successfully processed for AMS. The dependence of the magnetic susceptibility versus the temperature variations were measured by use of a furnace for high temperatures and a cryostat for low temperatures. The principal directions of magnetic susceptibilities were measured by using a kappabridge. The magnetic principle directions were analyzed and their relationship between the bedding, discontinuities, dislocations and direction of drilling were determined. Some plots derived from low magnetic rocks displayed the resultant direction was dependent on the drilling direction due to a contamination from the diamond-drill which left a thin layer of steel on the specimen surface (Fig. 2). The influence of the contamination reached values $X \times 10^{-5}$ SI. The magnetic fabrics of the majority of the Ordovician sediments are controlled by paramagnetic minerals, except orthoquartzites and siliceous rocks, in which fabrics are probably controlled by ferromagnetic minerals. Throughout the study, sedimentary, deformed and other magnetic fabrics were identified. Further studies will especially focus on deformed magnetic fabrics.

The study was supported by the grant project GAP210/10/2351.

Černý J. 2010. Magnetic anisotropy of the Ordovician sedimets from the Prague Synform. MSc. Thesis. Masaryk University. Brno. Czech Reublic.

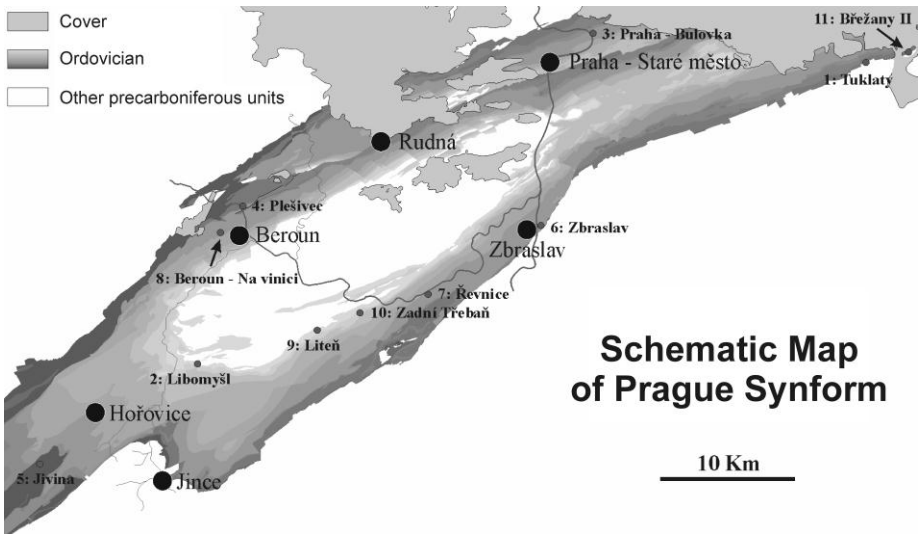

Fig. 1. Schematic map of the Prague Synform with localities and their numbers (black points). On these localities samples were drilled for AMS analyses.

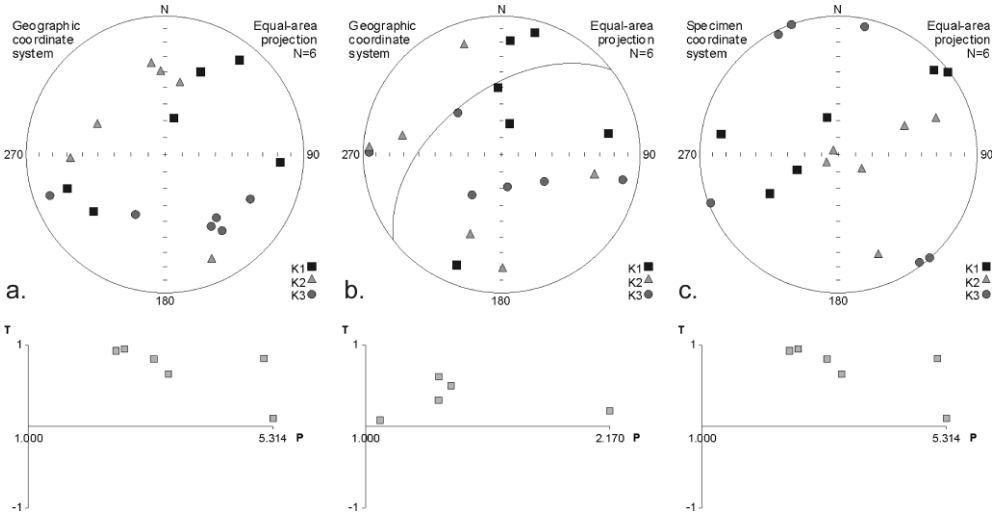

*Fig. 2. Analyses from Březany II locality. Selection of specimens were identified to have a high magnetic susceptibility (**a**). It was discovered that specimins which have an extremely high magnetic susceptibility were contaminated by a thin layer of steel which was emplaced on the specimin surface by the diamond-drill that was used. The results without a thin layer of steel are displayed in figure **b** (the layer of steel was removed). After removal of the steel coating, the average magnetic susceptibility dropped from 16–89 × 10^{-6} SI to 2–8 × 10^{-6} SI. Also, the parameter P rapidly decreased. The influence of the diamond-drill contamination can change the results in weakly magnetized rocks. In the specimens coordinate system, it is possible to see that the direction of minimum magnetic susceptibility, due to diamond drill contamination, is situated around the perimeter of the diagram circle (**c**). It is possible to explain that the direction of minimum magnetic susceptibility is perpendicular to the thin steel layer which is on the surface of the cylinder*

Geochemistry and petrology of the Neogene rhyolites from the Central Slovakia Volcanic Field, Western Carpathians

Rastislav Demko[1], Jakub Bazarnik[2], Pavol Šesták[1]

[1]*State Geological Institute of Dionýz Štúr, Mlynská dolina 1, 817 04 Bratislava 11, Slovakia (rastislav.demko@geology.sk)*
[2]*Institute of Geological Sciences, Polish Academy of Sciences, Krakow Research Centre, Senacka 1, 31-002 Krakow, Poland*

The Central Slovakia volcanic field (CSVF) is a product of Neogene volcanic activity linked to the collision of the Western Carpathians with the stabilized European platform. The volcanic activity started in the Middle Miocene with the production of andesites. The rhyolite volcanism operated during the Upper Sarmatian with the production of pyroclastics, extrusive domes and lava flows. After the rhyolitic volcanism ceased, an activity proceeded with the eruption of subalkaline basalts and later alkaline basalts. The ryolites are mainly of porphyric textures, but aphyric types and obsidians are also present. Phenocrysts consist of amphibole and plagioclase, Fe-Ti oxide (scarce), biotite, sanidine and quartz, which have crystallized in order how there are named. Accessory phases include zircone, allanite and rare apatite. The important petrographical feature is a separate presence of plagioclase, plagioclase with sanidine, or sanidine in phenocryst assemblages. These phenomenas tend to create a special rock names such as plagioclase rhyolites and sanidine rhyolites. Thermobarometric calculations based on two feldspar thermometry, Pl-Amf thermometry and Amf barometry yield magma temperatures between 830-760°C to 730°C. Barometric results correspond with pressure of 4,4-3,1 kBar, but only for rhyolites with amhiboles. The chemical composition of glass corresponds with haplogranitic system equilibration in near surface conditions below 0,5 kbar. Rhyolites chemically respond to subalcalic high-potassium peraluminous rhyolites with normative quartz and corund. The major composition is varied by volume and phenocryst types. The main chemical heterogeneities between rhyolites are based on Nb-La-Ti-Zr-Y systematics, where three petrogenetic groups are identified. The group I corresponds by petrography to sanidine – plagioclase and sanidine rhyolites, while plagioclase rhyolites correspond to the most primitive group III. The group II is combined by mix of the group I and the group III. Every one of these groups has typical geochemical features dictated by their petrogenesis and degree of fractionation. Focused to RE and HFS trace element data, chemistry of rhyolites were affected mainly by fractionation of zircon and amphibole. As for rhyolite petrogenesis, it is difficult to generate them by classical differentiation processes such as crystal fractionation, magma mixing and contamination or more complex MASH or filter pressing liquid extraction. Beside to basalt - andesites and rhyolite chemical differentiation, it is not possible to derive acid melts from parental intermedial liquids. The observed rhyolite chemical trends are results of melting, probably of a high solidified basic amphibole bearing pluton, by heat input from new injections of primitive magma. These ideas are in good agreement with radiogenic isotope study. Rhyolites belong to two isotope groups, but not corresponding with previous petrography and HFSE-REE systematics. The first one has εNd_1 between -1,57 and -1,41 with 87/86Sr 0,706537-0,706463 and the second one has εNd_2 between -3,9 to -3,33 with 87/86Sr 0,707150-0,710496. The isotopic composition of CSVF rhyolitic rocks overlaps other volcanics, such as andesites and basalts (data of Harangi et al., 2007). The rhyolite and basalt-andesite similarities of CSVF and strong differences with Western Carpathians basement rocks (metapelites, gneisses, granites) suggests petrogenetic relationship of all CSVF volcanics or continual source development. Looking for a global model of CSVF isotopic development and petrogenesis, radiogenic composition of previous andesites gradually changes through rhyolites to more primitive basaltic andesites and basalts. Rhyolite volcanism display physically connection during hiatus of intermediate and basic volcanism. All volcanic activity is affected by tectonics. Two pulses of previous intermediate and the next basic volcanism respond with higher tectonic interaction of the Western Carpathians and the European platform. The rhyolite volcanic pulse was derived during reduction of tectonic activity and changing of tectonic style from compression to transtension regime.

(This project was supported by Ministry of Environment of the Slovak Republic (No. 15 06):"The maps of paleovolcanic reconstruction of rhyolite volcanism in Slovakia and analysis of magmatic and hydrothermal processes".)

Harangi, S., Downes, H., Thirlwall, M. & Gméling, K., 2007. Geochemistry, Petrogenesis and Geodynamic Relationships of Miocene Calc-alkaline Volcanic Rocks in the Western Carpathian Arc, Eastern Central Europe. J. Petrology, 48, 2261-2287.

LA-ICP-MS U-Pb zircon dating of igneous, epiclastic and sedimentary rocks of the Jílové zone and the Davle Formation (Teplá-Barrandian unit, Bohemian Massif, Czech Republic)

Kerstin Drost[1], Jan Košler[1], Jiří Konopásek[1], Hege Fonneland Jørgensen[2]

[1]*Department of Earth Science and Centre for Geobiology, University of Bergen, Allegaten 41, 5007 Bergen, Norway (Kerstin.Drost@geo.uib.no, Jan.Kosler@geo.uib.no, Jiri.Konopasek@geo.uib.no)*
[2]*Petrology Group, StatoilHydro ASA, Forskningssenteret, P.Box 7190, 5020 Bergen, Norway (hfon@statoil.com)*

The Neoproterozoic basement of the Teplá-Barrandian unit in the centre of the Bohemian Massif has been subject to numerous studies including tectonics, metamorphism, the composition and geotectonic affiliation of igneous rocks, provenance and depositional environments of sedimentary rocks as well as paleontological studies. There is broad agreement on a subduction-related setting connected to the evolution of the Avalonian-Cadomian belt in the periphery of Gondwana, and on south-directed subduction beneath Teplá-Barrandian crust that must have lasted until ~550-540 Ma (Zulauf et al., 1999; Timmermann et al., 2004).

A key element in any reconstruction of the Neoproterozoic geotectonic evolution of the Teplá-Barrandian unit is represented by the rocks preserved close to the southeastern boundary with the Moldanunian Zone, namely the Davle Formation and the Jílové belt. These units are usually interpreted to represent remnants of a Cadomian magmatic arc or island arc at or close to the margin of Gondwana. This interpretation is based on field relations and some geochemical data (Waldhausrová, 1984) and has significant implications for the understanding of the latest Neoproterozoic and early Palaeozoic evolution of the Teplá-Barrandian unit and the peri-Gondwanan realm.

However despite of the key role attributed to the Davle Formation and Jílové belt by many authors, the ages of the (sub-)volcanic and volcaniclastic rocks and orthogneisses have never been sufficiently established. Moreover, the nature of the basement (continental/oceanic) of the assumed arc is unknown and the provenance of the sedimentary component of the Davle Formation has never been constrained.

Aiming to overcome these shortcomings, we collected samples from (1) orthogneisses of the Jílové belt and its continuation in the Sedlčany-Krásna Hora pendant, (2) intrusive and (sub-)volcanic rocks of the Jílové belt, (3) deposits of volcanic and volcaniclastic material with evidence of variable reworking (Davle Formation) as well as (4) siliciclastic sedimentary rocks of the Davle Formation for laser ablation inductively coupled plasma mass spectrometry (LA-ICP-MS) U-Pb zircon dating.

The data are acquired in order to shed light on the timing of the Precambrian magmatism and the provenance of the sedimentary component. The latter in combination with potential inheritance in the igneous rocks may in turn provide a clue to the affinity of the basement on which the evolution of the presently known Teplá-Barrandian unit started. Furthermore it can be evaluated whether or not pre-existing equivalents of the presently preserved igneous rocks may have served as a source for Ediacaran detrital zircon (and white mica) commonly found in Ediacaran and Palaeozoic siliciclastic rocks of the Teplá-Barrandian unit.

Preliminary results confirm an Ediacaran age for the igneous rocks of the Jílové Zone and the volcanic component of the Davle Formation. The sedimentary component in the Davle Formation appears to have a mixed provenance from Ediacaran and Palaeoproterozoic/Archean sources, whereas the latter may make up substantial proportions of the detrital zircon age spectra. Although no prove of pre-Neoproterozoic inheritance in purely magmatic rocks has been found so far, the age patterns in epiclastic (with unknown proportion of sedimentary contribution) and sedimentary rocks are clearly in favour of a setting on the continental crust.

Timmermann, H., Štědrá, V., Gerdes, A., Noble, S. R., Parrish, R. R. & Dörr, W., 2004. The Problem of Dating High-pressure Metamorphism: a U–Pb Isotope and Geochemical Study on Eclogites and Related Rocks of the Mariánské Lázně Complex, Czech Republic. Journal of Petrology, 45, 1311-1338.

Waldhausrová, J., 1984. Proterozoic volcanics and intrusive rocks of the Jílové zone in central Bohemia. Krystalinikum, 17, 77-97.

Zulauf, G., Schitter, F., Riegler, G., Finger, F., Fiala, J. & Vejnar, Z., 1999. Age constraints on the Cadomian evolution of the Teplá Barrandian unit (Bohemian Massif) through electron microprobe dating of metamorphic monazite. Z. dt. geol. Ges., 150, 627-639.

Structure and evolution of the Variscan Belt during Carboniferous times derived from gravimetric, magnetic and paleomagnetic data.

Jean-Bernard Edel, Karel Schulmann

Université de Strasbourg,, EOST, Institute de Physique de Globe, UMR 7516, 1 Rue Blessig, 67 000 Strasbourg, France

The object of the paleomagnetic study was to unravel the geodynamic motions leading to the present aspect of the Variscan belt during Devonian to Permian times. In parallel, using all available gravimetric and magnetic map as well as various transformations of these maps intending to optimize qualitative and quantitative interpretations, we produced a structural map of the whole European Variscides. This map shows the main tectonic features which delimitate the various terranes and blocs of the belt and facilitates the interpretation of the paleomagnetic data in terms of block motions.

Paleomagnetic investigations have been carried out in all Paleozoic massifs of stable Europe, from Armorican Massif to Polish Sudetes. One of the major results was the revealing of pervasive remagnetizations in Middle-Late Carboniferous times which hamper the knowledge of the early phases of the orogeny. Because of higher competence for late overprinting of sediments and scarcity of suitable sedimentary outcrops, investigations were mainly carried on Early Carboniferous volcanic, plutonic and seldom metamorphic rocks which are present in most massifs. Thanks to this strategy, Early Carboniferous motions could be detected in northern Vosges and Central Bohemian Pluton. Summing up the results from investigated massifs, the following evolution can be proposed.

340-330 Ma: a counterclockwise rotation by about 40° is detected in arc magmatic granitoids from northern Vosges and Central Bohemian pluton. This rotation concerns as well Saxothuringian, Bohemian and Moldanubian crustal blocks. It is associated with dextral shear along major transform faults presently striking NW-SE (Bray, Franconian-Bavarian, Elbe and Odra faults). These motions are likely driven by squeezing of the belt between northward drifting Gonwana and nearly stable Avalonia.

- 330-325 Ma: NNW-SSE extension leads to significant southeastward tilting of crustal fragments related to NW-SE extensional tectonics.
- 325-310 Ma: pervasive magnetic overprinting related to extensive magmatism and hydrothermalism affects all parts of the belt. The ENE or WSW paleomagnetic declinations reveal a large global clockwise rotation by about 70°. The pole of the rotation is located on the Teisseyre-Tornquist zone. The driving force is the westward rotation of Gondwana.
- 310-260 Ma: the clockwise rotation continues but, after final collision and thrusting of the Rhenohercynian margin on Avalonia, Avalonia and Baltica are driven by the same motion. The collision of Africa with Laurentia marks the end of the global clockwise rotation.

Metamorphism and tectonics of the Central Iranian Basement and their relation to closure of the Tethyan oceanic tracts

Shah Wali Faryad[1], Petr Jeřábek[1], Mahmoud Rahmati-Ilkhchi[1,2], František Holub[1],

[1]*Institute of Petrology and Structural Geology, Charles University, Albertov 2, Prague, faryad@natur.cuni.cz*
[2]*Geological Survey of Iran*

Metamorphic basement rocks, exposed beneath the very-low-grade to unmetamorphosed Upper Jurassic-Eocene formations north of the Torud fault zone within the Great Kavir Block, were investigated in order to elucidate the origin of their protoliths and their metamorphic history during Alpine and pre-Alpine orogenies. The basement, previously assumed as a pre-Cambrian metamorphic complex, is mostly formed by amphibolite facies orthogneisses (tonalite, granodiorite, and granite) with amphibolites and small amounts of metasediments-micaschists. Major- and trace-element geochemistry in combination with U-Pb age dating of zircon showed that the protoliths formed during Late Neoproterozoic continental arc magmatism that has also been identified in other tectonic blocks of Central Iran. This Neoproterozoic-Early Paleozoic orogenic system was active along the Proto-Tethyan margin of the Gondwanaland supercontinent (Rahmati-Ilkhchi, et al., 2011).

In addition to quartz, feldspar(s), micas in orthogneisses, and amphibole + plagioclase in amphibolite, all rocks may contain garnet. Kyanite was found only in Al-rich amphibolite together with gedrite. The PT conditions of the rocks estimated, based conventional geothermobarometry and pseudosection method, show a medium-pressure amphibolite facies metamorphism. Both igneous and sedimentary rocks show evidence of prograde metamorphism with subsequent cooling. This Barrovian-type metamorphism with field gradient of 20–22 °C/km was related to collision-induced crustal thickening. It was associated with D1 deformation phase, which occurred during prograde stage and D2 event that corresponds to post-collisional exhumational upflow of middle crust, resulting in updoming of the basement core and its top-to-the-Northwest unroofing along a low-angle detachment shear zone at the basement/cover boundary Rahmati-Ilkhchi et al., 2010). Ar-Ar age dating of muscovite reveals that this metamorphism occurred during Middle Jurassic (166 Ma). A mid-Cimmerian age for D1 and D2 events is considered, while they affected also the Lower Jurassic Shemshak Formation and are sealed by the Middle Jurassic conglomerates. The D3 folding event, characterised by NE–SW shortening, affected also the Cretaceous limestones, and it is sealed by Paleocene conglomerates. Considering the Late Cretaceous age of this deformation, it is related to the Late-Cimmerian–Early Alpine orogeny that resulted from the Cenozoic closure of the Neo-Tethys oceanic tract(s) and convergence between the Arabian and Eurasian plates. The D4 folding event, characterised by NW–SE shortening, affected also the Miocene conglomerates, implying its Late Miocene to post-Miocene age. This deformation event is associated with Late Alpine Alborz and the Zagros phase of convergence between Arabia and Eurasia during Late Cenozoic, and it could be combined with a left-lateral activity along the Great Kavir fault-bounding system. Petrologogical and geochronological data in combination with field structural relations indicate a relatively fast burial and subsequent exhumation of the basement units during middle Jurassic time. This was due to the NE-SW shortening of Central Iran basement units that related to closure of the Neotethys. This is is confirmed also by age data from from high-pressure rocks along the Sabzevar and Sanandaj-Sirjan zones that give Middle Jurassic to Cretaceous ages for their metamorphism (Davudian, et al., 2008, Rossetti, et al., 2009)

Davoudian, A. R. Genser, J. Dachs, E. and Shabanian, N. 2008. Petrology of eclogites from north of Shahrekord, Sanandaj-Sirjan Zone, Iran. Mineralogy and Petrology (2008) 92: 393–413

Rahmati-Ilkhchi, M. Faryad, SW, Holub, F.V.. Košler, J and Frank, W. 2011..Magmatic and metamorphic evolution of the Shotur Kuh metamorphic complex Central Iran. International Journal of Earth Sciences, 100, 45-62.

Rahmati-Ilkhchi, M., Jeřábek, P., Faryad, S. W., Koyi, H. A. 2010 published online. Mid-Cimmerian, Early Alpine and Late Cenozoic orogenic events in the Shotur Kuh metamorphic complex, Great Kavir block, NE Iran. Tectonophysics, 494, 101-117.

Rossetti, F., Nasrabady, M., Vignaroli, G., Theye, T., Gerdes, A., Razavi, M.H., Vaziri, H.M., 2009. Early Cretaceous migmatitic mafic granulites from the Sabzevar Range (NE Iran): Implications for the closure of the Mesozoic peri-Tethyan oceans in central Iran. Terra Nova, 22, 26-34.

Thermal and erosional history calibrated by vitrinite reflectance - comparison of Lazy, CSM, and Staříč profiles in the Upper Silesian Basin

Juraj Franců[1], Lada Navrátilová[2], Philipp Weniger[3], Jan Šafanda[4], Petr Waclawik[5], Rostislav Melichar[2]

[1]*Czech Geological Survey, Leitnerova 22, 65869 Brno (juraj.fancu@geology.cz)*
[2]*Institute of Geological Sciences, Masaryk University, Brno (lada.navrat@email.cz, melda@sci.muni.cz)*
[3]*Institute of Coal and Petroleum Geology, RWTH University Aachen, (philipp.weniger@lek-rwth.de)*
[4]*Institute of Geophysics Acad. Sci. Czech Republic, Boční II/1401, 141 31 Prague 4, Czech Republic (jsa@ig.cas.cz)*
[5]*OKD ČSM, Stonava 1077, 735 34 Stonava (petr.waclawik@okd.cz)*

Vitrinite reflectance and Rock-Eval pyrolytic T_{max} index were measured on core samples from the Lazy, CSM, and Staříč exploration wells to quantify thermal maturity of organic matter. The data show rather similar trends with depth with some vertical shift and indicate that the rocks were exposed to higher thermal stress in the geological past. The maturity distribution was used as calibration data of alternative heat flow, burial and uplift scenarios for the selected parts of the Upper Silesian Basin. PetroMod software (™ Schlumberger) for basin modeling was used as the principal tool to experiment with the effects of heat transfer and amount of erosion using finite elements method for non-steady state systems.

The first model presents the subsidence and deposition history based on the preserved thickness of the sedimentary strata encountered by the exploration boreholes with negligible erosion of the Upper Paleozoic units. The second model assumes continuing deposition of Namurian C and Stephanian and subsequent removal of these hypothetic strata during the Mesozoic and Paleogene.

Geothermic conditions were simulated as alternative scenarios of heat flow and distribution of thermal conductivities following the lithological profile. In the first step, the heat flow at the base of the sedimentary basin fill was assumed ca 150% of the present value. In every model, compaction of shale, coal, and sand were calculated to simulate the increase in thermal conductivity in time and depth of burial. In process of modeling the heat flow values were modified together with the amount of erosion until the predicted thermal maturity agreed with the measured one. Alternative modeled maturity profiles are shown suggesting the credibility of geological scenarios of basin history.

The first model with negligible erosion yields significant difference among the measured and predicted values (Fig. 1a). The absence of deeper burial was experimentally compensated by very high heat flow. This model resulted in a steeper maturation trend with depth and fitted only a single data point of vitrinite reflectance. The maximum number of measured data (Fig. 1b) was achieved by an optimized model where the paleo-heat flow was 75 mW/m^2 during the Late Carboniferous and 43 mW/m^2 for the geological present

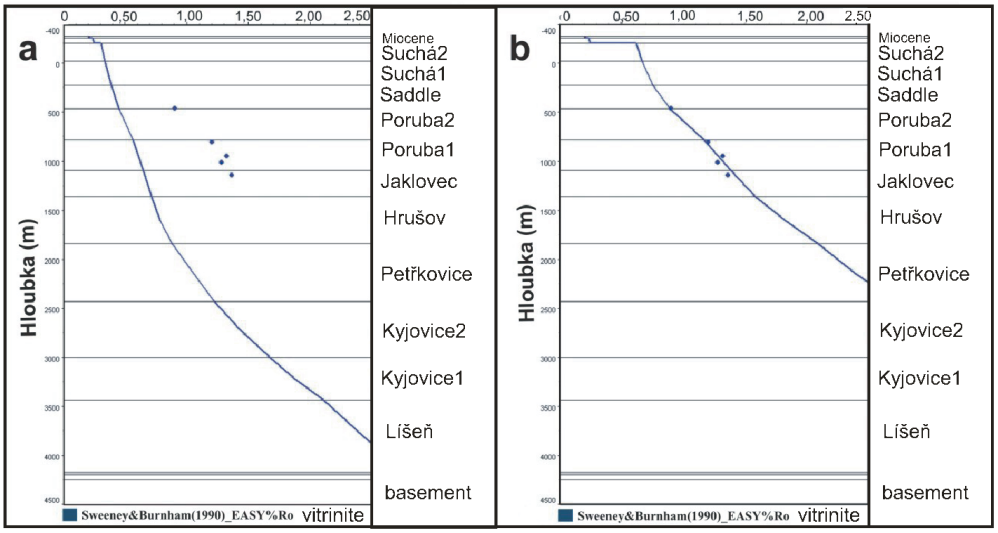

Fig. 1. Predicted profile (line) and measured vitrinite reflectance (points R_o) in Lazy 76/08: a) model with negligible erosion, b) model with erosion of 2300 m from top of the Suchá Mb.

associated with erosion of 2300 m in Staříč and 1800 m in CSM of the mostly Stephanian siliciclastic rocks with minor coal seams. These overburden strata were eroded during the Permian through Paleogene prior to deposition of the Lower Miocene of the Carpathian Foredeep.

In contrast to Dvořák and Wolf (1979) and Dvořák (1989) we conclude that the present Upper Silesian Basin is an erosional relict of a much bigger basin. The amplitude of unroofing is increasing from the Variscan foreland (present East) to the Variscan thrust-and-fold belt in the West. Similar pattern was observed in the Paleozoic in the SE Czech Republic by Francu et al. (2002).

Dvořák J., 1989. Anchimetamorphism in the Variscan tectogene in Central Europe – its relationship to tectogenesis, Věst. ÚÚG, 64, 1, 17–30.

Dvořák J. and Wolf M., 1979. Thermal metamorphism in the Moravian Paleozoic (Sudeticum, ČSSR). N. Jb. Geol. Paläont. Mh., 10, 596–607.

Franců E., Franců J., Kalvoda J., Poelchau H.S. and Otava J. 2002. Burial and uplift history of the Palaeozoic Flysch in the Variscan foreland basin (SE Bohemian Massif, Czech Republic). EGU Stephan Mueller Special Publication Series, 1, 167–179.

Fractal dimension of lineaments network in the Karkonosze-Izera Block (SW Poland)

Krzysztof Gaidzik, Jerzy Żaba

Department of Fundamental Geology, University of Silesia, Będzińska 60, PL-41-200 Sosnowiec, Poland (k.gaidzik@gmail.com, jzaba@interia.pl)

Fractality of lineaments network geometry was tested for the Karkonosze and Izera Mountains area. For this the cluster analysis and the box counting methods were employed (for details of used methods see: Mandelbrot, 1983; Turcotte, 1992, Idziak & Teper, 1996). The fractal geometry was proved for fault network of many areas (i.e.: Idziak & Teper, 1996; Teper, 1998), whereas such studies for lineaments haven't been taken.

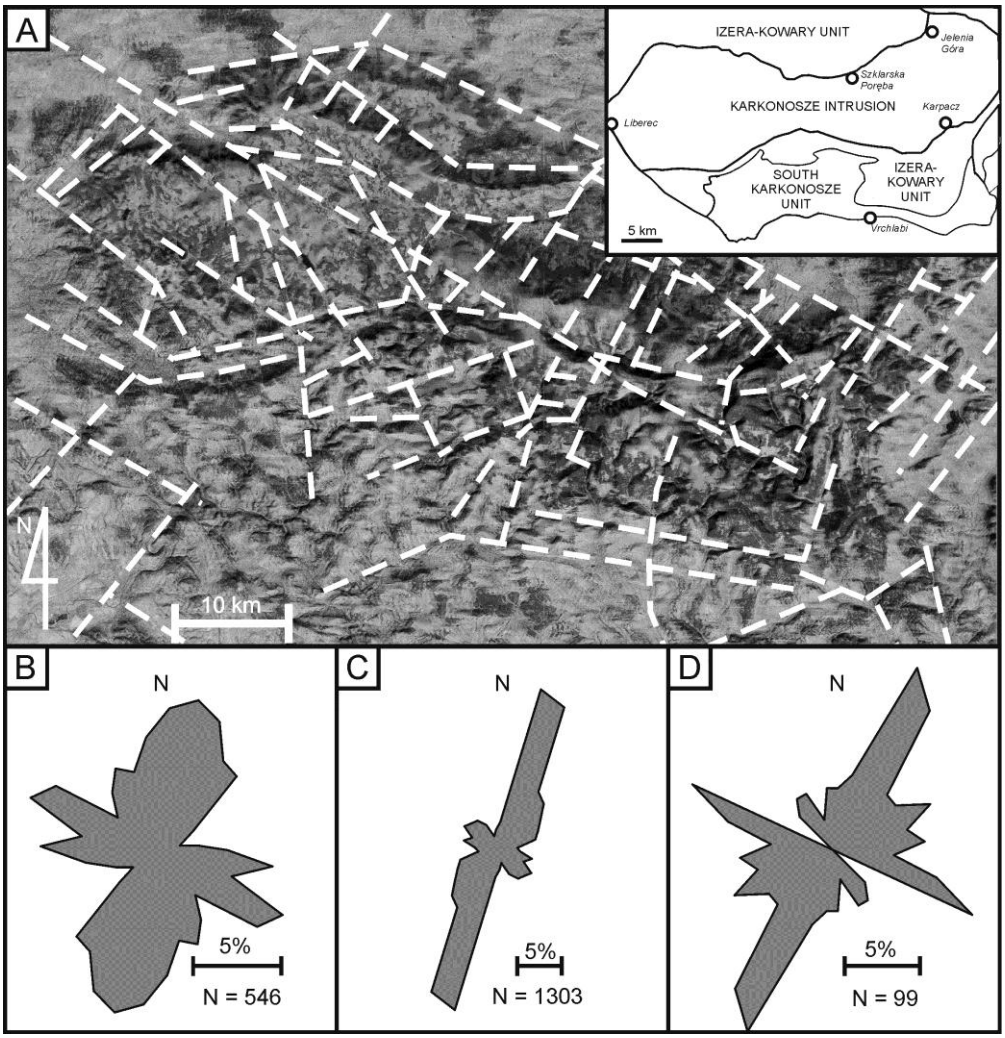

Fig. 1. Discontinuous structures network in the study area. A – the main linear structures in the studied area, B – discontinuous structures rose diagram of the Karkonosze intrusion (max: 9,2%, strike azimuth: 10-20°), C – discontinuous structures rose diagram of the Karkonosze intrusion envelope in the area of Karpacz (max.: 18,4%, strike azimuth: 10-20°), D - lineaments rose diagram of the studied area (max.: 13,1%, strike azimuth: 20-30°).

The morphotectonic studies were made for the area of over three thousands km^2 of the Karkonosze-Izera Block, on the basis of DTED-2 (Digital Terrain Elevation Data; resolution 20x30 m) received from Professor Stanisław Ostaficzuk, due to the cooperation with the Military Institute of Geodesy and Cartography (Fig. 1A & D), as well as geological maps of that area (Cymerman, 2004, as well as series of maps of the Detailed Geological Maps of Sudetes in scale 1: 25 000). The resulted lineaments network is very similar to actually stated, during field studies, joints and faults systems (Fig. 1B & C; Gaidzik & Żaba, 2009), as well as results obtained by other authors (Mroczkowski & Ostaficzuk, 1985; Migoń, 1996; Lysenko, 2007).

According to box counting method, the lineaments network of the studied area might be characterized by the fractal geometry with fractal dimension equals D = 1.56 (Fig. 2A). Similar results were obtained for fault systems from the Upper Silesian Coal Basin (Idziak & Teper, 1996; Teper, 1998). However the actual resulted boxing line isn't ideal straight. It might be caused by several reasons. Probably the most important include:

1 – imperfection of morphotectonic analysis (subjectivity of interpreter), 2 – lineaments aren't the same as faults, 3 – obtained lineament network contain structures of different deformation phases or stages, 4 – differences in lithology and tectonic evolution of geological units present on the studied area. The probability of lineament occurrence has no fractal character (Fig. 2B). Similar results were obtained for lineaments network grouped into definite tectonic units: the Karkonosze intrusion, the Izera-Kowary unit and the South Karkonosze unit.

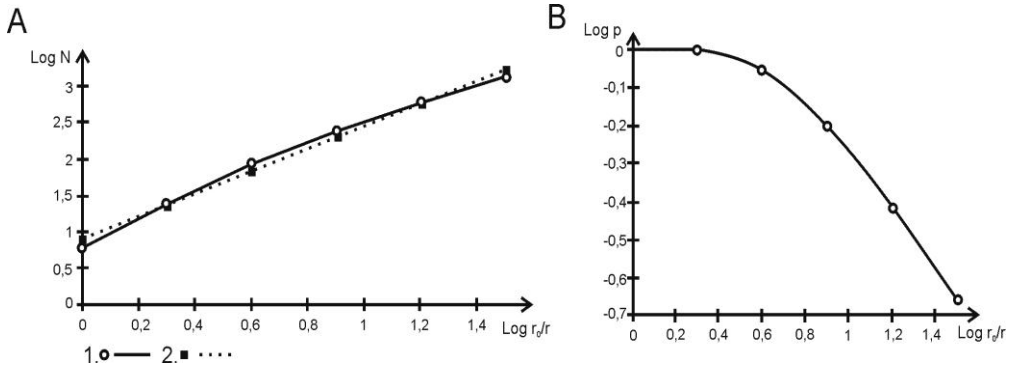

Fig. 2. Fractal analysis – log-log graphs. A – Log-log graph plotting minimum number of squares required to cover lineament lines versus normalized box size. B – Log-log graph plotting 2-D geometrical probability of lineament occurrence distribution versus normalized box size; 1 – actually obtained data, 2 – best fit line (least squares method), other explanation the same as in Fig. 1..

Authors would like to thank Professor Adam Idziak and Lesław Teper for inspiring studying fractals in tectonics as well as their helpful suggestions and comments.

Cymerman Z., 2004. Tectonic Map of the Sudetes and the Fore-Sudetic Block 1: 200 000. Polish Geological Institute, Warszawa.

Gaidzik K. & Żaba J., 2009. Brittle shears in the southern contact zone of the Karkonosze granite in the area of Karpacz relating to fractures on chosen example. In: Knapik R., Andrle J. (Eds.), 7th International Conference Geoecological Problems of the Karkonosze Mts Szklarska Poręba, 21-23.09.2009 (Book of Abstracts), 52-53.

Idziak A. & Teper L., 1996. Fractal Dimension of Faults Network in the Upper Silesian Coal Basin (Poland): Preliminary Studies. Pure and Applied Geophysics, 147 (2), 239-247.

Lysenko, V., 2007. Morphotectonic analysis of the Giant Mountains using the methods of remote sensing. Opera Corcontica, 44 (1), 37-42 (in Czech with English summary).

Mandelbrot B. B., 1983. The Fractal Geometry of Nature, Freeman, New York.

Migoń, P., 1996. Morphotectonic structure of the central part of the Western Sudetes in the light of densed contour map. Czasopismo Geograficzne, 67 (2), 233-244 (in Polish with English summary).

Mroczkowski, J. & Ostaficzuk, S., 1985. The Karkonosze Mts-Góry Izerskie Mts Block – geological map versus satellite image; an attempt of interpretation of fault tectonics. Geologica Sudetica, 20 (2), 121-130 (in Polish with English summary).

Turcotte D. L., 1992. Fractals and Chaos in Geology and Geophysics, University Press, Cambridge.

Teper L., 1998. Seismotectonics in the Northern Part of the Upper Silesian Coal Basin: Deep-seated Fractures-Conotrolled Pattern. Wydawnictwo Uniwersytetu Śląskiego, Katowice, 107 pp. (in Polish with English summary).

Variscan plate dynamics in the Circum-Carpathian area

Aleksandra Gawęda[1], Jan Golonka[2]

[1]*Faculty of Earth Sciences, University of Silesia, Będzińska st. 60, 41-200 Sosnowiec, Poland (aleksandra.gaweda@us.edu.pl)*
[2]*Faculty of Geology, Geophysics and Environmental Protection, AGH University of Science and Technology.; jan_golonka@yahoo.com*

The formation of European Variscides is interpreted as a result of the collision of microterranes, rifted away from the Gondwana margin and docked to Laurussia (Golonka et al., 2006). The resulting Upper Devonian – Carboniferous granitoid magmatism and metamorphism, as well as the tectonic zonation were described in detail from many Western European localities

The core mountains in the Carpatho-Balkan orogenic belt, being fragments of the Variscan continental crust, were subsequently incorporated into the Alpine units (i.e. Tatricum, Veporicum, Gemericum, Zemplinicum; Ebner et al., 2008). At present they bring a lot of information about the subduction and collision related voluminous granitoid intrusions and metamorphism, dated for the same Upper Devonian – Carboniferous period.

Three main periods of Pre-Variscan and Variscan development can be roughly defined on the basis of petrogenetic features of crystalline rocks:

1. Early Paleozoic basin development

Metamorphic rocks, forming original filling of the basin, were mostly metapelitic-metapsamitic, with intercalations of plume influenced tholeiites showing MORB-like affinity (Gawęda et al., 2000) and felsic volcanic and volcanoclastic rocks, dated for ca 500 Ma (Burda et al., 2010). These magmatic rocks were emplaced as sills and dykes into the clastic and volcanoclastic rocks, accumulated in an extensional basin, floored by the attenuated continental crust (Gawęda et al., 2000). The extension was a result of rifting of proto-Carpathian terrane from Avalonia. At ca 400 Ma the back-arc basin had been formed, marked by the ophiolitic remnants (transformed into leptyno-amphibolite complexes) and presence of OIB sequences in the Carpathian-Balkan crystalline cores (Hovorka et al., 1997).

2. Devonian – Early Carboniferous convergence

As a result of continuous subduction and possibly basaltic underplatting or slab break-off (Poller et al. 2000), hybrid Meso-Variscan granitoid magmas were formed and intruded in the interval of 370-335 Ma, conteporaneously with Variscan Nappes formation. VAG and CAG granitoid affinities suggest that melted metasediments were originally deposited both in the volcanic arc and intracontinental basins (Poller et al., 2000). Locally, the melting of accretionary prism resulted in formation of localized leucocratic melt pockets (called alaskites; Gawęda 2001), usually predating or synchronous with voluminous granitoid magmatism (Burda & Gawęda 2009). The subsequent uplift caused the exhumation of eclogitic remnants (Hovorka et al. 1997).

3. Late Carboniferous – Permian rifting

The extensional to transtensional regime and mantle lithosphere upwelling in the Late Carboniferous was followed by A-type magmatism during Permian (270-240 Ma) and associated with brittle tectonics (dominantly strike-slip lineaments and crustal-scale folds) as elsewhere in Europe (Bonin, 1990).

Bonin B., 1990. From orogenic to anorogenic setting: evolution of granitoid suites after a major orogenesis. Geol. J., 25, 261-270.

Burda J., Gawęda A., 2009. Shear-influenced partial melting in the Western Tatra metamorphic complex: Geochemistry and geochronology. Lithos, 110, 373-385.

Burda J., Gawęda A., Klötzli U. 2010 Hybridization event in the Tatra Granite, Western Carpathians, POLAND. Acta Mineralogica-Petrographica - Abstract series (IMA 2010), 6, 516.

Ebner, F., Vozarova, A., Kovacs, S., Krautner, H., Krstic, B., Szederkenyi, T., Jamicic, D., Balen, D., Belak, M., Trajanova, M., 2008. Devonian–Carboniferous pre-flysch and flysch environments in the Circum Pannonian Region. Geologica Carpathica, 59, 2,. 159-195.

Gawęda A., 2001. Alaskites of the Western Tatra Mountains: a record of Early-Variscan collision stage in the Carpathians pre-continent. University of Silesia Publishing House, Monograph series, No 1997, 142 pp.

Gawęda A., Winchester J., Kozłowski K, Narębski W., Holland., 2000. Geochemistry and peotectonic setting of amphibolites from the Western Tatra Mountains. Geol. J., 35, 69-85.

Golonka, J., Gahagan, L., Krobicki, M., Marko, F., Oszczypko, N., Ślączka, A., 2006. Plate Tectonic Evolution and Paleogeography of the Circum-Carpathian Region, in: Golonka J., Picha F. (Eds.), The Carpathians and their foreland: Geology and hydrocarbon resources. AAPG Mem., 84, 11–46.

Hovorka D., Ivan P., Méres Š., 1997. Leptyno-amphibolite complex of the Western Carpathians: its definition, extent and genetical problems. In Grecula P., Hovorka D., Putiš M (Eds.) Geological evolution of the Western Carpathians. Min. Slovaca - Monograph, 269-280

Poller, U., Janak, M., Kohut, M., Todt, W., (2000). Early Variscan magmatism in the Western Carpathians: U-Pb zircon data from granitoids and orthogneisses of the Tatra Mountains (Slovakia). Int. J. Earth Sci. 89, 336-349.

About microfacial character of selected profiles in the Western Orava part of Pieniny Klippen Belt - prelimenary results

Marína Gaži, Roman Aubrecht

Department of Geology and Paleontology, Faculty of Natural Sciences, Comenius University, Mlynská dolina G, 84 215 Bratislava (gazim@fns.uniba.sk, aubrecht@fns.uniba.sk)

The boundary between Outer Western Carpathians and Central Western Carpathians is a large scale suture zone called Pieniny Klippen Belt (PKB). Its evolution was effected by several tectonic events which resulted in contemporary complicated structure. Typical klippen appearance is caused by presence of Middle Jurassic to Lower Cretaceous limestone klippens (Oravic units) surrounded by less resistent Cretaceous to Paleogene marlstones and claystones (Non-oravic units). Klippens represent the remnants of Mesozoic sedimentary regions of PKB – Czorsztyn ridge and Pieniny basin. Performed field work was focused on the region around villages Istebné, Veličná and Revišné that are situated in the western Orava part of PKB. In the area of interest klippens are formed by rocks of Kysuca unit (deep marine strata) and Czorsztyn unit (shallow marine strata). The paleoenvironment of assigned units was locally changing in different parts of Oravic sedimentation space. This resulted in microfacial variability of strata in same successions. In the studied region attention was drown to two profiles. Analysis of profile Revišné 1 show unusual facies evolution in Kysuca unit. Common Tithonian-Neocomian Calpionella microfacies are replaced by Radiolarian microfacies without presence of Calpionella fossils. The replacement of Caplionella fossils by Radiolaria fossils may indicate a local deepining of basin (under CCD) or may be a result of a change in current flow that made the environment for Calpionella fossils unhostile. Strata of profile Revišné 2 extend from Tithonian to Aptian age, while in other localities of Czorsztyn unit age ranging to Aptian lacks. This age range was evidenced primarily by foraminifera assemblages. Profile Revišné 2 is also unique by the presence of Krasín breccia which until now was documented only in Púchov part of Pieniny Klippen Belt. Krasín breccia is a product of Jurassic synsedimentary tectonics and it was formed at the cliffs of Czorsztyn elevation. Both profiles Revišné 1 and Revišné 2 need further analysing in order to provide complete results.

The structure of the Carpathian Orogenic front near Pilzno (SE Poland) based on preliminary interpretation of 3D seismics

Andrzej Głuszyński

Institute of Geological Sciences, Wroclaw University, ul. Cybulskiego 32, 50-205 Wroclaw, Poland

The contact of the Carpathian orogen and its foreland basin is a prospective location of hydrocarbon accumulations in southern Poland and hence a rewarding object of geological and geophysical studies. Recent seismic data make it possible to elucidate many details of its structural geometry. Structural interpretation of 3D seismics acquired near to the town of Pilzno was carried out by the present author. The interpretation was completed with data from boreholes and geological maps. The interpretation was facilitated using Kingdom (™SeismicMicro) and Petrel (™Schlumberger) software packages, relying on, among others, seismic attributes.

The geological structure in the vicinities of Pilzno is tripartite. Its three components are major structural units: (1) the Miocene Carpathian foreland basin, overriden from the south by and partly deformed at the contact with (2) Cretaceous to Palaeogene flysch successions of the Outer Carpathian stack of thrust sheets and (3), Permo-Mesozoic strata underlying both (1) and (2), and representing the sedimentary cover of the post-Variscan platform.

The most intense tectonic deformation is displayed by the Outer Carpathian fold-and-thrust belt, in the northernmost part of which there is a triangle zone interpreted as such by Sieniawska & Aleksandrowski (2008) and Sieniawska et al. (2010) in the foredeep strata that became tectonically included as the Zgłobice unit in the frontal part of the orogenic wedge. Below the frontal backthrust of the triangle zone, tectonically thickened and folded Miocene evaporites occur, that attain as much as c. 700 m of the total thickness in the west, decreasing gradually down to several metres in the east. Above the frontal backthrust, folded Miocene strata were displaced toward the northeast along a lateral ramp in the west and were thrust upon a frontal ramp of E-W strike in the north. Fault-bend frontal anticlines developed over both the ramps. A SW-plunging syncline was also formed along the lateral ramp in the west. Its SE limb overlies the triangle zone's frontal backthrust and the syncline is cut by a N-vergent thrust of E-W strike in its NE part.

The Permo-Mesozoic basement of the Carpathian foredeep is dissected by SW-throwing normal faults together with accompanying subordinate lower order events. The throws on those faults reach up to several tens of metres.

The here described tectonic structures have been visualised in the form of a three-dimensional model, which is illustrative of the complex geometry of the object of study.

Sieniawska I. and P. Aleksandrowski (2008). Structural balancing of geological sections cutting across the orogenic front along regional transects 1-11., in The structure, evolution and hydrocarbon potential of the Carpathian orogenic front and its substratum between Andrychów and Pilzno", edited by P. Krzywiec, Part 8, pp. 1-86, unpublished report of research project no 03764/C.T12-6/2005, Polish Geological Institute, Warszawa [in Polish].

Sieniawska, I., P. Aleksandrowski, M. Rauch, and H. Koyi (2010), Control of synorogenic sedimentation on back and out-of-sequence thrusting: Insights from analog modeling of an orogenic front (Outer Carpathians, southern Poland), Tectonics 29, TC6012, 23 pp., doi:10.1029/2009TC002623. American Geophysical Union, Washington D.C.

Plate tectonic evolution of the Southern margin of Laurussia in the Paleozoic

Jan Golonka[1], Aleksandra Gawęda[2]

[1]*Faculty of Geology, Geophysics and Environmental Protection, AGH University of Science and Technlogy, Mickiewicza 30, 30-059, Krakow, Poland; jan_golonka@yahoo.com*
[2]*Faculty of Earth Sciences, University of Silesia, Bedzińska st. 60, 41-200 Sosnowiec, Poland (aleksandra.gaweda@us.edu.pl*

The role of an active margin of Eurasia during Mesozoic and Cenozoic times was well defined (Golonka, 2004). The trench-pulling effect of the he north dipping subduction, which developed along the new continental margin caused rifting, creating the back-arc basin as well as transfer of plates from Gondwana to Laurasia. The present authors applied this model to the southern margin of Laurussia during Paleozoic times. The supercontinent of Laurussia, defined by Ziegler (1989), included large parts of Europe and North America. It originated as a result of a closure of Iapetus Ocean and collision of Baltica, Avalonia and Laurentia.

Traditionally the continent of Avalonia included the Avalon Peninsula of eastern Newfoundland, much of Nova Scotia, southern New Brunswick, some coastal parts of New England as well as southeastern Ireland, England, Wales, the Ardennes of Belgium and northern France, terranes in northern Germany and northwestern Poland (Golonka, 2007). It was accreted into Baltica during Ordovician- Silurian times. The accretion of terranes in southern, southeastern Poland and further eastward to Baltica is quite speculative. These terranes

Fig. 1. Paleogeography of Laurussia margin in central-eastern Europe during Early Devonian. Plate position at 401 Ma. 1- Central-Sudetic ophiolite, 2 - Western Carpathian ophiolite, 3 - Balkan-South Carpathian ophiolite.

include Brunovistulicum, Inner Carpathian block, the Małopolska High with the southern Holy-Cross Mountains, Carpathian terranes, parts of Moesian and Balkan terranes, Scythian platform in southernmost Ukraine, Northertn Turkey (Pontides), Dzurilla Massif of Caucasus and part of Turan platform (Golonka et al., 2009, Kalvoda and Babek, 2009). It might be possible, that some of these terranes were accreted to Baltica together with the Avalonian blocks. The accretion was followed by the development of north dipping

subduction, along the new continental margin of Laurussia. That subduction caused rifting and creating the new back-arc basin. That basin was first recognized in central Europe as Rheno-Hercynian zone (Ziegler, 1989, Golonka, 2007 and references therein). The eastern extension of the Rheno-Hercynian Basin is marked by ophiolites in Sudety area in Poland and in the Carpahian-Balkan area. The Balkan-South Carpathian ophiolite belt yield the isotopic age of 406-399 Ma (Zakariadze et al, 2007), comparable with the Central-Sudetic ophiolites age being around 400 Ma (Kryza, Pin, 2010). The Western Carpathians ophiolite remnants revealing ages from 503 to 450 Ma, contemporaneous with felsic magmatism (Putiš et al., 2009) probably represent the oldest opening stage of the basin.

The Laurussian margin subduction is well marked in the Carpathian area by the granitoid magmatism and metamorphism of the host rocks (Burda and Gawęda, 2009). This subduction was followed by collision of microterranes with this margin, and finally by the involvement of Gondwana promontory (Golonka, 2007) After the collision of Gondwana with Laurussia during the Varican orogeny Laurussia became part of the supercontinent of Pangea (Golonka, 2007).

Burda J., Gawęda A., 2009. Shear-influenced partial melting in the Western Tatra metamorphic complex: Geochemistry and geochronology. Lithos, 110, 373-385.

Golonka, J., 2004. Plate tectonic evolution of the southern margin of Eurasia in the Mesozoic and Cenozoic, Tectonophysics, 381, 235-273.

Golonka J. 2007. Phanerozoic Paleoenvironment and Paleolithofacies Maps. Late Paleozoic. Kwartalnik AGH. Geologia, 33(2), 145-209.

Golonka, J., Krobicki, M., Poprawa, P., Paul, Z. & Khudoley, A. 2009. Early Paleozoik Evolution of the peri-Gondwana plates. Kwartalnik AGH. Geologia. 33(2/1), 339-344.

Kalvoda, J. & Bábek, O., 2010. The Margins of Laurussia in Central and Southeast Europe and Southwest Asia. Gondwana Research, 17 (2-3), 526-545.

Kryza, R. & Pin, C., 2010. The Central-Sudetic ophiolites (SW Poland): Petrogenetic issues, geochronology and palaeotectonic implications. Gondwana Research, 17 (2-3), 292-305.

Putiš M., Ivan P., Kohút M., Spišak J., Siman P., Radvanec M., Uher P., Sergeev S., Larionov A., Mères S., Demko R., Ondrejka M., 2009. Meta-igneous rocks of the West-Carpathians basement: indicators of Early Paleozoic extension and shortening events. Bull.Soc. Geol. France, 180, (6), 461-471.

Zakariadze, G. S.; Karamata, S. O.; Dilek, Y.; 2007. Significance of E. Paleozoic Paleo-Tethyan Ophiolites in the Balkan Terrane and the Greater Caucasus for the Cadomian-Hercynian Continental Growth of Southern Europe . American Geophysical Union, Fall Meeting 2007, abstract #V43B-1367

Ziegler P.A., 1989. Evolution of Laurussia. Kluwer Academic Publishers, Dordrecht, Netherlands.

Geology of the Žďárské vrchy area: a review

Pavel Hanžl[1], Rostislav Melichar[2], David Buriánek[1], Zuzana Krejčí[1], Lenka Kociánová[1]

[1]*Czech Geological Survey, Klárov 3, 118 21 Prague, Czech Republic (pavel.hanzl@geology.cz)*
[2]*Department of Geological Sciences, Masaryk University, Kotlářká 2, 611 27 Brno, Czech Republic*

The eleven geological map sheets on the 1 : 25,000 scale from the Protected Landscape Area Žďárské vrchy have been prepared within the mapping campaign in years 2002–2007. Geological maps of the Žďárské vrchy area are available in online shop (http://obchod.geology.cz/) of the Czech Geological Survey. Structural, petrological, geochemical and geochronological data were summarized in paper of Pertoldová et al. (2010) and in Special Issue of Journal of Geosciences (Volume 54/2009/2) devoted to Geological development of the region at the NE periphery of the Moldanubian Zone, eastern part of the Bohemian Massif.

The area covers geological units along the NE margin of the Moldanubian Zone of the Bohemian Massif east of the Přibyslav mylonite zone. The Strážek unit (part of the Moldanubian zone), Svratka and Polička units can be distinguished here from the SW to the NE. These units are separated by the Hlinsko unit from the Kutná Hora unit and Železné hory pluton in the NW.

The Strážek unit is structurally lowermost unit of the area composed of variegated high grade rocks corresponding with the Gföhl unit of the Moldanubian Zone and intruded by small irregular Variscan intrusions of durbachites. Variably oriented, relatively flat foliations were reoriented close to contact of the Strážek and Svratka units to directions parallel with this terrane boundary.

The Svratka unit lying in the hanging wall of the Strážek part of the Moldanubicum is characteristic by a lithological sequence, which can be correlated with the Orlice-Sněžník unit of the Lugian domain. Dominating red leucocratic migmatites with layers of micaschists and boudins of skarns were intruded by coarse-grained granites of the Cambrian age. Boundary with underlying Moldanubicum is indistinct in a field; nevertheless it is marked by a belt composed of retrogressed migmatites with boudins and lenses of amphibolites, serpentinites, eclogites and granulites. The belt of SE–NW strike is dipping to the NE and folded in the NW termination. This trend corresponds with dominating SE–NW oriented foliation folded by large brachyanticline in the NW. Dominating subhorizontal lineations parallel with contact of units indicate strike-slip reworking of the boundary between the Strážek and Svratka units.

The Polička unit in the hanging wall of the Svratka unit is composed of a various kind of metaigneous (amphibolites, metagranites) and metasedimentary rocks (gneisses, mica schist, marbles) in three subunits. Metasediments are intruded by numerous syntectonic plutonic bodies of Variscan age among them tonalites are more distinctive. The contact with the underlying Svratka unit is marked by a narrow discontinuous belt of amphibolites and was reworked by younger, steep NNW–SSE striking normal faults in the NE. Metagranites and augen gneisses interpreted as equivalents of the Polička unit trace an anticline structure of the Svratka unit in a narrow belt between villages of Borová, Krouna, Vortová and Cikháj. Similar rock was recognized in tectonic slice even inside Moldanubian migmatites near Stržanov village.

The Hlinsko unit is exposed in the N–S oriented fault through which broadens and rotates towards NE. Southern part consists of the Neoproterozoic–Lower Palaeozoic slightly metamorphosed flysh-like sediments with intercalations of metabasalts, metagabbros and various kinds of metarhyolites (Vítanov Fm.). The volcanic rocks absent in northern part of the Hlinsko unit; monotonous slightly metamorphosed Lower Palaeozoic flysh sediments (Hlinsko-Rychmburk Fm.) dominate here. Paleontological evidence on Silurian exists only in black shales with lydite horizon (Mrákotín Fm.). Contact with the Svratka and Polička units in the footwall is modified by outstanding normal fault, nevertheless some exposures near Borová and Perálec villages indicate lithological relationships between Polička and Hlinsko units.

Plutonic complex of Železné Hory is composed of two parts. The southern one, Železné Hory pluton, is of pre-Variscan age and formed by various types of deformed granodiorites and gabbros. Contact with Hlinsko zone is tectonic. The northern part, Nasavrky pluton is Variscan, primary intrusive contact with the Lower Palaeozoic sediments of the Hlinsko zone is partly modified by faults. Oval body of the Ransko massif with basic and ultrabasic rocks is bounded to the contact of the Kutná Hora unit and Moldanubicum on the S termination of the Hlinsko unit. Its geological position is still ambiguous.

Sediments of the Bohemian Cretaceous Basin cover Variscan consolidated basement of the area from the NE and dominate in a tectonically subsided narrow belt of the Dlouhá mez structure.

Pertoldová J, Verner K, Vrána S, Buriánek D, Štědrá V, Vondrovic L (2010): Comparison of lithology and tectonometamorphic evolution of units at the northern margin of the Moldanubian Zone: implications for geodynamic evolution in the northeastern part of the Bohemian Massif. J Geosci 55: 299–319.

Sense of movements analysis: shear zones from micro-structures in granitic mylonites (Bratislava Massif)

Michal Hoffman

Department of Geology and Palaeontology, Faculty of Natural Sciences, Comenius University, Mlynska dolina pav. G, SK 84215, Bratislava, The Slovak Republic, (hoffman.geology@gmail.com).

One of the most characteristic properties of mylonites (Lapworth, 1885) and some other rocks from ductile shear zone is the fabric elements and structures show monoclinic shape symetry. Thos effect is a result of the non-coaxial deformation in shear zones due to relative displacement of the wall rocks.

In the Southern part of the Malé Karpaty Mts. (Bratislava massif) were researched shears zones in granitic rocks. From this shears zones we take samples of rocks. Rocks were classificated as cataclasites – mylonites. Basically inner micro-structures were established sense of movement shears zones that transpierce across Bratislava granitoids body.

For the establish sense of movement in the study shear zones were used δ, σ structures, mica-fish structures, (Scholz, 2002), (Sibson, 1977), (Schmid and Handy, 1991) S-C (Berthé et al., 1979) and S-C` (Dennis and Secor 1987) structures .

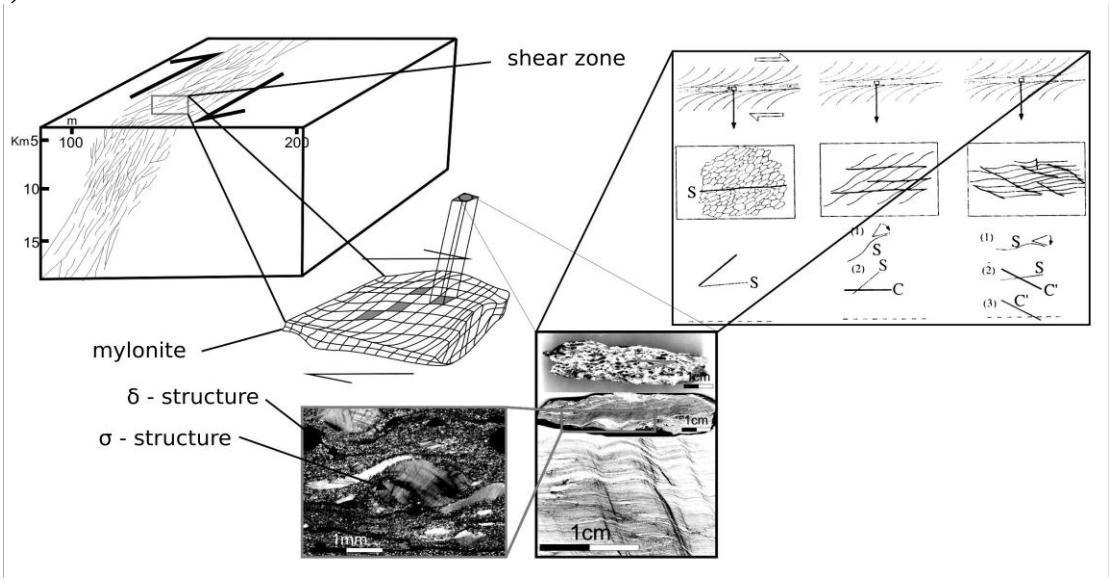

Fig. 1.: Diagram of metodic of analysis non-homogenous deformation in shear zone.

Mylonites are compose from muskovite, sericite, quartz, biotite and phengite. In this rocks is possible to observe S-C and S-C` structure with records of dynamic recrystallization, flattnenig and stretching of quartz porphyroclasts and transformation of feldspar and muscovite to dynamo-metamorphic phengite. These structural and material changes within the ductile shear zone were realized during the Alpine thrusting of Bratislava nappe to the west in pressure cca 400-600 MPa and temperature 300-350^{o} C. As youngest dynamic event, the normal brittle faulting was observed along this shear zone. It occured after exhumation, very probably in the Miocene. The last paleostress brittle-fault related event represents NNE-SSW tension, which is responsible for creation of the Upper Miocene Lamač gate depression along NW-SE normal faults. These are the youngest faults in the structural plan of the southern rim of Bratislava massif, even suspected form neotectonic activity (Hoffman et al., 2008 in Németh Z., & Plašienka D., 2008). (This work was supported by the Slovak Research and Development Agency under the contract No. APVV-0158-06 and APVV-0279-07.)

Berthé, D., P. Choukroune and P, 1979: Jegouzo, Orthogneiss, mylonite and non-coaxial deformation of granites: the example of the South Armoricain shear zone, Journal of Structural Geology.

Dennis, A.J., Secor, D.T., 1987: A model for the development of crenulations in shear zones with application from the Souther Appalachian Piedmont, Journal of Structural Geology 9: 809-817.

Hoffman M., Sulák M., Marko F., 2008: Faults and brittle-ductil shear zones in the southern rim of the Bratislava granitoid massif (Malé Karpaty Mts.) In: Németh Z., & Plašienka D., (Eds.), 2008: 6th Meeting of the Central Europe Tectonic Studies Group (CETeG), State Geological Institute of Dionyz Stur, Bratislava, 236p.

Lapworth, C. 1885: The Highland Controversy in British Geology: its causes, course and consequences. Nature, 32.

Scholz, Ch., H., 2002: Earthquakes and faulting,Second edition, Cabridge University Press, 460p.

Sibson, R.H. 1977: Fault rocks and fault mechanisms. Journal of the Geological Society (London) 133p.

Schmid, S. & M. Handy, 1991: Towards a genetic classification of fault rocks: Geological usage and tectonophysical implications. In: D. Müller, J. McKenzie and H. Weissert, Editors, Controversies in Modern Geology, Academic Press, London, pp. 339–361.

Reconstructing Pleistocene river terrace formation in the Budejovice Basin (Czech Republic) using field and borehole data in combination with OSL-dating

Dana Homolová[1], Johanna Lomax[2], Kurt Decker[1]

[1]*Department of Geodynamics and Sedimentology, Geocenter, University of Vienna, Althanstrasse 14, A-1090 Vienna, Austria (dana.homolova@univie.ac.at; kurt.decker@univie.ac.at)*
[2]*Institute of Applied Geology, University of Natural Ressources and Life Sciences (BOKU), Peter-Jordan-Strasse 70, A-1190 Vienna, Austria (johanna.lomax@boku.ac.at)*

Fluvial sediments of the rivers Vltava and Malse, accumulated during the whole Pleistocene and probably further in the past, occur in the Budějovice Basin as terrace bodies of different lateral and vertical extent. The Budějovice Basin, situated in Southern Bohemia, is a fault-bounded sedimentary basin overlying Variscan crystalline basement of the Bohemian Massif. The sedimentary basin fill mostly consists of Cretaceous (Klikov Formation) and Miocene sediments (Zliv and Mydlovary Formation) covered with Quaternary fluvial and colluvial deposits.

Mapping and dating of fluvial terraces in this area focuses on the establishment of a late Pleistocene chronology of terrace formation for a major European river having its source in a non-glaciated region. According to the scheme used in most European regions, influenced by the Pleistocene glacial cycles, these terrace staircases were previously assigned to the 4 or 5 main Alpine glacial periods by most scientists. Due to the fact that the catchments of the rivers were not glaciated during the Pleistocene, this correlation is not straightforward as terraces are not connected to moraine bodies like in the Alps. Additional stratigraphical errors may arise from the previous approach to correlate fluvial terraces along the streams solely using the elevation of the terraces above the receiving waters. Such correlations do not account for possible Pleistocene tectonics and vertical movements on faults crossed by the rivers. Since there is no data concerning the numerical age of the Quaternary sediment cover in the research area so far, OSL-dating is the key method in building a late Pleistocene stratigraphy of the basin sediment fill. Such correlations may be used to prove or disprove Pleistocene vertical movements of the boundary faults of the Budějovice Basin.

Current research particularly focuses on the fluvial terraces in the hangingwall and the footwall of the Hluboká fault. The fault forms the NW boundary of the Budějovice basin delimiting the Cretaceous to Miocene sediments of the basin fill from Variscan crystalline basement rocks to the NE. Currently available data is derived from more than 60 outcrops, hand drillings and 21 shallow boreholes. Stratigraphic correlations rely on more than 20 OSL ages. Additionally, archive data from more than 1000 drilling reports from the Czech Geological Survey (Geofond) in combination with a high-resolution DEM was used to create a 3D-model of the terrace bodies in the basin. It gives an overview of the horizontal and vertical extension of fluvial terrace bodies in the research area and represents an essential tool for terrace correlations and the assessment of the youngest slip history of the Hluboká fault.

Results from field mapping in the vicinity of Hluboká nad Vltavou show 5 terrace levels in the crystalline basement northeast of the Hluboká fault (Fig. 1) and at least 4 levels within the Budějovice Basin (Fig. 2). For the lower terraces, it was possible to create a consistent stratigraphy with ages ranging from about 80 ka to the Holocene, whereas the uppermost terrace levels are out of the dating range of the method. Data about the lateral and vertical extent of fluvial terrace bodies obtained from the 3D-model coincide with morphological data from field mapping, also showing up to five terrace levels in the research area.

Further mapping and dating, as well as sedimentological analyses are planned to create an inventory of terrace bodies in this area and to correlate their formation with tectonic and climatic evolution in this region.

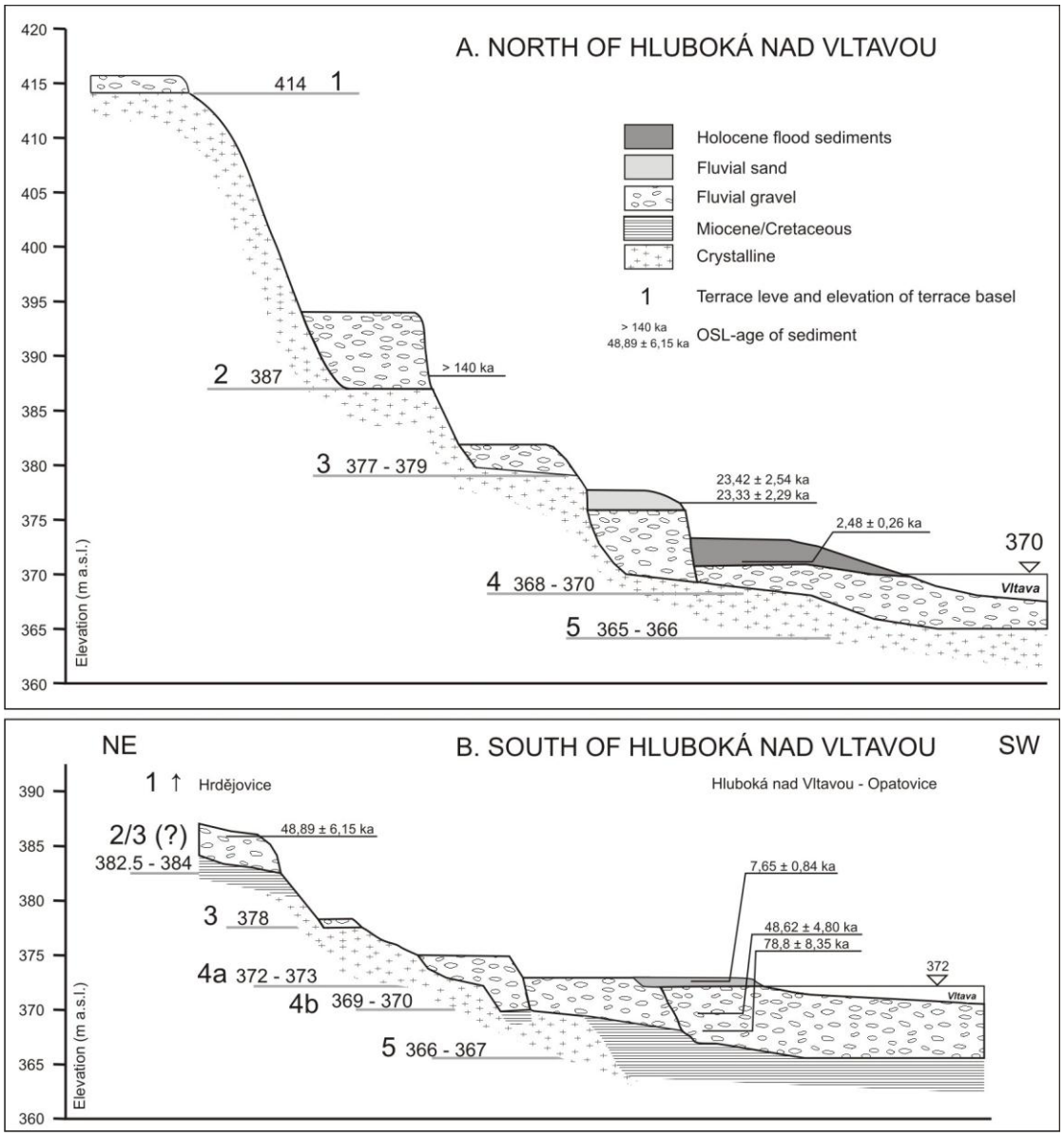

Fig. 1. Schematic sections across the Vltava river illustrating the Pleistocene terrace bodies overlying the footwall of the Hluboká Fault (A, North of Hluboká nad Vltavou) and the hangingwall South of the fault (B, South of Hluboká). Sections highlight elevations of the terrace base and OSL ages derived from the terrace sediments..

The granitic massifs of the Zamtyn Nuruu area, SW Mongolia

Kristýna Hrdličková[1], Pavel Hanžl[1], David Buriánek[1], Axel Gerdes[2]

[1]*Czech Geological Survey, Klárov 3, 118 21 Prague 1, Czech Republic (kristyna.hrdlickova@geology.cz)*
[2]*Institut für Geowissenschaften, J. W. Goethe Universität, Altenhöferallee 1 60438 Frankfurt am Main; Germany*

The Zamtyn Nuruu range as a part of the Gobi Altay Mountains is situated in the SW Mongolia, approximately 740 km SW of Ulaanbaatar. Area lies right along the large tectonic structure of the Ikh Bogd fault, which separates here two different lithotectonic units: the Cadomian–Caledonian Lake Zone in the north and the Variscan Gobi Altay Terrane in the south. The area is intruded by an amount of various plutons. Three massifs of different ages and geotectonic position are described to illustrate the evolution of the area in the time span between the Lower Palaeozoic and the Permian. The Cambrian Burd Gol Massif is situated along Burd Gol river. The Permian Shar Oroy Massif is exposed in the Khar Argalantyn Mountains SE of the Boon Tsagaan lake. These two massifs pertain to the Lake Zone Terrane. The Lower Carboniferous Chandman Massif lying south of the Chandman village represents intrusive body of the northernmost part of the Gobi Altay Terrane.

Burd Gol Massif intruded the crystalline complex of the Zamtyn Nuruu and the Cambrian continental sediments in footwall of it. The southern boundary of massif is limited by the Ikh Bogd fault. The massif is lithologically homogenous, composed of fine to medium-grained, leucocratic to biotite granite locally with muscovite. Septa of metamorphic rocks and thermally metamorphosed sandstones are exposed in the northern part of massif.

The geochemical character of the granites is calc-alkaline, peraluminous, with potassium content corresponding to high-K series. Trace elements signatures indicate volcanic-arc environment of granite evolution. Radiometric dating revealed the Upper Cambrian age. The laser ablation ICP-MS U–Th–Pb radiometric dating of monazites and zircons from these rocks yields intrusive ages between 506.4 ± 5.4 and 513.4 ± 4.3 Ma. The Ar–Ar dating of muscovite from a pegmatite dyke at 485.1 ± 3.2 Ma, documents the final stage of magmatic activity. Structural trends in volcano-sedimentary complexes in the exocontacts of the Burd Gol Massif were reoriented to asymmetric tails due to movements on the younger strike-slip faults.

Shar Oroy Massif is exposed in a few individual bodies intruding the upper Early to the lowermost Late Permian volcano-sedimentary complexes. The geological and geochemical relations between volcanic and plutonic rocks point to co-genetic evolution of these rocks. The felsic and mafic suites were distinguished in the Shar Oroy Massif. Biotite granites to amphibol-biotite syenites are predominant rock types of the felsic suite. Rocks of mafic suite form small enclaves in felsic rocks and small bodies up to several hundred meters in diameter. Gabbros and diorites of the mafic suite are medium- to coarse-grained and composed of plagioclase, amphibole, and/or clinopyroxene, which are partly replaced by actinolite. Olivine, and biotite are rare and often partially replaced by the secondary minerals.

Syenite and gabbro to diorite are sub-alkaline to alkaline, metaluminous. Granites yields peraluminous alkaline character. Trace elements signatures indicate within plate character of all above mentioned rocks. The U/Pb zircon age of 285 ± 1.3 Ma corresponds with Lower Permian age of the intrusion.

Chandman Massif intruded the HT metamorphic rocks of the Chandman Khayrkhan complex in the north and slightly metamorphosed volcano-sedimentary complex of supposed Cambrian age in the south. The Quaternary sediments cover an eastern termination of the Chandman Massif.

The Chandman Massif can be subdivided into the two separate parts. Porphyritic, biotite granodiorite with anatectic textures forms the southern part, whereas biotite to biotite-amphibole granodiorites and tonalites are exposed in the northern part. The internal deformational fabrics evidence the syntectonic intrusion of the massif. The youngest magmatic member represented by granites is present in both parts of the pluton. Anatectic granite pertains to calc-alkaline high-K series and is peraluminous. Granodiorites and tonalites have medium to low-K abundances and metaluminous character. Both groups show the volcanic-arc granite character. The U-Th-Pb ICP-MS dating of the Chandman granite yields the age of 345 ± 2 Ma (Lower Carboniferous), which is interpreted as the time of granite crystallization.

The different ages and geotectonic enviroments of the studied granite massifs quite well illustrate the geological evolution along the contact between the Lake Zone and Gobi Altay Terranes in the Zamtyn Nuruu area. The intrusion of the eldest Burd Gol Massif closed final stage of southward oriented accretions of geological domains between microcontinents of the Baydrag and Zamtyn Nuruu blocks during the Cambrian.

The character of the Lower Carboniferous Chandman Massif reflects evolution in a collision stage of the Variscan orogeny within the volcanic arc environment.

The intrusion of the Shar Oroy Massif is coeval with extensive terrestrial volcanic activity in the lower Permian related to the evolution of the Gobi Altay rift.

Inhomogeneous changes in magnetic fabric during retrogressive metamorphism of eclogites in the Mariánské Lázně Complex (West Bohemia, Czech Republic)

František Hrouda[1,2], Shah Wali Faryad[2], Marta Chlupáčová[1]

[1]*AGICO Inc., Ječná 29a, Brno, Czech Republic (fhrouda@agico.cz)*
[2]*Institute of Petrology and Structural Geology, Charles University, Albertov 6, Praha, Czech Republic*

The Mariánské-Lázně Complex (MLC) is a Cambro-Ordovician terrane with metabasites of oceanic crust affinity and it is tectonically emplaced between the Saxothuringian Zone and the Teplá-Barrandian Unit. The MLC is formed by amphibolites (retrogressed after eclogites), eclogites, serpentinized peridotites and coronitic metagabbros. Available geochronological data give Ordovician age for magmatic crystallization and Variscan ages for the eclogite facies metamorphism and subsequent amphibolite facies reequilibrium (Bowes et al., 1991; Timmermann et al., 2004; Zulauf, 1997).

The eclogites are restricted to the central part of the complex, where they occur as boudins and lenticular masses up to 3.5 km long within rutile-garnet amphibolite. They preserve garnet, omphacite and rutile, but mostly they are retrogressed, where first form symplectites of diopside + amphibole with plagioclase and then coarse-grained amphibole overgrowing the symplectites. Rutile is replaced by ilmenite and partly rimmed by titanite. Both eclogites and amphibolites show foliation, which is defined by amphibole, locally by biotite, quartz and zoisite. Metagabbros still preserve igneous pyroxene and amphibole with tabular plagioclase, which is replaced by albite. Among metamorphic minerals they contain amphibole, biotite, albite and locally garnet and kyanite. Peridotite contained medium-grained olivine, idioblastic amphibole, and spinel (now chlorite) prior to serpentinization. Olivine is replaced by serpentine and magnetite.

Metamorphic fabrics of mafic and ultramafic rocks of the MLC were investigated by means of the anisotropy of magnetic susceptibility (AMS), which indicates the preferred orientation of magnetic minerals in a rock. The most voluminous rock type of the MLC, amphibolite, is characterized by large scatters in the spatial orientations of both magnetic foliation poles and magnetic lineations. The magnetic foliations are only exceptionally parallel to the mesoscopic metamorphic schistosity. The degree of AMS, indicating the intensity of the preferred orientation of magnetic minerals, is also relatively variable, ranging from very low values (near magnetic isotropy) to relatively high values indicating considerable preferred orientation. The magnetic fabric shape ranges from strongly prolate to very strongly oblate, being mostly oblate. In peridotite, both the magnetic foliations and magnetic lineations are moderately to strongly steep, the degree of AMS being moderate and the magnetic fabric shape being variable. In eclogite, the magnetic foliations are flat or inclined moderately, while the magnetic lineations are flat. The degree of AMS is variable as well as the fabric shape. In gabbro, both the magnetic foliations and magnetic lineations are scattered largely, the degree of AMS being moderate and the fabric shape ranging from moderately prolate to moderately oblate.

Results of petrological investigations show that the amphibolites originated through retrogression of eclogites. Their AMS indicates that this process was rather inhomogeneous from the fabric point of view, giving rise to large scatters both in magnetic foliation and magnetic lineation. The overprint of the original eclogite fabric by the secondary amphibolite facies fabric was only imperfect resulting in relatively large angles between the magnetic foliation and mesoscopic metamorphic schistosity. The intensity of the modification of the original fabric in peridotite and eclogite by the retrogression in amphibolite facies conditions is difficult to estimate because of the large scatters of magnetic foliations and lineations in amphibolites.

Nature and tectonic setting of Jurassic felsic igneous activity in the Victory Glacier area (Graham Land, Antarctic Peninsula)

Vojtěch Janoušek[1,2], Axel Gerdes[3], Jiří Žák[1,4], Igor Soejono[1], Zdeněk Venera[1], Ondrej Lexa[1,2]

[1]*Czech Geological Survey, Klárov 3, 118 21 Prague 1, Czech Republic (vojtech.janousek@geology.cz)*
[2]*Institute of Petrology and Structural Geology, Charles University, Albertov 6, 128 43 Prague 2, Czech Republic*
[3]*Institut für Geowissenschaften, Abt. Geochemie & Petrologie, Altenhöferallee 1, D-60438 Frankfurt, Germany*
[4]*Institute of Geology and Paleontology, Charles University, Albertov 6, 128 43 Prague 2, Czech Republic*

The Victory Glacier at the eastern coast of Graham Land (Antarctic Peninsula) separates two large outcrops of the Permian to Middle Triassic quartzose metasandstones, metagreywackes, and metapelites of the Trinity Peninsula Group intruded by large volumes of Jurassic felsic igneous rocks. At the more easterly Pitt Point, the rhyolite dykes define a large-scale chocolate-tablet structure, implying biaxial principal extension in the ~WNW–ESE and ~N–S directions. Along the northeastern slope of Mount Reece, further to the W, the ~NNE–SSW set dominates suggesting local variations in the direction and amount of extension. Most of the Mt. Reece nunatak is built by coarse grained biotite granites, though.

The geochemical signatures of granites and rhyolites are practically mutually indistinguishable. These siliceous rocks (SiO_2 > 73.8 wt. %) are high-K calc-alkaline, subaluminous to slightly peraluminous in nature. The NMORB-normalized spiderplots are characterized by strong LILE enrichment (Cs, Rb, Ba, Th, U and Pb) and conspicuous depletion in Nb, Ta and Ti, typical of magmas generated at active continental margins or having originated by an anatexis of mature continental crust. A range of geotectonic diagrams points to arc-related genesis as well. A characteristic feature is a fair degree of LREE/HREE enrichment (LaN/YbN = 2.7–7.0); the chondrite-normalized contents of individual HREE exceed 10 (LuN = 11.2–15.6) and the patterns feature deep negative Eu anomalies (Eu/Eu* = 0.45–0.24). Altogether, the whole-rock geochemical signatures are those of highly differentiated melts derived exclusively by low-P (residue lacking Grt), low-T (monazite and zircon saturation T ~ 770 °C) anatexis of mature crustal sources (metapsammites or orthogneisses), most likely within the attenuated crust.

The LA-ICP-MS zircon dating of rhyolite dykes yielded concordant U–Pb ages of 174.2 ± 0.6 Ma (2σ), 175.2 ± 0.7 Ma (Mt. Reece) and 178.6 ± 0.7 Ma (Pitt Point). The granitic magmatism at Mt. Reece was constrained between 184.9 ± 0.7 Ma (lighter Bt granite) and 165.7 ± 0.9 Ma (darker, restite-rich granite, containing abundant ~181 Ma inheritance). The voluminous felsic igneous activity in the studied part of the Graham Land was clearly rather short-lived; the granite pulses both pre- and postdated the felsic dykes.

New geochemical and geochronological results confirm the notion that the Early–Middle Jurassic (Toarcian–Aalenian) felsic magmatism in Graham Land can be correlated with (nearly) contemporaneous, petrologically and geochemically analogous rocks in Patagonia, forming together a single silicic large igneous province (Pankhurst et al. 2000). It is widely accepted that this magmatic flare-up records the incipient lithospheric extension that continued in the opening of the Weddell Sea (e.g., Riley et al. 2001, 2010). This reflects most likely massive crustal anatexis in a back-arc position relative to the Antarctic Peninsula arc (Riley et al. 2001).

The biaxial extensional stress regime required for emplacement of the highly fractionated dykes could have developed (1) locally, i.e. above a large, subsurface granitic pluton, whose existence at depth may be in line with the presence of large-scale negative gravity anomaly in the region (Jordan et al. 2009) and obtained zircon age spectra from the two granite phases dated, or, on a more global scale (2) above the upwelling mantle plume taken by many authors as a trigger of the Gondwana break-up. Such a mantle plume upwelling resulted in analogous Mid-Jurassic biaxial extension in South Africa and the Dronning Maud Land, northern Antarctica.

Jordan T.A., Ferraccioli F., Jones P.C., Smellie J.L., Ghidella M. and Corr H. 2009. Airborne gravity reveals interior of Antarctic volcano. Phys Earth Planet Int., 175, 127–136.

Pankhurst R.J., Riley T.R., Fanning C.M. and Kelley S.P. 2000. Episodic silicic volcanism in Patagonia and the Antarctic Peninsula: chronology of magmatism associated with the break-up of Gondwana. J. Petrol., 41, 605–625.

Riley T.R., Leat P.T., Pankhurst R.J. and Harris C. 2001. Origins of large volume rhyolitic volcanism in the Antarctic Peninsula and Patagonia by crustal melting. J. Petrol., 42, 1043–1065.

Riley T.R., Flowerdew M.J., Hunter M.A. and Whitehouse M.J. 2010. Middle Jurassic rhyolite volcanism of eastern Graham Land, Antarctic Peninsula: age correlations and stratigraphic relationships. Geol. Mag., 147, 581–595.

P-T-d-t record of metasedimentary rocks in the Staré Město belt, NE Bohemian Massif: insights into polyphase evolution of the Variscan suture zone

Mirosław Jastrzębski[1], Jarosław Majka[2] Mentor Murtezi[1], Andrzej Żelaźniewicz[1], Ilya Paderin[3]

[1]*Institute of Geological Sciences, Polish Academy of Sciences, Wrocław, Poland*
[2]*Uppsala University, Department of Earth Sciences, Uppsala, Sweden*
[3]*Centre of Isotopic Research, All-Russian Geological Research Institute, St Petersburg, Russia*

The Staré Město Belt (SMB) is located at the northern continuation of the Moldanubain Thrust. This c. 55 km long, NNE-SSW–trending narrow tectonic zone separates the tectonically upper Orlica-Śnieżnik Dome in the west from the tectonically lower Moravosilesian domain in the east. The SMB forms an east-verging thrust stack consisting of three NNE-trending narrow lithotectonic units. Two marginal units are dominated by metasedimentary rocks whereas the middle unit comprises elongated body of the MORB amphibolites. Scaterred inlayers of migmatites and mica schists and an elongated body of the Carboniferous granitoids occur within the amphibolites (e.g. Štípská et al. 2004). All units contain dispersed small-scale leucocratic patches and veins.

The conducted integrated research (structural studies, MnNCKFMASH pseudosection and isopleth thermobarometry, U-Th-Pb monazite and U-Pb zircon geochronology) of the metasedimentary rocks from the SMB reveals that its present-day tectonic architecture results from the polyphase Variscan evolution including the Late Devonian collision between Saxothuringian/Moldanubian terrane and Brunovistulia terrane, and their subsequent Early Carboniferous mutual displacements along the WNW-dipping suture zone.

During the WNW-ESE directed collision (in the present day co-ordinates), the structurally highest unit ("Hranična series") experienced two cycles of tectonic burial separated by a short-term episode of uplift. The foremost recognized thickening stage was related to burial to depths corresponding to c. 10 kbar at c. 490 °C and the subsequent decompression to c. 6.5 kbar associated with slight temperature increase to c. 520 °C. Continuation of the ESE-directed thrusting resulted in another deepening of the upper unit and burial of the middle and lower units to depths corresponding to c. 7.5 kbar at c. 650 °C. The following, main stage of uplift could be related to continuous indentation and underthrusting of the Brunovistulia (e.g. Skrzypek et al. 2011) or gravitational instability of the thickened orogen (e.g. Murtezi, 2006, Jastrzębski 2009). Subsequently, the metasedimentary rocks of the SMB underwent dextral (top-to-the-NNE) shearing, locally associated with the nearly isobaric heating to c. 680 °C at depths corresponding to 5.5-6.0 kbar possibly related to the emplacement of the granitoid body. The metapelites of the middle unit underwent high grade metamorphism which concurs with granulite facies conditions obtained for the surrounding amphibolites (Parry et al. 1997; Lexa et al. 2005). The boundaries between the lithotectonic units of the belt are considered to be originally thrust faults which were later reactivated during subhorizontal dextral shearing.

Monazite in the upper unit yielded three distinct ages of 368±6Ma, 355±5Ma and 342±7Ma. The oldest age was obtained on the low-Y metamorphic rim of composite monazite grain exhibiting detrital core and two metamorphic overgrowths. Low Y content in the internal rim suggests that this zone was presumably growing in presence of stable garnet. External rim of this composite grain yielded an age of c. 340 Ma and that particular zone seems to be dating D3 dextral shearing (since the zone itself is a kinematic indicator). The c. 340 Ma age was also obtained on several other grains. Monazite of this age occurs both as inclusions in garnet and in the matrix. Notably, one of the c. 340Ma grains co-existing with xenotime, yielded minimum crystallization temperature of c. 625°C based on Y-saturation thermometer of Pyle et al. (2001). Importantly, one grain from the upper unit yielded an age of 355±5Ma. This grain forms an elongated prism enclosed in garnet and is characterized by relatively low-Y content. Generally, there is no correlation between age and microtextural context of monazite in regard to garnet. This might be simply an effect of fluid flow connected with re-heating events. It is quite possible, since all of the dated monazites enclosed in garnet are connected via cracks with the matrix. Monazite in the middle unit (both, matrix- and garnet-located) yielded only uniform age of 336±4Ma. It cannot be excluded however that some older monazites have also preserved in the rock.

Local in-situ partial melting of metamorphic rocks and development of associated melt patches and veins could be either coeval with the termination of the eastward thrusting or emplacement of the granitoid sill coeval with the dextral shearing. SHRIMP zircon dating of a leucocratic patch developed at the boundary between upper and middle unit yielded zircon crystallization age of 356±2Ma.

In conclusion, the studies on P-T-d-t record of the Staré Město Belt reveal multistage tectonic evolution of this zone. The sequence of Variscan events may be described as follows: D1- the continent-continent collision and related eastward thrusting that led to tectonic burial and regional metamorphism presumably ending with

the Famenian/Tournasian partial melting of the metamorphic rocks, D2 – uplift during Tournasian/Visean (Jastrzębski, 2009) and D3 – Visean subhorizontal dextral (top-to-the-NNE) strike-slip movements.

Jastrzębski M. 2009. A Variscan continental collision of the West Sudetes and the Brunovistulian terrane: a contribution from structural and metamorphic record of the Stronie Formation, the Orlica-Śnieżnik Dome, SW Poland. International Journal of Earth Sciences 98, 1901¬–1923.

Lexa O., Štípská P., Schulmann K., Baratoux L. and Kröner A., 2005. Contrasting textural record of two distinct metamorphic events of similar P-T conditions and different durations. Journal of Metamorphic Geology 23, 649–666.

Murtezi M., 2006. The acid metavolcanic rocks of the Orlica–Śnieżnik Dome: their origin and tectono-metamorphic evolution. Geologia Sudetica 38, 1–38.

Parry M., Štípská P., Schulmann K., Hrouda F., Ježek J. and Kröner, A., 1997. Tonalite sill emplacement at an oblique boundary: northeastern margin of the Bohemian Massif. Tectonophysics 280, 61–81.

Pyle J. M., Spear F. S., Rudnick R. L. and McDonough W. F. 2001. Monazite-xenotime-garnet equilibrium in metapelites and a new monazite-garnet thermometer. Journal of Petrology, 42, 2083–2107.

Štípská P., Schulmann K. and Kröner A., 2004. Vertical extrusion and middle crust spreading of omphacite granulite: a model of syn-corvengent exhumation (Bohemian Massif, Czech Republic). Journal of Metamorphic Geology 22, 179-198.

Skrzypek E., Štípská, P. Schulmann, K. Lexa O and Lexova M., 2011, Prograde and retrograde metamorphic fabrics – a key for understanding burial and exhumation in orogen (Bohemian Massif). Journal of Metamorphic Geology, in press.

Volcano-sedimentary series from the Sudetes Mts.: discordant geochronological record from two sides of the Nýznerov thrust

Mirosław Jastrzębski[1], Mentor Murtezi[1], Izabella Nowak[1], Alexander N. Larionov[2], Nickolay V. Rodionov[2]

[1]*Institute of Geological Sciences, Polish Academy of Sciences, Wrocław, Poland*
[2]*Centre of Isotopic Research, All-Russian Geological Research Institute, St Petersburg, Russia*

One of the characteristic feature of the northern continuation of the Moldanubian trust is that it divides orthogneisses predominantly Neoproterozic in age (Brunovistulia terrane) from Early Palaeozoic ones of the Saxothuringian/Moldanubian terrane (e.g. Kröner et al 2000, Oberc et al. 2003; Klimas et al 2009; Mazur et al 2010). In the Sudetes Mts., the Variscan suture zone is defined by thrust fault sheets of mainly supracrustal successions bounded by few WNW-dipping, regional-scale tectonic boundaries (Don et al. 2003). The Bialskie thrust divides gneisses of Orlica-Śnieżnik Dome from metavolcano-sedimentary succession (so-called "Hranična series") that directly overlain the NNW-trending, elongated body of Cambro-Ordovician MORB-like amphibolites. The East Nýznerov thrust, traditionally considered to be the most important tectonic boundary in this zone (e.g. Schulmann and Gayer, 2000), divides the lowermost unit Staré Město Belt from metavolcano-sedimentary rocks of the Velké Vrbno Dome. The Ramzová thrust separates the Velké Vrbno Dome from Branna Unit and Keprnik Dome.

We examined the protolith ages of metavolcano-sedimentary successions of the uppermost unit of the Staré Město Belt and the Velké Vrbno Dome to reveal affinity of the "Hranična series" and determine the significance of the Bialskie, Nýznerov and Ramzová thrusts in the regional lithotectonic architecture.

The U-Pb SHRIMP zircon dating of the felsic metavolcanitic rock in the upper unit of the Staré Město Belt provides the age of 493±4 Ma (based on 17 analytical points) which is interpreted as the age of crystallization of felsic lavas within the sedimentary succession. Inherited age of 575±18 Ma (5 analytical points) indicates that the felsic magma originated from melting of a continental crust that had been consolidated by the Cadomian-age plutons. The zircons retrieved from the studied sample commonly have thick metamorphic rims with characteristic high U content (1100-8400 ppm). Microprobe dating of the rims (6 analytical points) gave U-Pb ages ranging from 365 to 314 Ma, that could be referred to the high temperature event related to the Variscan regional metamorphism (see Jastrzebski et al. – this volume). These results well correlate with zircon age record from volcano-sedimentary Stronie formation of the Orlica-Śnieżnik Dome to the east of the Bialskie thrust (e.g. Murtezi and Fanning 2005, Jastrzębski et al. 2010).

For the metavolcanic rocks of the Velké Vrbno Dome, analytical points were located in zircons both retrieved from felsic and mafic member of bimodal metavolcanic suite forming interlayers in mica shists. In contrast to the ages from the Staré Město Belt the felsic metavolcanic rocks and the mafic metavolcanites of the Velké Vrbno Dome yield older SHRIMP zircon ages of 558±Ma and 557±4 Ma respectively. These ages are interpreted as the age of crystallization of lavas within the sedimentary succession. Inter-fingering contacts of metavolcanic rocks and metasedimentary rocks (Don et al. 2003) and the observed sequence with thin interlayers of the metavolcanic rocks and mica schists of the Velké Vrbno Dome strongly suggest the continuous character of the volcano-sedimentary series. Similar to the felsic metavolcanic rock sample of the Staré Město Belt, few analyzed zircons from its equivalent from the Velké Vrbno Dome gave ages ranging from 367 to 315 Ma.

New SHRIMP data stay in accordance with the earlier Pb-Pb dating performed for metavolcanic rocks of both studied units (Kröner et al. 2000). This study reveals connection of the "Hranična series" to the Orlica-Śnieżnik Dome and the Velké Vrbno Dome to the western Brunovistulia. It stresses the importance of the East Nýznerov thrust as a frontier separating not only gneisses but also the enveloping supracrustal volcano-sedimentary rock successions of dissimilar ages of formation.

Don J., Skácel J. and Gotowała R., 2003. The boundary zone of the East and West Sudetes on the 1:50 000 scale geological map of the Velké Vrbno, Staré Město and Śnieżnik Metamorphic Units. Geologia Sudetica, 35, 25–59.

Jastrzębski M., Żelaźniewicz A., Nowak I., Murtezi M. and Larionov A. N., 2010. Protolith age and provenance of metasedimentary rocks in Variscan allochthon units: U–Pb SHRIMP zircon data from the Orlica–Śnieżnik Dome, West Sudetes, Geological Magazine, 147, 416–433.

Klimas, K., Kryza R. and Fanning C. M., 2009. Palaeo- to Mesoproterozoic inheritance and Ediacaran anatexis recorded in gneisses at the NE margin of the Bohemian Massif: SHRIMP zircon data from the Nowolesie gneiss, Fore-Sudetic Block (SW Poland). Geologia Sudetica, 41, 25–42.

Kröner A., Štípská P., Schulmann K. and Jaeckel P., 2000. Chronological constraints on the pre-Variscan evolution of the northeastern margin of the Bohemian Massif, Czech Republic. In: W. Franke, V. Haak, O. Oncken & D. Tanner (Eds.) Orogenic processes: Quantification and Modelling in the Variscan Belt,. Geological Society of London, Special Publication no. 179, 175–197.

Mazur S., Kröner A., Szczepański J., Turniak K., Hanzl P., Melichar R., Rodionov N. V., Paderin I and Serggev S. A., 2010. Single zircon U–Pb ages and geochemistry of granitoid gneisses from SW Poland: evidence for an Avalonian affinity of the Brunian microcontinent. Geological Magazine, 147, 508–526.

Murtezi M. and Fanning M., 2005. Petrogenesis, Age and Tectono-Metamorphic Evolution of the Acid Metavolcanites of the Stronie Formation (Orlica-Śnieżnik Dome, Sudetes, SW Poland). Geolines, 19, 85.

Oberc-Dziedzic T., Klimas K., Kryza R. & Fanning C. M. 2003., SHRIMP zircon geochronology of the Strzelin gneiss, SW Poland: evidence for a Neoproterozoic thermal event in the Fore-Sudetic Block, Central European Variscides. International Journal of Earth Sciences, 92, 701–711.

Schulmann K. and Gayer R., 2000. A model of an obliquely developed continental accretionary wedge: NE Bohemian Massif. Journal of Geological Society London, 156, 401–416.

Solid phase inclusions in garnets from felsic granulite, eclogite and peridotite from the Kutná Hora Complex (Moldanubian zone, the Bohemian Massif)

Radim Jedlička, Shah Wali Faryad, Helena Klápová

Institute of Petrology and Structural Geology, Charles University, Prague, Czech Republic (radim.jedi@gmail.com)

High-temperature eclogite and garnet peridotite boudins and lenses are common within felsic granulites and granulite gneisses in the Bohemian Massif. Ultra high-pressure conditions for some of these rocks were demonstrated by mineral inclusions (coesite and microdiamonds) and by conventional geothermobarometries. Similar lithologies are present in the Kutná Hora complex, which is correlated with the Gföhl unit in the eastern part of the Moldanubian zone (Synek and Oliveriová, 1993). Thin sections and mineral separates of felsic granulite, eclogite and garnet peridotite from the Kutná Hora complex were investigated. As all these rocks underwent granulite facies reequilibrium and subsequent cooling, most inclusions are transformed into secondary phases (Faryad, 2009). In addition to olivine, orthopyroxene and clinopyroxene, garnet from garnet peridotites usually contains accessory chromium spinel with up to 40 wt % Cr_2O_3. The host garnet around inclusions shows Cr-rich domains as results from Cr diffusion from spinel to garnet. Rare ilmenite inclusions with high MgO content (up to 27 % geikelite end-member) with small amounts of spinel were also observed in garnet. Ilmenite of similar composition is present in clinopyroxene which is partly enclosed by garnet. Pentlandite with composition $Ni_{4.8}Fe_{5.2}S_8$ was also observed as inclusion in garnet. Similar inclusions were reported in pyrope garnet from Kolín area by Vrána (2008). When compare composition of pyroxene in the inclusions and with that in the matrix, the the latter have lower Al and higher Na in the ortophyroxene and clinopyroxene, respectively.

Two varieties of eclogites are present in the granulite. The first variety forms small bodies within garnet peridotites, which may additionally contain layers of clinopyroxenites and garnetites. Garnet from eclogite contains inclusions of omphacite, apatite and rutile. In addition to relatively large grains, oriented lamellae of rutile are also present in garnet. Apatite is common in garnetite and it is characterized by the presence of monazite exsolution lamellae oriented parallel to c-axes of apatite crystals. The second variety of eclogite occurs within felsic granulite and does not associate with garnet peridotite. It contains prograde zoning garnet grains with inclusions of omphacite, kyanite, quartz and rutile.

Inclusions of Ti-rich phengite were found in garnet from several samples of felsic granulites. It is mostly replaced by Ti-rich biotite with quartz and other Al-, Si- rich phases. Radial cracks around some inclusions with unidentified composition (SiO_2 = 48 and Al_2O_3 = 34 wt %) and low K_2O, FeO and MgO contents suggest replacement of former dense mineral(s). In one case a polyphase inclusion of pargasitic hornblende with plagioclase was found. The mass balance indicated for taramite amphibole or omphacite with quartz and small amounts of phengite.

The presence of spinel inclusions and the decrease of Al content in orthopyroxene, associated with olivine, as well as the increase of jadeite content in clinopyroxene from garnet peridotite in the Kutná Hora complex suggest an increase of pressure and decrease of temperature during metamorphic history of these mantle lithologies. In addition to eclogite with prograde zoning garnet, a prograde PT path for the host granulite is assumed by the presence of phengite inclusions in garnet.

Faryad, S.W. (2009). The Kutná Hora Complex (Moldanubian Zone, Bohemian Massif): A composite of crustal and mantle rocks subducted to HP/UHP conditions. Lithos 109, 193–208.

Faryad, S.W., Nahodilová, R., Dolejš, D. (2010). Incipient eclogite facies metamorphism in the Moldanubian granulites revealed by mineral inclusions in garnet. Lithos 114, 54–69.

Synek, J., Oliveriová, D. (1993). Terrane character of the northeast margin of the Moldanubian Zone—the Kutná Hora crystalline complex, Bohemian Massif. Geologische Rundschau 82, 566–582.

Vrána, S. (2008). Mineral inclusions in pyrope from garnet peridotites, Kolín area, central Czech Republic. Journal of Geosciences, 53, 17–30.

Transition from fracturing to viscous flow at lower crustal conditions - evidence for a strong lower continental crust

Petr Jeřábek[1], Holger Stünitz[2], Pritam Nasipuri[2], Florian Fusseis[3], Erling J. Krogh Ravna[2]

[1]*Institute of Petrology and Structural Geology, Faculty of Science, Charles University, Czech Republic (jerabek1@natur.cuni.cz)*
[2]*Institutt for Geologi, Universitetet i Tromsø, Norway*
[3]*School of Earth & Environment, University of Western Australia, Australia*

The Hasvik gabbro of the Seiland Igneous Province in northern Norway represents a piece of lower continental crust. The gabbro contains the primary magmatic assemblage of plagioclase (X_{An}=0.53), clinopyroxene (X_{Mg}=0.85), orthopyroxene (X_{Mg}=0.65) and minor amount of biotite and rutile. In the gabbro, narrow shear zones with an extremely sharp strain gradient are developed. The gabbros and the shear zones lack any signs of low-temperature overprint or weathering.

The immediate vicinity of highly localized, 1 to several cm wide shear zones is fractured with typical synthetic, antithetic Riedels, and P-geometries. These fractures cross-cut all magmatic phases with minor offsets and are filled with small (<10 microns) fragments of magmatic as well as small (~10 microns) grains of newly formed metamorphic phases. The newly formed minerals are amphibole, clinopyroxene II, orthopyroxene II, plagioclase II and accessory biotite II, quartz, ilmenite. Among, the newly formed mineral phases, the composition of amphibole varies significantly (X_{Mg} = 0.84 core – 0.78 rim, X_{Ca} = 0.94 core – 0.85 rim). The appearance of amphibole demonstrates hydration of the gabbro by aqueous fluids via the fracture network. Phase equilibrium modelling using PERPLEX (hp04ver.dat, solut_08.dat) of this assemblage* (cAmph(DP), Opx(HP), Cpx(HP), Pl(h)) confirmed lower crustal PT conditions of 800-850 °C at 0.400 to 0.500 GPa for the nucleation of metamorphic amphibole. However, the conventional geo-thermobarometry yeilds 100-150 °C lower temperature at 0.400-0.600 GPa pressure. The cracks are cut by the localized shear zones which are sub-parallel to P-fractures. Typically, the viscous shear zones are formed by through-going bands of fine grained aggregates of newly formed metamorphic phases. Numerous relics of magmatic grains are also present as porphyroclasts within the bands. The minerals in the cracks and the viscous shear zones have the same composition. The bands are up to 200 microns thick. Some are monomineralic, but most of them are formed by a phase mixture that is usually dominated by one of the phases. Electron back-scattered diffraction analysis of all minerals present within the fractures and the shear zones shows a random, host-grain unrelated CPO for plagioclase and ortopyroxene, and host-grain-controlled nucleation of amphibole and clinopyroxene II in the vicinity of magmatic clinopyroxene porphyroclasts. With increasing distance from the host-grain, this primary CPO changes to a random one for clinopyroxene and a weak CPO for amphibole. The amphibole CPO with [001] axes distributed along single girdle parallel to the shear zone boundaries is best explained by oriented growth. The results of our EMPA and EBSD analyses suggest that the displacement within the shear zones is accommodated by viscous flow during diffusion creep at lower crustal conditions.

Synchrotron x-ray tomography shows a considerably higher porosity in the cracks filled with clinopyroxene and plagioclase and in phase mixtures compared to amphibole-filled parts of the rock and monophase mineral aggregates. This observation suggests a greater dynamic permeability in cracks and mixed phase aggregates. The deformation of the gabbro commenced by fracturing, thereby facilitating fluid infiltration due to an increased permeability and subsequent switch in deformation mechanism to diffusion creep. The switch in deformation mechanisms is caused by the fine grain size of the newly nucleated phases. In these aggregates, permeability appears to remain high, even though porosity is most likely not generated by fracturing any longer. The initial fracturing requires very high stresses, indicating a high strength of the lower crust. The subsequent hydration weakens the crust in localized shear zones. Thus, lower crustal strength may vary considerably, depending on fluid content, fluid infiltration, and deformation history.

* Mineral nomenclature is according to PERPLEX solut_08.dat

Relationship between fracture network geometry and diverse alteration processes of the Mórágy granite, SW Hungary

Rita Kamera, Tivadar M. Tóth

University of Szeged, Department of Mineralogy, Geochemistry and Petrology, H-6701, Szeged P. O. Box 651, kamera@geo.u-szeged.hu, mtoth@geo.u-szeged.hu

It is of basic importance to get reliable information of fracture networks of the different geological formations, in order to understand fractured hydrocarbon reservoirs, to optimize radioactive waste depository or even to exploit geothermal energy. Depending on the degree of deformation, a fracture network can be divided into a central slip zone and a damage zone (Fig. 1/a), which play different roles in the fluid migration. Moreover, along fractures the fluid flow may have different influence on the host rock by its special chemical and physical features. There are two basic types of the fluid migration concerning fluid-rock interactions. In case of positive feedback systems solution and alteration of the host rock is typical, which can help fluid flow, while in negative feedback systems fractures get cemented blocking migration.

The low- and intermediate-level radioactive waste depository is under construction in the Variscan Mórágy Granite Complex (MGC) in SW Hungary. This is an intensely fractured hard rock body cut up by numerous intensely deformed zones forming typical central slip zones. Because of safety reasons it is essential to know well the fracture network geometry and its long-range behaviour. One aim of the study was to calculate a standardized algorithm for determining the geometric parameters (length: *E*; fractal dimension: *D*) of the fracture network, which can further be used for the 3D fracture network modelling. Besides this simulation the connectivity of individual fractures was estimated using the percolation threshold (*P*) concept, which depends on the above geometric data. A further goal of the study was to estimate degree of element mobilization processes in a both a central zone and the damage zone around it. Mobilization processes may cause significant mass-, and volume changes in the host rock.

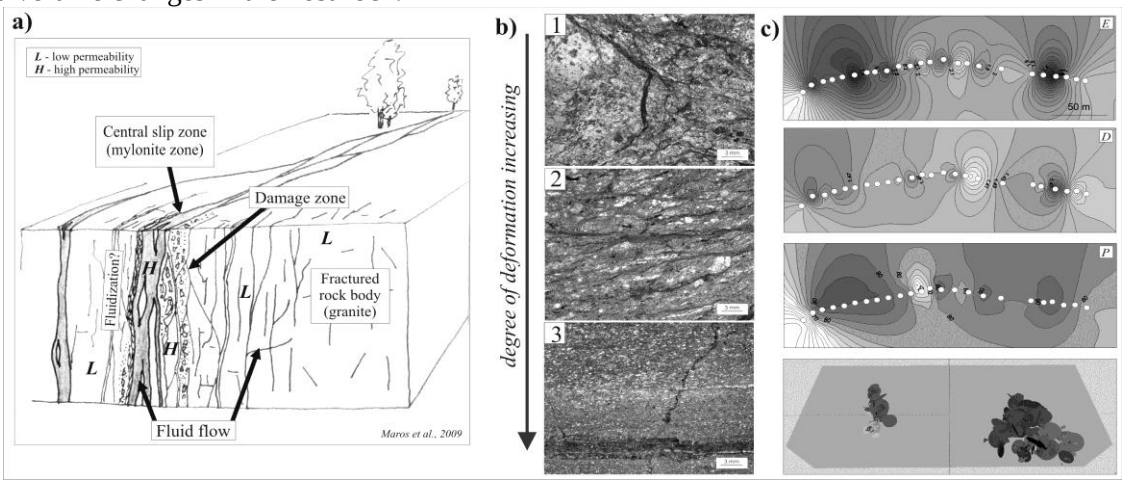

Fig. 1. a) Shematic sketch about the structure of a fracture network b) Decrease of amount of feldspar and of grain size during the shearing c) Distribution of E, D and P values and the 3D fracture network model, where the fracture network is highly heterogeneous with two intesely communicated zones (central zone)

The first part of our research was to measure and calculate essential geometric parameters of the fracture system both along 20 wells (M. Tóth, 2004) and in numerous headings of the repository site itself. Digital images of fracture patterns of over 30 headings were processed using image analysis approaches to get fracture length distribution (*E*), follows power low distribution N(L) = F*L-E (e.g..: Min et al., 2004). Secondly, using a box-counting algorithm the fractal dimension (*D*) was calculated from the fracture midpoint distribution. Finally, from the determined *E, D, α* values the 3D fracture network model was set up based on the REPSIM code (M. Tóth, 2010). We used fracture orientation data sets (dip, strike – *α, β*) of previous structural geological studies.

In the second part of the study the role of element mobilization processes along a shear zone was estimated. The degree of deformation had different influence on more mafic and felsic zones (Fig. 1/b), so they were interpreted separately. The isocon method (Gresens, 1967; Grant 1986) was used for the explanation of the element mobilization processes.

Results of the fracture network modelling suggest that around 90% of the fractures in the studied part of the repository site communicate with each other giving a connected network. The maps of the *E* and *D* values

outline two central, highly deformed zones, where the fluid migration processes could probably be the most intensive (Fig 1/c). This is supported by the element mobilization processes in the shear zone studied. Owing to the intensive shear strain towards the core of the shear zone the amount of feldspar decreases significantly and its components (K, Al, Si) were removed by the fluid flow (Fig. 1/b). However, the amount of Ca increases a little bit due to the secondary carbonatization in the more mafic portions of the host rock. To summarize the observations, the core zones serve as a positive feedback system concerning fluid-rock interaction, where the migrating fluid caused ~55% mass- and ~45% volume depletion in the felsic zones, whereas ~10% mass gain and ~20% volume depletion can be estimated in the mafic zones.

Grant J. A. 1986. The Isocon-diagram – a simple solution of Gresen's equation for metasomatic alteration. – Economic Geology 81, 1976-1982.

Gresens R. L. 1967. Composition.volume relationships of metasomatism. – Chemical Geology 2, 47-65.

M. Tóth T. 2004. Adatbázis repedéshálózat fraktál geometriai alapú szimulációjához a Bátaapáti kutatási területenmélyült mélyfúrások alapján. Manuscript, , RHK Kht., 13-85.

M. Tóth T. 2010. Determination of geometric parameters of fracture networks using 1D dating. Journal of Structural Geology 32/7, 878-885.

Maros Gy., Koroknai B., Palotás K., Dudko A., Balogh K., Pécskay Z. 2009: Törészónák a Mórágyi Gránitban: Szerkezeti és K/Ar adatok. In: Magmás és metamorf képződmények a Tiszai Egységben, Geolitera, Szeged, 43-62.

Min K. B., Jing L., Stephansson O. 2004. Determining the equivalent permeability tensor for fractured rock masses using a stochastic REV approach: Method and application to the field data from Sellafield, UK. Hydrogeology Journal, 12/5, 497-510.

Stratigraphy fault-cut diagrams and stratigraphic separation diagrams methods

Martin Knížek[1,2], Rostislav Melichar[2]

[1]*ARCADIS Geotechnika a.s., Geologická 988/4, 152 00 Praha 5, Czech Republic (kniza@mail.muni.cz)*
[2]*Department of Geological Sciences, Faculty of Science, Masaryk University Brno, Kotlářská 2, 611 37 Brno, Czech Republic (melda@sci.muni.cz)*

This analysis of a fault in a sedimentary complex is a based on the study of geometric components of displacement and fault surface geometry in relation to the bedding. The fault cut-off geometry in deeper levels can be precisely presented in 3D models. These diagrams plot the depths of the hanging wall and footwall cut-off lines for specific stratigraphic markers against distance along the fault. These same results, however, may be simply obtained by using stratigraphy fault-cut diagrams (SFDs) and stratigraphic separation diagrams (SSDs). These diagrams can be quatitatively constructed by using only surface data and require data for the spatial positions of fault and stratigraphic-marker surface, i.e. the exact location of cut-off lines.

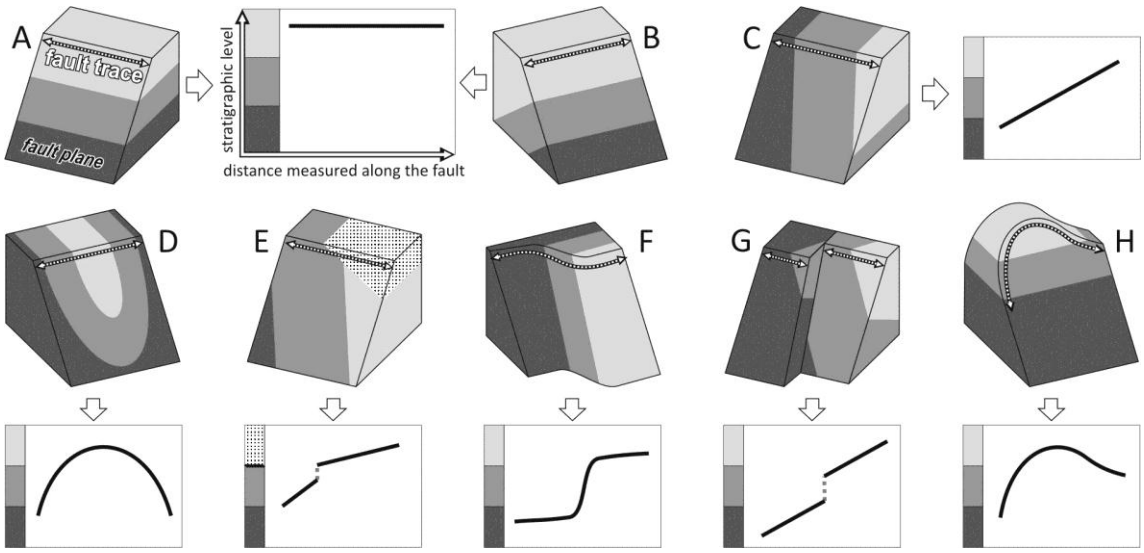

Fig. 1: *Different patterns of fault surface geometries in relation to bedding and stratigraphy fault-cut diagrams:* ***A*** *– fault crosscutting horizontal bedding;* ***B*** *- strike fault crosscutting inclined bedding;* ***C*** *– oblique fault crosscutting inclined bedding;* ***D*** *– fault crosscutting older fold structure;* ***E*** *– fault crosscutting unconformity;* ***F*** *– fault with flat-ramp-flat geometry;* ***G*** *–fault cut by transversal fault;* ***H*** *- fault trace respects rugged relief*

Fault surface geometries in relation to bedding can be sketched in stratigraphy fault-cut diagrams (SFD). This type of diagram plots the stratigraphic level of one fault wall against length of any fault trace which is usually a map trace (Fig. 1). Such fault-cut lines in SFD represent two points of information: the stratigraphic amplitude of the fault wall and fault surface/bedding geometry. Rubey (1973) used SFD for stratigraphic analysis to show the stratigraphic amplitude of a hanging wall of the fault that was researched. SFD is also powerful for a fault analysis as the inclination of the fault-cut line in SFDs is proportional to dip of the bedding surface and also to the angle between fault and bedding dip directions. The fault-cut line in a SFD is horizontal if the fault trace is parallel to the cut-off line (Fig. 1a, b). Inclined fault-cut line indicates other geometrical cases (Fig. 1c). Older folds produce curved patterns in SFD as the bedding is facing to opposite sides in different fold limbs (Fig 1d). It is significant that synclines are represented by convex arches (upward) and anticlines by concave arches (downward). Unconformities are marked by disconnected fault cut lines (Fig 1e) and faults with flat-ramp-flat geometry led to a similar geometry in SFDs but with continuous steps (Fig 1f). Typical steps in the diagram coincide with ramps, while long horizontal portions mark the locations of the flats. Recognition of various ramp types has been discussed by Wilkerson et al. (2002). Only if the fault is bedding-parallel (e.g. flat) the fault-cut line is horizontal and continuous for very long distance in the SFD. This is very important evidence for the determination of flats and possible flat-and-ramp fault geometry.

SSD combines information presented in SFD and stratigraphic separation and makes possible to understand fault surface geometry and tectonic transport along fault in one plot. SSD plots the stratigraphic level of both fault walls against the distance along some fault trace. In such a way, the two lines in the diagram represent the stratigraphic levels of two fault walls. There are two possibilities for their relative position: 1) if the line representing the stratigraphic level of the hanging wall is situated above the footwall line, there is a clear

stratigraphic gap in the SSD; 2) vice versa, if the footwall line is above the hanging wall, there is stratigraphic duplication along the fault.

After SSD construction, we can interpret the fault kinematics. Constant value of stratigraphic separation in some direction between fault walls is typical for transport-parallel SSDs or for translatory block faults (Fig. 2). Constant stratigraphic and strike separations at the same time are typical for slip faults that cut the monoclinal bedding which make straight fault-cut lines in the SSD (Fig. 2a) and the fault kinematics are unknown in trace slip component. If the fault-cut lines are more complex (curved or with steps), the kinematics might be determined more easily. Dip-slip faults have constant stratigraphic separations while strike separation might be variable (Fig. 2b) and analogously strike-slip faults produce stable values of strike separation with possible variations in stratigraphic separation (Fig. 2c). Variable stratigraphic and strike separations are typical for oblique-slip faults (Fig. 2d). Completely different patterns in SSDs are produced by flat-ramp-flat faults. The ramps appear in distinct stratigraphic positions on one or on both fault wall lines as well as flats (décollements) which are situated in other stratigraphic levels (Fig. 2e). There are no constant separations in SSDs and fault-cut lines of hanging wall and footwall are usually different (Fig. 2f).

Stratigraphic separation diagrams demonstrate their applicability and effectiveness as tools for the tectonic analysis of faults. Detailed stratigraphy and good geological maps are important requirements for the use of SSDs, but when these are available, this method is economical, simple and effective.

Rubey W.W., 1973. New Cretaceous Formations in the Western Wyoming Thrust Belt. Geological Survey Bulletin, 1372-I, 1–35.
Wilkerson M.S., Apotria T. and Farid T., 2002. Interpreting the geologic map expression of contractional fault-related fold terminations: lateral/oblique ramps versus displacement gradients. Journal of Structural Geology, 24, 593–607.

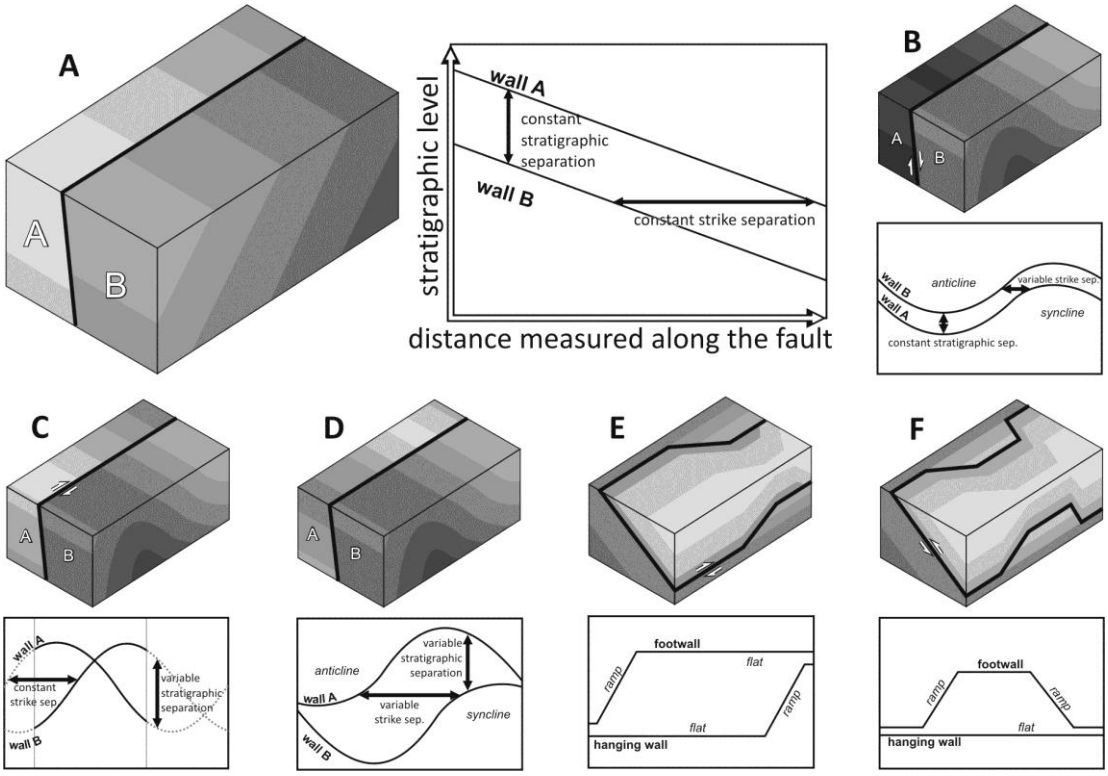

Fig. 2: Different patterns in stratigraphic separation diagrams: A – fault crosscut monoclinal bedding; B – true dip-slip fault crosscutting older fold structure; C – true strike-slip fault crosscutting older fold structure; D – oblique-slip fault crosscutting older fold structure; E – thrust fault with flat-ramp-flat geometry (transport-parallel SSD); F – thrust fault with flat-ramp-flat geometry (longitudinal SSD).

The Rochovce granite – witness of the Alpine tectonic processes in the Western Carpathians

Milan Kohút[1], Martin Danišík[2], Pavel Uher[3]

[1]*Dionyz Štúr State Institute of Geology, Mlynská dolina 1, 817 04 Bratislava, Slovakia (milan.kohut@geology.sk)*
[2]*The University of Waikato, Hamilton, New Zealand (m.danisik@waikato.ac.nz)*
[3]*Department of Mineralogy and Petrology, Comenius University, Mlynská dolina G, 842 15 Bratislava, Slovakia (puher@fns.uniba.sk)*

The Rochovce granite is a subsurface intrusion in the south-eastern part of the Veporic Unit near the contact with overlying Gemeric Unit in the Central Western Carpathians (CWC). The hidden granite body was discovered in the end of seventies by the drill-hole KV-3, situated in the centre of a magnetic anomaly. As revealed by this drill-hole, granitic rocks intruded mostly into the metapelitic to psammitic micaschists and phyllites of the so-called Slatviná Formation, whereby direct contact form a 100 m layer of metagabbro. Subsequent drilling exploration revealed that this granite intruded also into the quartz-sericite schists of the Ochtiná Formation (Gemeric Unit) in the SE part, and into the Permian psammitic to psephitic rocks of the Rimava Formation in the S part. The Alpine contact metamorphism is bound exclusively to these Carboniferous and Permian metasedimentary rocks. The Rochovce magmatic body was formed by two intrusive phases. *The first phase* comprises two petrographic varieties: (*i*) coarse-grained biotite monzogranites with the pink K-feldspars phenocrysts, locally with mafic microgranular enclaves (central part of the body); and (*ii*) granite porphyries (marginal part). *The second phase*, forming mainly S to SE part of the magmatic body, is more evolved type represented by medium- to fine-grained biotite leucogranites and leucogranitic porphyries. Narrow veins of leucogranite randomly penetrate coarse-grained granites of the first phase. Since the first appearance of the granite samples from drill-core KV-3, they attracted researchers not only for fresh pinkish colour, but mainly for its undeformed character that is rather unusual for the Western Carpathians granites. The Rochovce granite varieties have normal to elevated SiO_2 values (66 ~ 77 wt. %), a typical calc-alkaline, subaluminous to peraluminous character (Shand's index – A/CNK = 0.9 ~ 1.4), high concentrations of Ba, Rb, Li, Cs, Mo, Nb, Y, V, W, Cr, F, Th, U and low concentrations of Sr, Zr and Be. The low to moderate initial Sr isotope ratios (I_{Sr} = 0.7083 ~ 0.7126), together with negative $\varepsilon_{Nd(i)}$ = -3.0 ~ -2.1, zircon $\varepsilon Hf_{(80)}$ = -5.2 ~ 0.2 and depleted stable isotopes values ($\delta^{18}O_{(VSMOW)}$ = 8.0 ~ 8.3‰; $\delta^{34}S_{(CDT)}$ = -2.1‰; $\delta^{7}Li$ = 4.7‰) indicate a lower crustal meta-igneous protolith. Although the first K/Ar cooling ages on biotites 88 ~ 75 Ma indicated the Cretaceous (Alpine) age, some researchers preferred the Permian age of emplacement established by means of Rb/Sr (WR) isochron (253 ± 2 Ma). The Cretaceous magmatic age for the Rochovce granite was first proven correct by U-Pb zircon dating using conventional multi-grain TIMS method (82 ± 1 Ma), and later by cathodoluminescence controlled single grain method and SHRIMP yielding the ages of 75.6 ± 1.1 Ma 81 Ma, respectively. The Late Cretaceous age was recently confirmed by Re-Os molybdenite dating from granite-porphyry and host rock – stockwork mineralization with age 80 Ma.

The Rochovce granite was intruded to relative shallow level. The ultimate depth of the granite emplacement estimated on the basis of contact metamorphism is 200 ~ 100 MPa. However, besides of contact metamorphism there is known regional metamorphism in the SE Veporic territory related to the development of a metamorphic core complex during Cretaceous orogenic events. The Late Cretaceous exhumation of these metamorphic terrains is interpreted in terms of post-collisional, orogen-parallel extension and unroofing along low-angle detachment faults. The following scenario for the generation and emplacement of the Rochovce granite was inferred: during the Late Jurassic – Early Cretaceous, continental collision and crustal stacking followed the closure of the Meliata ocean. Crustal thickening together with some heat input from the mantle triggered partial melting and generation of granite in the lower crust. During the mid-Cretaceous period, shortening and crustal stacking continued and propagated outwards in the CWC. Shortening in the rear of the Veporic wedge triggered its exhumation and orogen–parallel extension. During the final stages of exhumation, the Rochovce granite was emplaced into the extensional shear zones. The sources of Rochovce granitic melts can be seen in the lower crustal meta-igneous root, not exposed at the surface. Noteworthy, that the Rochovce granite records a thermal event in the Middle to early Late Miocene, which was likely related to mantle upwelling, volcanic activity, and increased heat flow. During the thermal maximum between ~17 and 8 Ma, the granite was heated to temperatures ≥ 60 °C. Increase of cooling rates at ~12 Ma recorded by the apatite fission track and (U-Th)/He data is primarily related to the cessation of the heating event and relaxation of the isotherms associated with the termination of the Neogene volcanic activity. (Acknowledgment: This work was supported by the Slovak Research and Development Agency under the contract No. APVV-0549-07, and APVV-0557-06.)

The influence of intracrystalline diffusion and partial resorption of garnet on the reproducibility of metamorphic pressure-temperature paths

Jiří Konopásek[1,2], Mark J. Caddick[3]

[1]*Department of Earth Science and the Centre for Geobiology, University of Bergen, Allegaten 41, N-5007 Bergen, Norway (jiri.konopasek@geo.uib.no)*
[2]*Czech Geological Survey, Klarov 3, 118 21 Praha 1, Czech Republic (jiri.konopasek@geology.cz)*
[3]*Institute for Geochemistry and Petrology, ETH Zurich, Clausiusstrasse 25, 8092 Zurich, Switzerland (mark.caddick@erdw.ethz.ch)*

With the advance of thermodynamic modeling techniques, the chemical zoning preserved in garnet crystals is now commonly used for reconstruction of pressure-temperature histories of metamorphic rocks. However, pristine growth zoning is rarely preserved in its original form because of variably extensive subsequent modification by intracrystalline diffusion. Moreover, partial resorption of garnet typically accompanies decompression and removes outer parts of the established growth zoning profile, irreversibly losing evidence for parts of the pressure-temperature history.

In this contribution, we present growth and intra-crystalline diffusional relaxation models for garnet crystals produced along several pressure-temperature (P-T) paths that involve prograde heating and burial along various geothermal gradients, followed by decompression. Our modeling tests two end-member behaviors for metamorphic rocks. In the first case, the calculated amount of garnet follows equilibrium thermodynamic constraints, changing crystal volume accordingly during both growth and decomposition. In the second mode, disequilibrium is imposed by preventing dissolution of the garnet modeled crystal, but still allowing chemical exchange between its rim and the rock matrix. The resultant chemical zoning profiles through model garnet crystals are then inverted to estimate the pressure-temperature path that they would imply if they were preserved as natural samples.

The results can be summarized as follows:

1) In the studied example of a pelitic system composition, the prograde part of the P-T path involves garnet growth, whereas decompression is usually associated with its resorption (unless the decompression path is accompanied by substantial additional heating). As a consequence, the peak pressure of the prograde path is typically recorded by compositions at or near the outermost garnet rim. This suggests that for many combinations of rock composition and P-T path, any partial garnet resorption during decompression can seriously obscure estimates of the peak temperature and pressure conditions.

2) For all but the fastest modeled metamorphic histories, the chemical record of equilibrium conditions occurring during the onset and early stages of garnet crystallization is removed by diffusive re-equilibration well before peak conditions are reached. Apparent pressure-temperature paths inferred from preserved profiles will therefore almost always begin at higher temperatures than actually experienced.

3) For cases in which we suppress garnet resorption during decompression, Fe-Mg changes at the crystal rim still cause rapid re-equilibration of outer parts of the crystal (see the discussion in Caddick et al. 2010), strongly modifying the chemical composition apparently corresponding to peak pressure and temperature.

4) The effect of the processes described above is magnified with a) increasing peak temperature, b) decreasing size of the garnet crystal and c) increasing heating or cooling durations.

Our analysis suggests that the zoning of garnets from samples reaching temperatures of the greenschist and lower amphibolite facies may yield apparent P-T paths that correspond well with the actual path experienced by the sample. This match improves with increasing garnet diameter and increasing exhumation rate. On the other hand, it is extremely difficult to reconstruct correctly P-T paths from the modified chemical zoning of garnets that have reached temperatures of the upper amphibolite and the granulite facies, unless very large crystal sizes or high exhumation rates are used.

Acknowledgement: JK appreciates financial support of the Ministry of Education, Youth and Sports of the Czech Republic through the Scientific Centre “Advanced Remedial Technologies and Processes (identification code 1M0554)”.

Caddick M. J., Konopásek J. and Thompson A. B., 2010. Preservation of garnet growth zoning and the duration of prograde metamorphism. J. Petrol., 51, 2327-2347.

U-Pb zircon provenance of Moldanubian metasediments in the Bohemian Massif

Jan Košler[1,2], Jiří Konopásek[1,2], Jiří Sláma[1], Stanislav Vrána[2], Martin Racek[2], Martin Svojtka[3]

[1]*Centre for Geobiology and Department of Earth Science, University of Bergen, Norway (jan.kosler@geo.uib.no)*
[2]*Czech Geological Survey, Klárov 3, Prague 1, Czech Republic*
[3]*Institute of Geology, Academy of Sciences, Rozvojová 269, Prague 6, Czech Republic*

Metamorphosed Moldanubian sediments constitute a large part of the exposed Variscan orogenic root in the southern part of the Bohemian Massif. The sources of these sediments and their deposition ages have only been partly identified (Kröner et al., 1988; Finger et al., 2007). Their composition corresponds to a mature upper continental crust source. Metasedimentary rocks in the Moldanubian crustal stack have been internally divided into several nappes (units) that were primarily defined by their lithological contents and assumed deposition ages (Fuchs and Matura, 1976). These include (1) the Gföhl Unit consisting of high-grade gneisses and granulites, (2) the Varied Unit consisting of amphibolites, marbles and gneisses of presumably Palaeozoic age and (3) the Monotonous Unit that is made of gneisses and migmatites with a presumed Neoproterozoic age of deposition. The goals of this study were to constrain the deposition ages of sediments that now constitute the Moldanubian metasedimentary units, to test for possible differences in sedimentary sources among the three Moldanubian units and to evaluate the implications of such differences for the tectonic evolution of the Variscan orogen.

Here we report new U-Pb laser ablation ICP-MS ages derived from detrital zircons that were extracted from metasediments of the three Moldanubian units in southern Bohemia, Moravia and Lower Austria. The range of samples and units explored makes this the most complete provenance study of the Moldanubian so far. The age spectra of all 15 samples (consisting of more than 60 detrital zircon ages per sample) are dominated by a large Neoproterozoic peak and series of Palaeoproterozoic ages that probably reflect the widespread periods of magmatism that were also recorded by detrital zircon ages in the Teplá-Barrandian Unit (Drost et al., 2011). Discrete age peaks corresponding to Cambrian/Ordovician, Silurian and Devonian zircons were found in metasediments from both the Varied and Monotonous units in southern Moravia and Lower Austria, but they have not been found in the metasediments of the Monotonous Unit in southern Bohemia. This observation is not consistent with the previously proposed Neoproterozoic deposition age for the sedimentary precursor of the Monotonous Unit (e.g., Fiala et al., 1995) as a coherent group. Rather it indicates a previously unrecognised heterogeneity, at least in southern Moravia and Lower Austria. The new data also suggest that lithological differences between the metamorphosed clastic sediments of the Varied and Monotonous units may not correspond to differences in their respective sources of detrital material and ages of deposition. Despite the composition differences between the studied Moldanubian metasediments and the Neoproterozoic-Lower Palaeozoic sediments of the Teplá-Barrandian Unit (Kröner et al., 1988; Drost et al., 2007), the available detrital zircon ages suggest that the two terrains were supplied by sedimentary material that originated from sources with similar zircon crystallization ages. This may also suggest their spatial proximity during the deposition of the sediments.

*) The project is supported by the Czech Science Foundation (GACR P210/11/1904).

Drost K., Romer R.L., Linnemann U., Fatka O., Kraft P. and Jarda M., 2007. Nd–Sr–Pb isotopic signatures of Neoproterozoic–Early Paleozoic siliciclastic rocks in response to changing geotectonic regimes: a case study from the Barrandian area (Bohemian Massif, Czech Republic). Geol. Soc. Am. Spec. Pap., 423, 191– 208.

Drost K., Gerdes A., Jeffries T., Linnemann U. and Storey C., 2011. Provenance of Neoproterozoic and early Paleozoic siliciclastic rocks of the Teplá-barrandian unit (Bohemian Massif): Evidence from U-Pb detrital zircon ages. Gondwana Research, 19, 213-231.

Fiala J., Fuchs G. and Wendt J.I., 1995. Moldanubian Zone-Stratigraphy. In: Dallmeyer R.D., Franke W., Weber K.: Pre-Permian Geology of Central and Eastern Europe. Springer Verlag, Berlin, 417-428.

Finger F., Gerdes A. and Knop E., 2007. Constraints on the sedimentation of the Monotonous Series in the Austrian part of the Bohemian Massif from U-Pb Laser ICP-MS zircon dating. Mitt. Osterr. Miner Ges., 153.

Fuchs G. and Matura A., 1976. Zur Geologie des Kristallins der südlichen Böhmischen Masse. Jahrb. Geol. B.-A., 119, 1-43.

Kröner A., Wendt I., Liew T.C., Compston W., Todt W., Fiala J., Vaňková V. and Vaněk J., 1988. U-Pb zircon and Sm-Nd model ages of high-grade Moldanubian metasediments, Bohemian Massif, Czechoslovakia. Contrib. Mineral. Petrol., 99, 257-266.

Diamond and coesite in Bohemian granulites

Jana Kotková[1,2], Patrick J. O´Brien[3], Martin A. Ziemann[3]

[1]*Gzech Geological Survey, Klárov 3, 118 21 Prague 1, Czech Republic (jana.kotkova@geology.cz)*
[2]*Institute of Geosciences, Masaryk University, Kotlářská 2, 611 27 Brno*
[3]*Institut für Erd- und Umweltwissenschaften, Universität Potsdam, Karl-Liebknecht-Str. 24-25, 14476 Potsdam-Golm, Germany (patrick.obrien@geo.uni-potsdam.de, martin.ziemann@geo.uni-potsdam.de)*

High-pressure (HP) granulite occurrences are characteristic of the basement of European Variscides in the Czech Republic, Poland, Austria, Germany (cf. CETEG) and France. Recent decade has brought robust evidence for their undisputed regional tectonic importance and high-pressure and high-ultrahigh-temperature character, documented by characteristic mineral assemblage of hypersolvus ternary feldspar, quartz, garnet, kyanite and rutile in felsic quartzofeldspathic varieties (Saxony-type granulites) and garnet and clinopyroxene in more intermediate ones (Kotková, 2007). Common association of the serpenitized garnet peridotites with HP granulites clearly reflects crust-mantle interactions, and models explaining their apparently tectonic intercalation and involving Variscan compression, deep subduction and rapid exhumation have been proposed. What remained puzzling was the substantial difference of c. 2 GPa between the peak pressures recorded by HP granulites and peridotites, invoking questions as the possible exhumation mechanism of the heavy mantle rocks from depth concerns.

We discovered micro-diamond and coesite in HP granulites of North Bohemia (Ohře/Eger Crystalline Complex and České středohoří Mts. basement). This area was selected for focused search for these phases clearly indicative of the ultra-high pressure metamorphism due to the absence of HT/MP overprint during rapid granulite exhumation, association with garnet peridotites, and also not yet explained historical finds of macroscopic diamonds in pyrope-bearing gravels.

Micro-diamonds occur as single inclusions of 5-30 μm in diameter in garnet and kyanite. They range from well-formed octahedra in kyanite to ragged, sub-rounded crystals in places forming clusters of different-sized grains in garnet. Coesite with a thin quartz rim was identified as an inclusion in kyanite, which is itself completely enclosed in garnet, in one of the samples containing polycrystalline quartz aggregates. Presence of both diamond and coesite has been confirmed by micro-Raman spectroscopy.

The micro-diamonds have been found both in felsic quartzofeldspathic and intermediate garnet-pyroxene granulites from the exposures as well as drill cores. This along with their occurrence below the polished surface of the thin-sections, variable size and morphology and breakdown to graphite confirms their in-situ origin, as opposed to introduction during the preparation of samples. The discovery of coesite in granulite samples, considered as most reliable UHP indicator, strengthens these arguments further. Thus the north Bohemian crystalline basement can be added to a short list of accepted locations where diamond has been confirmed in situ in continental crust rather than mantle rocks (i.e. the Kokchetav Massif, Kazakhstan; Saidenbachtal, German Erzgebirge; Rhodope Massif, Greece and the Qinling Mts., China).

Coesite and diamond stability is restricted to pressures of above 3 and 4 GPa, respectively, exceeding conditions reached by even the deepest present-day orogenic crustal roots. Our discovery thus strongly supports the model of deep crustal subduction into the mantle (Willner et al., 2002) and challenges the homogeneous crustal thickening models (e.g. Schulmann et al., 2008) for formation of the high-pressure Bohemian granulites. It further shows that upper crustal rocks were brought into contact with peridotites at mantle depth and the exhumation of both crustal and associated mantle rocks was facilitated by buoyancy of quartzofeldpathic crustal rocks, as envisaged e.g. for Dabie-Sulu belt. The buoyancy of the Bohemian granulites was enhanced by their melting at depths (Kotková and Harley, 2010).

Kotková J., 2007. High-pressure granulites of the Bohemian Massif: recent advances and open questions: J. Geosci., 52, 45–71.

Kotková J., Harley S.L., 2010. Anatexis during high-pressure crustal metamorphism: evidence from garnet-whole rock REE relationships and zircon-rutile Ti-Zr thermometry in leucogranulites from the Bohemian Massif. J. Petrol., 51, 1967-2001.

Schulmann K., Lexa O., Štípská P., Racek M., Tajčmanová L., Konopásek J., Edel J.-B., Peschler A. and Lehmann, J., 2008. Vertical extrusion and horizontal channel flow of orogenic lower crust: key exhumation mechanisms in large hot orogens? J. Metamorph. Geol., 26, 273–297.

Willner A.P., Sebazungu E., Gerya T.V., Maresch W.V. and Krohe, A., 2002. Numerical modelling of PT-paths related to rapid exhumation of high-pressure rocks from the crustal root in the Variscan Erzgebirge Dome (Saxony/Germany). J. Geodyn., 33, 281–314.

Magnetic fabric in a highly serpentinized ultramafic body from orogenic root

Vladimír Kusbach[1,2], Stanislav Ulrich[3], Karel Schulmann[2], František Hrouda[4]

[1]*IPSG, PřF Charles University in Prague, Albertov 6, 120 00 Prague 2, Czech Republic (kusbach@gmail.com)*
[2]*EOST, Université de Strasbourg, 1 Rue Blessig, 67 000 Strasbourg, France*
[3]*Geophysical Institute Acad. Sci. Czech Republic, Boční II/1401, 141 31 Prague 4, Czech Republic 4, AGICO s.r.o., Ječná 29a, 621 00 Brno, Czech Republic*

The studied Mohelno peridotite body is the largest of spinel to garnet peridotites enclosed within retrogressed felsic granulite of the eastern part of the Moldanubian domain. The peridotite underwent complex tectonometamorphic history starting with recrystallization associated with emplacement into the lower orogenic crust followed by ascent to mid-crustal levels and folding by large scale, upright and E-W trending fold. Lattice preferred orientations of olivine and orthopyroxene shows that viscous creep of peridotite occurred during folding at the temperature range 700-800°C. An attempt is made to understand magnetic fabric from this highly serpentinized peridotite, its link to the olivine and pyroxene microstructure and tectonic evolution of the whole area. Temperature limit of serpentinization with respect to the development of the mylonitic microstructure in the Mohelno peridotite indicate, that serpentinization occurs as static post-folding process. Serpentinization of the studied peridotite is mostly expressed by presence of the antigorite and iron oxides. Density measurement recalculations projected against bulk magnetic susceptibility reveals that widespread serpentinization alters 50% to 100% of the rock volume. Study of low temperature and high temperature variation of susceptibility divides the peridotite samples into three main groups. Group I shows susceptibilities lower than 10^{-3} S.I. that corresponds to paramagnetic minerals only, while Group II and Group III show magnetic susceptibilities 10^{-3}-10^{-2} S.I. and higher than 10^{-2} S.I. which require presence of ferromagnetic minerals. Analysis of thermomagnetic curves revealed that a magnetite in Groups II and III is accompanied with both high and low temperature variety of maghemite and in some specimens also by a mineral from magnetite – chromite or magnetite – spinel series. The AMS patterns from the massif can be divided in three main types according to shape of magnetic ellipsoid, degree of anisotropy and orientation of susceptibility directions. The Type I fabric is characterized by clustered K_1 directions, girdle distribution of K_2 and K_3 directions, prolate shape of AMS ellipsoid and low degree of magnetic anisotropy. The Type II of fabric reveals clustered K_3 directions, girdle distribution of K_2 and K_3 directions, mainly oblate shapes of AMS and intermediate to high degree of magnetic anisotropy. The most common Type III fabric pattern is marked by clustered K_1, K_2, K_3 directions, plane strain to oblate fabrics and generally high degree of susceptibility. The least serpentinized samples corroborates with least magnetic samples of the Group I which also coincide with rarely preserved coarse-grained or core and mantle microstructure with large opx porphyroclasts. This group of samples reveals presence of the Type I AMS patterns. The samples of Groups II and III show generally mylonitic fine-grained microstructure marked by strong serpentinization. Both groups of samples reveal presence of the Type II and mainly Type III patterns. Spatial distribution of K_m and P parameters implies advancing serpentinization from the margins to the center of the body marked by presence of Group I samples in the core of the body. Orientation of magnetic foliations and lineations changes from the Group I to the Group III. Magnetic foliation follows the fold shape of the peridotite in the Group I and II, while in the Group III there are randomly oriented foliations as well as one strong subgroup of foliations dipping to the west at moderate angles. Magnetic lineation is gently plunging in the foliation without preferred orientation in the Group I, while in the Group II and III it is either gently plunging to the south or it concentrates around the peridotite fold axis moderately plunging to the west. The intensity of fabric alignment increases from the Group II towards Group III in conjunction with increasing bulk susceptibility. We suggest that the the Group I samples reflect either pre-folding olivine fabric or fabric defined by large opx porphyroclasts rotated to the easy-glide orientation within the syn-folding mylonitic matrix. Advanced serpentinization and ferromagnetic fabric measured in the Group II and III can be explained as a result of two competing factors: 1) the penetration of H_2O-rich fluids along the grain boundaries in the fine-grained microstructure and crystallization of magnetite following grain boundary network mimetize the shape of olivine and pyroxene within mylonitic microstructure, 2) the deformation superimposed on almost random serpentine and magnetite matrix bearing well oriented olivine and pyroxene. In our model, the weak strain is able to reorient random magnetite crystal but does not modify strong inherited fabric of olivine and pyroxene. We propose a tectonic scenario coherent with regional structural pattern supporting the latter model.

Structural and AMS records of granitoid sheets emplacement during growth of continental gneiss dome

Jérémie Lehmann[1,2], Karel Schulmann[1], Jean-Bernard Edel[1], František Hrouda[3,4], Josef Ježek[5], Ondrej Lexa[2,3], Francis Chopin[1,6], Pavla Štípská[1], Jakub Haloda[2]

[1]*Institut de Physique du Globe de Strasbourg, IPGS - UMR 7516, CNRS and Université de Strasbourg, F-67084 Strasbourg, France (jerelehmann@gmail.com)*
[2]*Czech Geological Survey, Klárov 3, 118 21 Praha 1, Czech Republic*
[3]*Institute of Petrology and Structural Geology, Univerzita Karlova, Albertov 6, Praha 2, Czech Republic*
[4]*Czech AGICO Ltd, Ječná 29, Brno 62100, Czech Republic*
[5]*Institute of Applied Mathematics and Computer Science, Charles University, Prague, Czech Republic*
[6]*U.M.R. 6526, GéoAzur, Université de Nice-Sophia Antipolis, Nice, France*

Emplacement of granitoid magmatic sheets accompanies the oblique growth of a crustal scale gneiss dome in the Lugian domain, at the eastern margin of the Bohemian Massif. There, pene-contemporaneous magmas (~ 345-338 Ma) were emplaced in two disctincts settings and surround the Orlica-Śnieżnik gneissic bulge.

The magmatic sheets emplaced along the eastern transpressive margin of the Staré Město Belt show strong mechanical coupling with high grade metapelites and gneisses of the hanging-wall and are structurally decoupled with respect to the eastern stiff banded amphibolites of the buttress. We show that the magma was first injected parallel to the subhorizontal anisotropy of the buttress producing an important rheological weakening of the host rock. This weakening of the melt-host rock multilayer led to the rheological collapse of rock structures and development of a major transpressional shear zone along which the major synconvergent magmatic sheet is emplaced. The microstructures and AMS of intrusive rocks support this model by an E-W fabric zonation (perpendicular to the strike of the magmatic sheets) represented by a solid state fabric and oblate to plain strain AMS ellipsoid in the West, subhorizontal magmatic fabric, oblate to plain strain symmetry of low intensity in the East and a transitional fabric with neutral to prolate ellipsoid associated with a girdle of AMS foliation in the centre of the magmatic sheet.

In contrast, the supracrustal Zábreh unit rocks at the southern margin of the gneissic dome reveals existence of a vertical fabric in metapelites intruded by sills, and an intense normal shear zone developed in the upper part of the gneiss dome. The sills are folded by asymmetrical folds associated with a subhorizontal AMS foliation and roddings, both parallel to the sill's strike and fold axis. Quartz fabrics and AMS document a variation from a magmatic fabric with oblate symmetry and steep magnetic foliation and lineation parallel to the walls, changing to a transitional magmatic to solid state fabric marked by development of a sub-horizontal magnetic lineation, girdle of magnetic foliation and neutral to prolate symmetry to finally evolve in a greenschist solid-state fabric with oblate symmetry and subhorizontal magnetic foliation. These variations of AMS and quartz fabrics are attributed to the overprint of an original steep magmatic fabric by continuous normal shearing.

The AMS modelling suggest the importance of overprinting of the intrusive fabrics during progressive transpressional deformation in the Staré Město belt and during normal shearing in the Zábreh area.

The coeval activities of the extensional and compressional magmatic emplacement along the periphery of a growing gneissic dome are related to the asymmetry of the dome structure, and the oblique growth process. The structural study of sills is therefore an excellent tool for understanding growth dynamics of gneiss domes in hot orogens.

Products of the basic volcanism from the area of Osobitá peak in the West Tatra Mts. – their strathigraphy and character of the volcanic activity

Jozef Madzin[1], Milan Sýkora[1], Ján Soták[2]

[1]*Department of Geology and Paleontology, Faculty of Natural Science, Comenius University, Mlynská dolina G, 842 15 Bratislava, Slovakia (madzin@fns.uniba.sk; sykora@fns.uniba.sk)*
[2]*Geological Institute, Slovak Academy of Sciences, Ďumbierska 1, 974 11 Banská Bystrica, Slovakia (sotak@savbb.sk)*

The basaltic volcanic rocks occur in the High Tatra Mesozoic cover unit (Osobitá succession) in the West Tatra Mts. in the Predná Kremenná valley, Široky žľab, Suchá valley and Bobrovecká valley in complex of limestones of the Lowermost Cretaceous age. They are composed of hyalobasanites, hyaloclastites – hydroclastic breccias and hyaloclastic tuffites. The main aim of this work is to verify their stratighraphic position on the basis of microfacies analysis of limestones and index microfossils. Limestones below the volcanites have nature of the intraformational fine-grained breccias and conglomerates consisting of lithoclasts of limestones of different facial types and age. Most frequent are lithoclasts of organodetritic limestones, oolitic limestones and micritic limestones. All types of lithoclasts contain calpionellid microfauna. Youngest form found in the underlying limestones was *Calpionella alpina* Lorenz, *Calpionella minuta* Houša *Calpionella elliptica* Cadish. They correspond to *Calpionella zone* and *elliptica* subzone. Age of this zone is upper part of the Lower Berriasian. The age of the fine-grained limestone breccias and conglomerates was determined as Upper Berriasian. Overlaying rocks above the volcanites are reddish and gray crinoidal limestones. They comprise mainly of packestones and grainstones, containing foraminiferas *Meandrospira favrei* (Charollais, Brönnimann & Zaninetti), *Montsalevia salevensis* (Charollais, Brönniman & Zaninetti), *Haplophragmoides cf. joukowskyi* Charollais, Brönnimann & Zaninetti of the Valanginian – Lower Hauterivian age. Volcanic activity took place in various less intensive phases since Upper Tithonian, what is approved by occurrence of calcified volcanic clasts in underlying fine-grained limestone breccias, which are underlying the volcanites. The age of main phase of the volcanic activity in the area of Osobitá peak is determined as the Upper Berriasian –Lower Valanginian.

Emplacement mode of a composite post-collisonal pluton in the Klamath Mountains (California, USA)

Matěj Machek, Prokop Závada, Aleš Špičák

Institute of Geophysics, Academy of Sciences of the Czech Republic, Boční II/1401, 141 31 Prague 4, Czech Republic (mates@ig.cas.cz, zavada@ig.cas.cz, als@ig.cas.cz)

The Klamath Mountains represent an accreationary complex on the northwest California and southwestern Oregon. It consists of four arcuate belts representing terranes of former island archipelago environments that span in age from Paleozoic to Jurrasic and are divided by eastward dipping thrust faults (Snoke and Barnes, 2006). During and after the accretion, the entire thrust sheet was penetrated by numerous plutonic bodies. The Castle Crags pluton was selected for detailed internal fabrics to understand the emplacement mode of post-collisional plutons. Castle Crags pluton that intruded the Eastern Klamath terrane and in particular ultramafic Trinity Complex subterrane is an elliptical NW-SE elongated pluton with 12 km and 7 km in its long and short dimension, respectively. It is a well exposed composite plutonic body with about 1 km vertical crossfall. The pluton is affected by prominent NW-SE trending vertical joints and another less well developed vertical set perpendicular to the first one. The pluton is zoned and consists of three following igneous varieties: 1) marginal fine-grained granodioritic facies with abundant subsolidus shear zones, 2) coarse-grained granodiorite and 3) central, circular in plan-form and about 2 km in diameter, domain of trondhjemite. Numerous miarolitic cavities with macroscopically measurable trends mark the transition between the central trondhjemite and surrounding granodiorite (Vennum, 1980 a,b). Macroscopic foliations, jointing and sampling on the Castle Crags was carried out along the main crest of the pluton and numerous sideway crests and valleys gaining about 70 samples. The internal magmatic foliations and magnetic foliations show a concentric pattern of margin-parallel vertical foliations. The magnetic lineations reveal plunge trends parallel to the margins of the pluton and continuously increasing plunge angles from the margin to the core of the pluton. The zonality and fabric pattern of the pluton can reflect either divergent flow during emplacement of the pluton of an upward widening magmatic stock or alternatively by helicoidal flow or balooning. The miarolitic cavities could reflect the dilatancy of the granodioritic crystal mush during emplacement of the central trondhjemite with vertical fabrics.

Snoke, A. W. and Barnes, C. G. (2006). The development of tectonic concepts for the Klamath Mountains province, California and Oregon, In: Geological studies in the Klamath Mountains Province, California and Oregon (Ed.: Snoke, A. W. and Barnes, C. G.), The Geological Society Of America Special Paper 410, 1-29.

Vennum W. R. (1980a) Petrology of the Castle Crags pluton, Klamath Mountains, California: Summary, Geological Society of America Bulletin, Part I, 91, 255-258.

Vennum W. R. (1980b) Petrology of the Castle Crags pluton, Klamath Mountains, California, Geological Society of America Bulletin, Part II, 91, 1332-1393.

Numerical model of crustal indentation: Application to the Variscan evolution of the Bohemian Massif

Petra Maierová[1], Ondrej Lexa[2], Ondřej Čadek[1], Karel Schulmann[3]

[1]*Department of Geophysics, Faculty of Mathematics and Physics, Charles University in Prague, Czech Republic*
[2]*IPSG, Faculty of Science, Charles University in Prague, Czech Republic*
[3]*EOST, Université de Strasbourg, Strasbourg, France*

Recent considerations of detailed petrological, geochronological, geophysical and structural data allow us to make progress in understanding mechanisms of crustal-scale exhumation of orogenic lower crust associated with lithospheric indentation. Current numerical models (e.g. Beaumont group) suggest an emplacement of "hot-nappes" in subsurface channel-flow powered either by gravity potential or by an indentation of a weak hot root with a lower crustal rigid promontory attached to the subducting plate.

We investigate by means of numerical modelling an example of several thousand square kilometres of a flat-lying orogenic lower crust underlain by a basement promontory located at the retroside of the Variscan orogen along a 300 km long collisional front (Poland, Czech Republic and Austria). Gravity surveys show that the limit of the basement promontory extends about 100 kilometres towards the internal part of the orogenic root from the todays exposure of the orogenic front. Combined structural and petrological studies revealed that the orogenic lower crust (high-pressure granulites and mafic eclogites) was vertically extruded from depths of about 60 kilometres along the steep margin (ramp) of the basement promontory. The observed transition from steep to flat fabrics occurs in different depths from 35 to 15 kilometres and is marked by different P-T-t paths of exhumed lower crustal blocks. The vertically extruded rocks are reworked by flat fabrics reflecting the flow of hot material into some horizontal channel developed between the upper boundary (flat) of the basement promontory and the overlying orogenic lid.

We present a thermomechanical model of the indentation process and the consequent viscous deformation of the orogenic lower crust. The modeling is performed using the open source finite element software for multiphysical problems Elmer (http://www.csc.fi/english/pages/elmer) which was extended for this purpose by user-written procedures for compositional convection, visco-plastic deformation of crustal materials, surface processes (erosion and sedimentation) and isostatic compensation. The modeling is carried out in a two-dimensional Cartesian domain representing a vertical cross section through an orogenic root and a stiff indentor. The initial stratification of the model domain and the rheological properties of individual layers correspond to the expected composition of the Brunia basement and the Variscan orogenic root prior to the indentation process. One of the specific features of Moldanubian root was a felsic heat-productive lower crust which was emplaced beneath the previously thinned Moldanubian domain during the initial stage of the continental collision (Lexa et al., 2011). These rocks belong to the so-called Gföhl unit and they can also be observed in gravity and seismic data (Guy et al., 2010; Růžek et al., 2007). We show that the presence of this anomalous layer significantly influences the indentation dynamics since it has a lower density and, owing to the large amount of radiogenic sources, also significantly lower viscosity than the upper and middle crust. The values of the model parameters, including the initial thicknesses of the layers, indentation rate, radiogenic heat production in the felsic lower crust, etc., are tuned in such a way that the pressure-temperature paths computed for the exhumed lower- and middle-crust rocks agree with the observed ones. The models constrained in this way mostly reproduce also the processes inferred from the geological record in the studied region (crustal scale folding, diapirism, channel flow, flat deformation of the exhumed rocks) as well as the basic signature found in the geophysical observation (Bouguer anomaly pattern).

Guy A., Edel J.-B., Schulmann K., Tomek Č., Lexa O., 2010. A geophysical model of the Variscan orogenic root (Bohemian Massif): Implications for modern collisional orogens. Lithos, article in press, doi:10.1016/j.lithos.2010.08.008

Lexa, O., Schulmann, K., Janoušek, V., Štípská, P., Guy, A. & Racek, M., 2011. Heat sources and trigger mechanisms of exhumation of HP granulites in Variscan orogenic root, Journal of Metamorphic Geology, 29, 1, 79-102.

Růžek B., Hrubcová P., Novotný M., Špičák A., Karousová O., 2007. Inversion of travel times obtained during active seismic refraction experiments CELEBRATION 2000, ALP 2002 and SUDETES 2003. Studia Geophysica et Geodaetica, 51, 141-164.

Tectonic stress field evolution and map-scale faulting at the northern margin of the Danube Basin, Slovakia (Western Carpathians)

František Marko

Comenius University Bratislava, Faculty of Natural Sciences, Department of Geology and Paleontology, Mlynská dolina, 842 15 Bratislava, Slovakia (marko@fns.uniba.sk)

Early Miocene sediments – remnants of a destroyed wrench furrow basin (sensu Montenat et al. 1987) are exhumed at the northern periphery of the Danube basin, at the Bánovce kotlina depression which occupies the nothernmost bay of the basin. Early Miocene sediments are from the south tectonically juxtaposed along the Jastrabie fault to a younger, Mio - Pliocene basin fill which occupies the downthrown block (Brestenská et al. 1980). The northern rim of the of the Danube basin is strongly affected by map-scale faults, tilting and erosion. Following Angelier`s principle of scale-invariancy, small-scale brittle deformational structures were used for dynamic interpretation of large-scale, regionally important faults. As a basic tool, fault-slip related paleostress analysis was applied, and the behavior of map-scale faults in reconstructed paleostress field was inferred. The most frequent meso-scale faults observed in the field are steeply diping strike-slips. Stress regimes reconstructed in the focused area had predominantly compressional and strike-slip characteristics. Six, Miocene to Quaternary(?) fault producing tectonic events were recognized, and records of distinctive block tilting were observed in the field. The orientation of the maximum principal stress axis (σ_1) during the Cenozoic tectonic evolution apparently rotated from WNW-ESE through NNW-SSE, NNE-SSW, NE-SW to the ENE-WSW direction. These stress directions represent five directionally independent events which operated in the Neogene-Quaternary time span. The succession of single events was interpreted according to the superposition of structures observed in the field and to the similarity of described stress/deformation events with already restored tectonic evolutionary histories in the surrounds. The results of paleomagnetic investigation in the neighbouring areas (Kováč and Tunyi, 1995) confirm the Early-Middle Badenian CCW block(s) rotation, which occured during several etaps. Although this structural scenario could also be expected in the studied area, no paleomagnetic data from the Bánovská kotlina depression are currently available. Pre-rotational records of tectonic events are not in situ, but are now in the changed - rotated positions. Whether the rotation was un-block (whole Carpathians), or domino-style rotation located within the strike-slip, wrench corridors remains open. We presume, that a small rotation at the begining occured as un-block, and the next, dominant rotational events happened inside the wrench corridor. The dominant large-scale structural phenomenon in the area is indeed an ENE-WSW wrench corridor, which operated in the Early Miocene as a transpressional dextral brittle shear zone, responsible for the origin of Eggenburgian-Karpatian wrench furrow basin. In the Middle Miocene, it operated as a transtensional sinistral brittle shear zone, where CCW block rotations took place, most likely throgh a book-shelf mechanism. Therefore, inside the wrench corridor, records of original N-S compression sinistraly rotated to cca NW-SE directions and NNE-SSW to ENE-WSW postrotational compressional events in the original directions. Dextral strike-slip faults formerly in N-S directions, now rotated to cca NW-SE direction, could have operated as accomodational antithetic faults controlling CCW block rotations inside the wrench corridor in a domino-style mechanism. The apparently last event in the recognized succession is ENE-WSW compresional one, and it could be Quaternary in age. The most distinctive-frequent event in the structural record appears to be a NNW-SSE compresion. We assume, that these records comprisize two single events, a rotated N-S Early-Middle Miocene one, which is overprinted by not rotated records of a NNW-SSE Quaternary compression, WSW-ENE tension respectively. The last event is the final one, sixth in order, and it explains the prevalence of N-S normal map-scale faults in this area. (Acknowledgements: This work was supported by the Academic scientific grant agency VEGA under the contract No. 1/0712/11 and by the Slovak Research and Development Agency under the contract No. APVV-0279-07.)

Brestenská, E., Havrila M., Kullmanová A., Lehotský I., Remšík A., Vaškovský L., Gross P. and Maheľ M. 1980. Geological map and explanations of the Bánovská kotlina (1:50 000). Manuskript, Geofond, Bratislava, 109pp. .(in Slovak)

Kováč M. and Tunyi I. l995. Interpretation of paleomagnetic data from the western part of Central Western Carpathians. Min. slovaca, 27, 2l3-220

Montenat Ch., Ott D´Estvou and Masse P. 1987. Tectonic-sedimentary characters of the Betic Neogene Basins evolving in a crustal transcurrent shear zone (SE Spain). Soc. Nat. Elf Aquitaine, Pau, France, 1-22.

Seismic response to tectonic movements in the southern part of the bird's head triple point

Radka Matějková, Aleš Špičák, Jiří Vaněk

Institute of Geophysics, Academy of Sciences of the Czech Republic, Boční II/1401, 141 31 Prague 4, Czech Republic (rmatejkova@ig.cas.cz)

We analyse spatial distribution of earthquakes in the Banda Sea region (1°-10°S and 124°-135°E), southern part of the Bird's Head triple point. The EHB global hypocentral determinations (Engdahl et al., 1998) covering the period 1964-2007 and fault plane solutions determined by Global CMT Project covering the period 1976-2009 have been used. Such an analysis enabled to distinguish between earthquakes belonging to the Wadati-Benioff zone(s) from those occurring in the overriding plate or at the lithospheric boundary between the Pacific and Indo-Australian plates (Fig. 1). Subsequent analysis of grouping of earthquake foci in combination with fault plane solutions led to a delimitation of several domains of shallow earthquakes of different character. Spatial distribution of earthquake foci, accompanied by thorough review of available geological information, does not indicate westward dipping subduction in the strip between 4.5°S and 6°S. Instead, this area seems to be

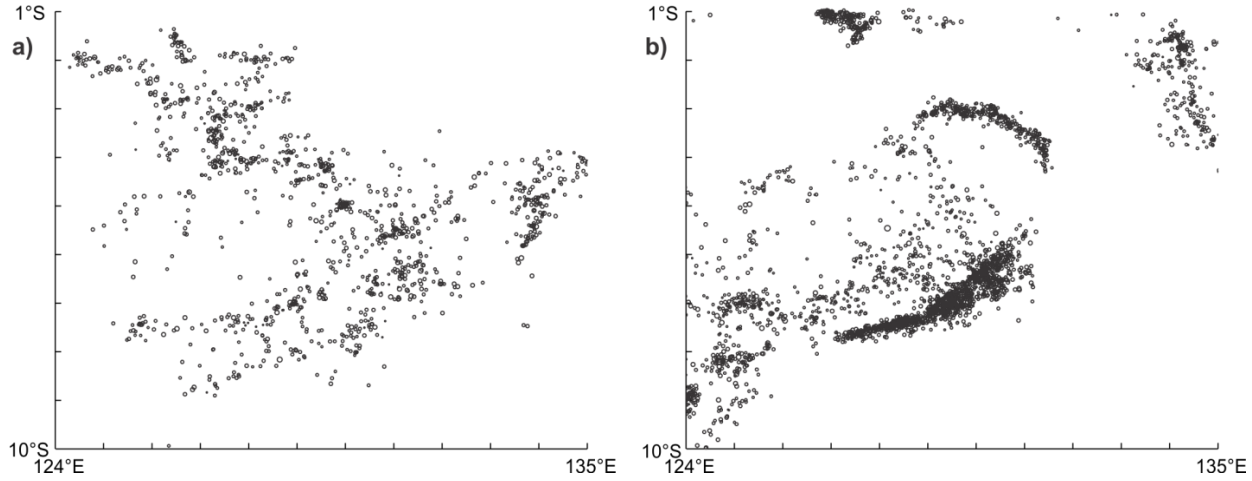

Fig. 1. Distribution of earthquakes of the Banda Sea region. a) Epicentral map of shallow earthquakes. b) Epicentral map of earthquakes belonging to the Wadati-Benioff zones and surrounding seismicity.

strongly influenced by westward movement of the Pacific plate relative to the Indo-Australian plate as indicated by dominance of left-lateral displacement documented by fault plane solutions. This left-lateral movement is mainly focused to two parallel fault zones Tarera-Aiduna I and Tarera-Aiduna II (TAFZ I and TAFZ II). These two parallel faults also divide the Banda Sea region into northern and southern parts with two different subduction zones. Vertical distribution of earthquake foci between parallels 126°-132°E, south of TAFZ I and TAFZ II, reflects several episodes of the subduction process of the Indo-Australian plate beneath the Banda Sea - Sunda block (Banda subduction) during the last 8 My, interrupted by a collision in several segments. The recent subduction has already reached a depth of about 100 km decisive for arc magma formation (Damar, Teon, Nila volcanoes). Within the northern subduction, north of the TAFZ I and TAFZ II, its shallow part has been the most active recently.

Engdahl, E.R., Van Der Hilst, R.D. & Buland, R., 1998: Global teleseismic earthquake relocation with improved travel times and procedure for depth determination. Bull. Seism. Soc. Am., 88, 722-743.

Microstructures and P-T estimates of a meta-peridotite from the exhumed hot crust-mantle fragments in a Variscan shear zone (the North-Veporic Basement, Western Carpathians)

Martin Michálek, Marián Putiš

Faculty of Natural Sciences, Comenius University in Bratislava, Mlynská dolina, 842 15, Bratislava, Slovakia (michalek@fns.uniba.sk; putis@fns.uniba.sk)

Horizontal zonation of the basement complexes, and even their vertical tectonostratigraphy, remained prominent features of the Variscan southward progressing orogeny at the territory of the Western Carpathians (Putiš, 1992). The Upper Variscan structural Unit, composed of paragneisses, orthogneisses, amphibolites, rare calc-silicate marbles, migmatites, is intruded by meso-Variscan granitic plutons. The sheared base contains layered amphibolites, lenses of Grt-Cpx amphibolites, eclogites, granulites and antigorite serpentinites, accompanied by Ky-Grt ortho- and paragneisses (Filová and Putiš, 2004; Janák et al., 2007; Michálek and Putiš, 2009). Part of these rocks was tectonically emplaced into the MT-MP micaschists to gneisses of the underlying Middle Variscan structural Unit.

The major mineral metamorphic assemblage in studied meta-peridotite lens contains Ol, Opx, Cpx, Am, Grt, Spl. Accessory minerals are Cr-Spl, Fe-Ti oxides, apatite. Microstructural relationships between these minerals indicate the evolution P-T path through the eclogite/HP granulite- to amphibolite facies. According to mineral relationships, we distinguished a few metamorphic stages of this mantle fragment within a Variscan shear zone. The hosting rocks are partially melted Ky-Grt gneisses, amphibolites and orthogneisses with eclogite lenses.

Grt ($Alm_{43}Prp_{34}Grs_{20}$) with Opx_2 and Cpx_2 ($En_{46}Fs_6Wo_{48}$, X_{Di}=0.83) is overgrowing relics of Am_1 in symplectite-like aggregates or "prograde" coronas (Fig. 1a), probably due to metamorphic reactions incorporating Spl and Mg-Hbl_1.

Inclusions of Am_1 (Mg-Hbl) are observable in Opx_1 (Fig. 1b). Am_2 is represented by porphyroblasts of Mg-Hbl (Fig. 1c) with Cr-Spl inclusions and Ilm exsolutions(?). Am_3 (Mg-Hbl to Tr in the rim) occurs in aggregates replacing Am_2 (Fig. 1c). Am_3 (Mg-Hbl to Tr) is overgrowing metamorphic matrix of Ol, Opx and Cpx of the different generations (Fig. 1a, d).

Ol_1 porphyroblasts surrounded by coarse-grained Opx_1 can be the metamorphic pseudomorphs after magmatic Ol and Opx in a porphyric structure. Ol_1 (X_{Fo} 0.74) is metamorphic olivine with inclusions of Am_1 (Mg-Hbl), Opx_1 and Cpx_1 ($En_{46}Fs_7Wo_{47}$, X_{Di}=0.8) and Cr-Spl. Ol_1 is replaced by intergrowths of Ol_2 and Opx_3 in a reaction (decompression) corona (Fig. 1b, d).

Opx forms porphyroblasts (Opx_1), or inclusions in Ol_1 and $Am_{2,3}$. Opx_2 creates the intergrowths with Grt and Cpx_2 around relics of Am_1 (Fig. 1a). Opx_3 and Ol_2 are preserved in coronas around Ol_1 (Fig. 1a, d).

Cpx forms porphyroblasts (Cpx_1), or inclusions in Ol_1 and $Am_{2,3}$. Cpx_2 with Grt and Opx_2 occurs in symplectite-like (prograde) coronas overgrowing relics of Am_1 (Fig. 1a).

The replacement of Am_1 by the porphyroblasts of Ol_1 and Opx_1, as well as the breakdown of Am_1 due to reactions including Am_1 (Mg-Hbl) and Spl, forming symplectite-like aggregate or a prograde corona of Grt, Opx_2 and Cpx_2, could be referred to a transition from amphibolite to eclogite or HP granulite facies of metamorphism, where the newly formed metamorphic mineral assemblage of Ol-Opx-Cpx-Grt is stable (Evans in Robinson et al., 1981).

Estimation of P-T conditions of metamorphic evolution of meta-mafic fragment is based on the geothermobarometric data (Ol, Opx, Cpx, Grt). Due to absence of plagioclase it is hardly to accurate pressure of formation of mineral assemblage of Opx_1 and Ol_1, and so just estimation of temperature (~830°C at 1.0 – 1.5 GPa) was obtained according to a Ca content in Opx at a given pressure (Brey and Köhler, 1990) and represent granulite facies conditions of metamorphism. P-T conditions of garnet formation were 733±22°C at 1.1±0.02 GPa using PT Average function in THERMOCALC (Holland and Powell, 1998, v. 3.31). Decomposition of Ol_1 into Ol_2-Opx_3 represents medium-P granulite facies and estimated temperature is ~700°C at 0.7 – 1.0 GPa (Ca content in Opx at a given pressure, Brey and Köhler, 1990). $Am_{2,3}$ aggregates represent amphibolite facies of metamorphism.

Acknowledgement: This work was supported by the APVV agency grant No. APVV-0279-07.

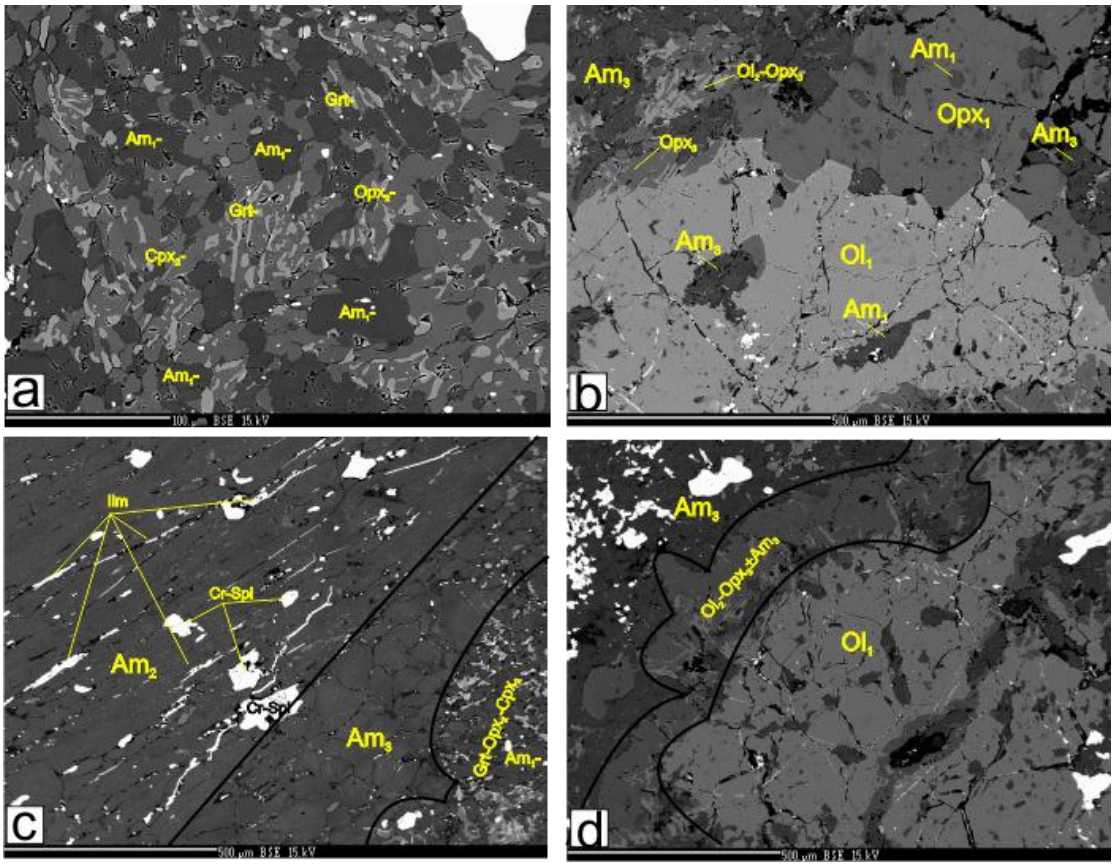

Fig. 1 Microstructures of meta-peridotite. a) Relics of Am_1 surrounded by Grt-Opx_2-Cpx_2 aggregate (a prograde corona). b) Ol_1 and Opx_1 with inclusion of Am_1. The rim of Ol_1 replaced by a decompression corona of Ol_2-Opx_3 ±Am_3. c) Am_2 porphyroblasts with inclusions of Cr-Spl and exsolutions(?) of Ilm needles, surrounded by Am_3 aggregate. d) Reaction (decompression) corona around Ol_1 consiting of Ol_2-Opx_3 ±Am_3.

Brey, G. P. and Köhler, T., 1990. Geothermobarometry in four phase lherzolites, part II: new thermobarometers, and practical assessment of existing thermobarometers: J. Petrol., 31, 1353 – 1378.

Filová, I. and Putiš, M., 2004. Lithological-petrographical study of meta-mafics in the North-Veporic basement. Mineralia Slovaca 36, 195-204.

Holland, T.J.B. and Powell, R., 1998. An internally consistent thermodynamic data set for phases of petrological interest. J. Met. Geol., 16, 309 – 344.

Janák, M., Méres, Š., Ivan, P., 2007. Petrology and metamorphic P-T conditions of eclogites from the northern Veporic unit of the Western Carpathians. Geol. Carpath., 58, 121 – 131.

Michálek, M. and Putiš, M., 2009. P-T-d evolution of eclogitic metabasites and Neoproterozoic orthogneiss in the North-Veporic basement of the central Western Carpathians. Mineralia Slovaca, 41, 1 – 22.

Putiš, M., 1992. Variscan and Alpidic nappe structures of the Western Carpathian crystalline basement. Geol. Carpath., 43, 369 – 380.

Robinson, P., Spear, F.S., Schumacher, J.C., Laird, J., Klein, C., Evans, B.W. and Doolan, B. L., 1981. Phase relations of metamorphic amphiboles: natural occurrence and theory. In: D.R.Veblen and P.H. Ribbe, (Eds.): Amphiboles: Petrology and experimental phase relations. Reviews in Mineralogy and Geochemistry, 9B, Mineralogical Society of America, Washington, D.C., 1 – 228.

Complex evaluation of Kiskunhalas-NE fractured metamorphic HC-reservoir, Pannonian Basin

Ágnes Nagy, Tivadar M. Tóth

University of Szeged, Department of Mineralogy Geochemistry and Petrology, H-6701, Szeged P. O. Box 651, mtoth@geo.u-szeged.hu, nagyagnes85@gmail.com

On the basis of macroscopic and microscopic studies of borecore samples, four main rock types were identified. In the ideal rock column at the lowermost structural position unaltered orthogneiss is characteristic. This gneiss variety that contains amphibolite xenoliths and was intruded by mica-poor postmetamorphic granitoid developed at a two-stage evolution with D_1: bio+kfp+pl+ilm+qtz±sill±grt (T~700-850 °C) and D_2: bio+mu+pl+qtz+ilm+mt (T~530-580 °C) assemblages (Zachar & M. Tóth, 2004). The next lithological zone upward consists of gneiss mylonite exhibiting extensional textural features (SC structure, apatite bookshelf, plastically deformed quartz grains), while, on the basis of its mineralogy and relic textures the protolith is identical to the lowermost orthogneiss. The quartz grain boundary thermometer (Kruhl & Nega, 1996) suggests temperature for mylonitic deformation T_{def} ~470 °C. Further upward mylonites occur with similar extensional fabric elements (SC structure, apatite bookshelf, feldspar boudinage, plastically deformed quartz grains), but significantly different mineralogy. The bio+kfp+pl+qtz assemblage clearly suggest a low-grade metamorphic protolith in this case. Based on the Raman spectroscopic measurements and the carbonaceous material thermometry (Beysacc etal, 2002; Rahl etal, 2005), for the peak metamorphic temperature of the original metamorphic rock ~420 ± 50 °C can be estimated. Using the method of Kruhl & Nega (1996) mylonite formed at T_{def} ~440 °C. Strongly fractured borecore samples of this rock unit are often oil spotted. In the uppermost structural position graphitic carbonate phyllite appears with T_{max}~375±50 °C (Figure 1/a).

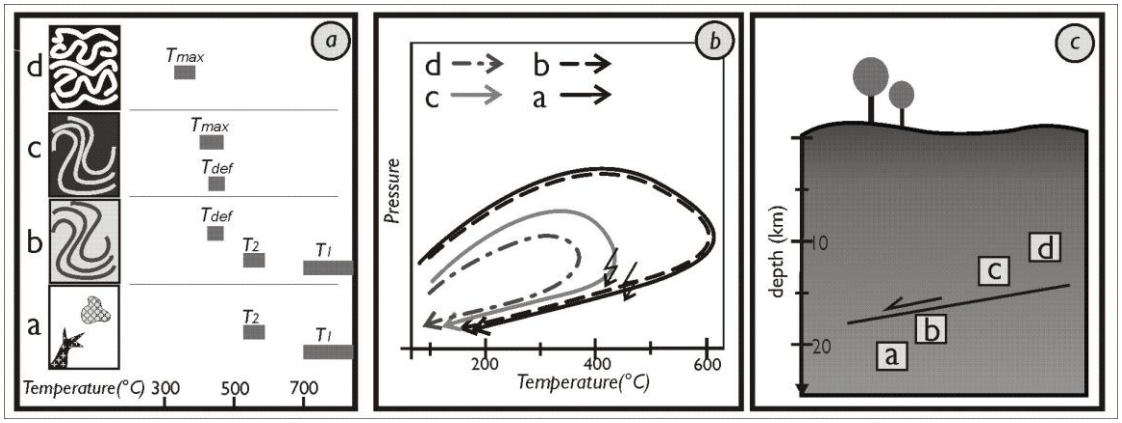

Fig. 1. a) *The ideal rock column of the field with the characteristic temperatures b) The PT path of the four main rock type* ***c)*** *The outline of the development of the rock body along the shear zone. Legend: a – orthogneiss, b – orthogneiss mylonite, c – low grade metamorphic mylonite, d – graphitic carbonate phyllite.*

Results of previous and current geothermometry calculations suggest that there is ~200 °C difference between the peak temperatures of the two extreme lithologies in the rock column is (Figure 1/b). That means 5-10 km difference in formation depth depending on the one-time geothermal gradient. This result together with presence of the extensional mylonites implies that the study area evolved in an extensional stress regime; the blocks of different metamorphic conditions got juxtaposed along a shear zone at a depth corresponds to ~450 °C (Figure 1/c). The entire rock column behaved uniformly during the following tectonic development; at shallower position it deformed in a brittle way.

In order to extrapolate petrologic information to reservoir scale, well-log data (gamma-ray logs) were utilized. In the first step of the analysis the petrologically identified intervals were characterized by geophysical data. Afterwards, using this information all lithologies can be extended using only well-logs and, finally, borders of the neighboring lithologies got marked along each well. Using diverse 2D horizontal and vertical sections a reliable 3D geological framework model for the whole study area was put together. Spatial position of the mylonite zone suggests a characteristic NW dip for the whole studied basement high. Appearance of a sequence of tilted blocks with NW dip may imply development along an antitetic fault system not uncommon in the basement of the Pannonian Basin. This structure was further complicated by a younger normal fault system that formed horst-graben structure with dip directions perpendicular the previous.

To get information about the fracturing tendencies of the four basic rock types of the reservoir, the samples were examined by rock mechanical tests and CT (computer tomography) methods both parallel and

perpendicular to the foliation. The results show that all mechanical parameters are highly anisotropic. There grow significantly more single fractures parallel to the foliation in all cases, while fracture intensity (cumulative length at unit area) of the induced fracture system is the highest for low grade metamorphic mylonite samples suggesting that this zone may serve the best reservoir characteristics.

As a summary we can state that the Kiskunhalas-NE fractured metamorphic reservoir is characterized by a series of NW dipping tilted blocks composing of rock types with different metamorphic and structural evolutions. On the basis of the complex investigation, structurally separated blocks of the low grade metamorphic mylonite zone owns the most favorable reservoir features being in coincidence with the HC production data.

Beysacc, O., Goffé, B., Chopin, C. and Rouzaud, N., 2002: Raman spectra of carmonaceous material in metasediments: a new geothermometer. J. metamorphic Geol., 20, 859-871

Kruhl, J. H. and Nega, M., 1996: The fractal shape of sutured quartz grain boundaries: application as a geothermometer. Geol. Rundsch. 85., 38-43.

Rahl, J. M., Anderson, K. M., Brandon and M. T., Fassoluas, C., 2005: Raman spectroscopic carbonaceous material thermometry of low grade metamorphic rocks: Callibration and application to tectonic exhumation in Crete, Greece. Earth ans Planetry Science Letters, 240/2, 339-354.

Zachar, J. and M. Tóth, T., 2004: Pertology of the metamorphic basement of the Tisza Block at the Jánoshalma High, S Hungary. Acta Geologica Hungarica, 47/4, 349-371.

Possible soft-sediment deformation features of the Jurassic slope and basin facies rocks in the SW part of the Bükk Mts.

Norbert Németh

Department for Geology and Mineral Resources, University of Miskolc, 3515 Miskolc-Egyetemváros, Hungary (foldnn@uni-miskolc.hu)

The SW part of the Bükk Mts (NE Hungary) exposes Middle Jurassic slope and basin facies rocks lying over Triassic limestone formations. A recent research project was aimed to ascertain the sedimentological character and specify the age of the rocks of this Jurassic succession (Haas et al. 2006; 2010; in press). The sedimentological and paleontological results were interpreted so, that these rock assemblage was formed as an accretionary complex with several olistostromes and even 10-100 m scale blocks. A considerable part of the material was redeposited from a carbonate platform, which is not known in the present-day area.

This model implies mass movements and syndepositional deformations in unconsolidated or semi-consolidated state, which are characteristic in recent analogous environments. The results of these processes driven either by gravity or by tectonics of a basin closure are very similar to post-lithification structures in general, and the unambiguous distinction is possible in special cases only. Unfortunately, the rocks were affected by an anchi-epizonal metamorphism and several deformation phases, so the observed deformation features (ductile and brittle as well) were attributed to synmetamorphic or later events. Obvious cases are the only exceptions: small-scale, stratabound convolutions were reported in siltstone (Konrád 1990) and in sandstone (Less et al. 2005) as soft-sediment deformation structures.

Beyond these, several observed features could have a soft-sediment origin. In shale-sandstone-limestone assemblages the bedding surfaces often show anastomosing pattern with curved ramps truncating the beds and, in consequence, sigmoidal dm-scale spaced cleavage was formed. Sandstone and limestone beds in shale matrix show boudinage to irregularly various extents without corresponding folding. Boudins are sometimes imbricated, indicating extension followed by shortening. One outcrop also exposes a typical slump fold in a few metres thick sequence: there are similar folds with axial planes parallel with the general bedding; thickness of the beds changes irregularly; competent beds are stacked in the hinge zone. The features are not equally well developed in every outcrop; in large areas there are parallel beds and a regular slaty cleavage within similar or the same lithology.

The textural characteristics also support rather an early, soft-sediment than a hard-rock ductile deformational origin of these features. Triassic limestone and shale formations with similar style boudinage of the Central Bükk area contain abundant signs of dynamic recrystallization and a folding-related cleavage. The Jurasssic limestone beds here show bedding-parallel flattening and the stylolitic spaced cleavage of certain domains only. This resembles to the direct underlying Triassic formations also preserving sedimentary texture with the same flattening, indicating a different deformation path during the period of metamorphism in contrast with the Central Bükk.

There are, however, further structures beyond cleavage which clearly overprint these features. The wide-spread zigzag folding with mostly gentle and open folds and with kink bands may reflect the SE-vergent thrust of the rock assemblage. The faulting can be correlated with Cenozoic phases. In summary, detaching the subsequent structures, the remaining, early ductile and conjugated brittle features could have a prediagenetic origin in an accretionary complex, in agreement with the sedimentological model. (Investigations were supported by the Hungarian Science Found (OTKA) project K61872.)

Haas J, Görög Á, Kovács S, Ozsvárt P, Matyók I. and Pelikán P. 2006: Displaced Jurassic foreslope and basin deposits of Dinaridic origin in Northeast Hungary. Acta Geologica Hungarica 49/2, pp. 125-163.

Haas J, Pelikán P, Görög Á, Ozsvárt P, Józsa S. and Kövér Sz. 2010: Subduction related Jurassic gravity deposits in Bükk-Darnó area, Northeast Hungary. Proceedings 19th Congress of the CBGA, Thessaloniki, Greece, pp. 149-156.

Haas J, Pelikán P, Görög Á, Józsa S. and Ozsvárt P. in press: Stratigraphy and facies characteristics of Jurassic formations in the SW part of the Bükk Mts, North Hungary. Geological Magazine

Konrád Gy. 1990: Adatok a Szarvaskő környéki anchimetamorf palaösszlet képződési körülményeiről [Data on the origin of the anchimetamorphic slate sequence at Szarvaskő, NE Hungary]. Annual Report of the MÁFI [Hungarian Geological Institute] from the year 1987, pp. 131-136. (in Hungarian)

Less Gy, Kovács S, Pelikán P, Pentelényi L. and Sásdi L 2005: A Bükk hegység földtana. Magyarázó a Bükk hegység földtani térképéhez (1:50000) [Geology of the Bükk Mts. Explanations to the 1:50000 map of the Bükk Mts]. MÁFI [Hungarian Geological Institute], Budapest, 284 p.

Origin of the peridotites from the Ditrău Alkaline Massif (Romania) by the mineralogy and mineral chemistry

Elemér Pál-Molnár , Enikő E. Almási , Edina Sogrik

Department of Mineralogy, Geochemistry and Petrology, University of Szeged, P.O. Box 651, Hungary (palm@geo.u-szeged.hu, almasieniko@geo.u-szeged.hu)

The Ditrău Alkaline Massif [DAM] is a Mesozoic alkaline igneous complex and situated in the S-SW part of the Ghiurghiu Mountains belonging to the Eastern Carpathians (Romania). Petrographically the DAM is exceptionally diverse, and consists of different types of rocks: peridotites, gabbros, diorites, monzodiorites, monzonites, nepheline syenites, granites, monzosyenites, syenites, quartz syenites, alkali feldspar syenites, lamprophyres and tinguaites. The massif is the result of a long lasting (Middle Triassic – Lower Cretaceous) two phases (Middle Triassic – Upper Triassic and Lower Cretaceous) magmatic process (Pál-Molnár, 2010). The peridotites (hornblendites), gabbros, nepheline syenites and granites belong to the first magmatic phase, the syenites and alkali feldspar syenites derive from the second phase. While peridotites are the most primitive rocks of the DAM, the determination of their mineralogy and mineral chemical composition is essential for understanding the magma processes which formed the DAM. Olivine-pyroxene hornblendite and plagioclase-pyroxene hornblendite from the northern part of the DAM which composition is near to the primitive magma were chosen for investigation.

Cameca SX-50 (accelerating voltage: 15 kV, sample current: 20 nA) electron microscope was used to determine the chemical composition for the all samples.

The main rock forming minerals are amphibole (51–59 wt%), pyroxene (10–32 wt%), plagioclase (3–10 wt%), olivine (0–20 wt%), and a few amount of apatite (0–5 wt%), titanite (2–9 wt%) and opaque minerals (0–4 wt%). Amphiboles are represented by pargasites, kaersutites, ferro-kaersutites and magnesiohastingsites. Pyroxenes are diopsides, aegirin-augites, and augites. Olivine is often altered, its Fo ratio is 74–98%, which refers to crystallization from a relatively primitive magma. The plagioclase is albite (Ab_{78-98}), which is a result of late stage processes.

The crystallization pressure and temperature were calculated by the chemical composition of amphiboles and pyroxenes. Using the correlation of Filippo (2010) amphibole formation is estimated in the max 1000 °C, and 7–10 kbar using the method of Anderson and Smith (1995), Hollister et al. (1987). According to Letterier et al. (1982) Ti vs Al ratio of pyroxenes indicates high pressure crystallization. The pyroxenes formed under the following p-T conditions: max 1150 °C and 18–22 kbar (evaluated by Nimis, 1999). Based on the evaluated pressure and temperature values of amphiboles and pyroxenes magnesiohastingiste and pargasite crystallised max 51 km depth, diopside and augite formed max 67 km depth. The examination of amphiboles and pyroxenes of the DAM peridotites show that the primitive melt derived from the upper mantle, more than 70 km depth. This correlates well with the results of the whole-rock geochemical investigations of the DAM peridotites (Pál-Molnár 2010).

Anderson J.L. and Smith D.R., 1995. The effects of temperature and FO2 on the Al in hornblende barometer Am Mineral, 80(4): 549-559.

Filippo R., Alberto R. and Matteo P., 2010. Stability and chemical equilibrium of amphibole in calc-alkaline magmas: an overview, new thermobarometric formulations and application to subduction-related volcanoes, Contrib. Mineral Petrol, 160, 45-66.

Hollister L.S., Grissom G.C. Peters E.K., Stowell H.H. and Sisson V.B., 1987. Confirmation of empirical correlation of Al in hornblende with pressure of solidification of calc-alkaline plutons. American Mineralogist, 72, 231-239.

Letterier J., Maury R. C., Thonon P., Girard D. and Marchal M., 1982. Clinopyroxene composition as a method of identification of the magmatic affinities of paleo-volcanic series. Earth and Planetary Science Letters, 59, 139-154.

Pál-Molnár E., 2010. Rock-forming minerals of the Ditrău Alkaline Massif. In: Szakáll S, Kristály F Mineralogy of Székelyland, Eastern Transylvania, Romania. Sepsiszentgyörgy; Csíkszereda, 63-88.

Semi-brittle deformation in shear experiments at elevated pressures and temperatures: Implications for crustal strength profiles

Matěj Peč[1], Holger Stünitz[2], Renée Heilbronner[1]

[1]*Department of Geosciences, University of Basel, Basel, Switzerland (matej.pec@unibas.ch)*
[2]*Institutt for geologi, Universitetet I Tromsø, Tromsø, Norway*

Many of the largest earthquakes in the continental crust nucleate at the bottom of the seismogenic layer in depths around 10 – 20 km indicating that the build-up stresses can be released by brittle failure under elevated confining pressures and temperatures. In addition, experimental studies, field observations and theoretical models predict that the strength of the lithosphere should be at its peak around these depths and that the rocks reach maximum compressive strength deforming by "semi-brittle" flow. Thus, the understanding of processes taking place under these conditions is of great interest for a better understanding of the seismic cycle and the rheology of faults in general.

We performed a series of experiments where crushed Verzasca gneiss powder (grain size ≤ 200 μm) with varying water content ("pre-dried" and 0.2 wt% H_2O added) was placed between alumina and Verzasca forcing blocks pre-cut at 45° and weld-sealed in gold and platinum jackets. The experiments were performed at 500, 1000 and 1500 MPa confining pressure, at temperatures of 300°C and 500°C and shear strain rates of ~ 1.5 x 10^{-4} sec^{-1} in a solid medium deformation apparatus (modified Griggs rig). The peak strength of the gouge at 500 MPa confining pressure is similar to that of intact rocks of the same material irrespective of the forcing blocks used. All but one sample show strain hardening in the examined shear strain range (up to ~ 2.6) and we observe that the 300°C experiments are systematically stronger by 100 - 500 MPa than the 500°C experiments, irrespective of the water content. At higher confining pressures (1000 and 1500 MPa) we observe a peak strength at shear strains of ~1 – 1.5 followed by strain weakening which eventually evolves into a steady state flow at a stress level ~ 60-130 MPa lower than peak strength. The strength difference between 300°C and 500°C samples is 200 – 300 MPa and does not increase with increasing confining pressure.

Microstructural observations at different strains show the development of an S-C-C' fabric with C' slip zones being the dominant feature. At low strains, the gouge zone is pervasively cut by closely spaced C' shears containing extremely fine-grained material (< 50 nm grain size). With increasing strain, deformation localizes into less densely spaced C' – C slip zones that develop predominantly in feldspars and show "flow" structures (grain size is below the resolution limit of a field emission SEM). Quartz grains show the least fragmentation and represent the rheologicaly strongest phase. Feldspar grains fracture more easily and are the weakest phase. The development of the microstructure evolves with finite strain and does not show any dependence on temperature.

CL observations and EDX maps show complex changes in chemical composition (especially in Ca, Na and K) of both plagioclase and K-feldspar in highly strained domains indicating that mechanical disintegration of the grains leads also to changes in mineral chemistry even on short time scale (~ 3 hours).

Our results indicate that in "semi-brittle" flow, fracturing produces large amounts of extremely fine-grained and amorphous material, which is a pre-cursor to viscous deformation accompanied by mass-transfer processes in the vicinity of slip zones. We conclude that the observed strength difference at different temperatures is caused by a) dissolution – precipitation creep in the finely fractured feldspars b) viscous flow of the possibly amorphous material in the slip zones, which act simultaneously with fracturing.

New data about structure of the Pieniny Klippen Belt in surroundings of town Púchov (western Slovakia)

Ľubomír Pečeňa

Department of Geology and Palaeontology, Faculty of Science, Comenius University, Mlynská dolina G, 841 05 Bratislava (pecenal@fns.uniba.sk)

The area among the town of Púchov, Biela Voda and Zubák valleys is characterized by a presence of the contact zone between the Pieniny Klippen Belt and the Biele Karpaty Unit (Javorina Member of the Lopeník Formation). This N–S trending contact zone is represented probably by a normal fault where the eastern hanging wall was subsided. The Pieniny Klippen Belt units were thrust on the Biele Karpaty Unit in the following order (from bottom to the top): Czorsztyn, Kysuca, and Klape units. The study area, which is built up by aforementioned tectonic units, was subsided and tilted during the Neogene. Therefore the units of the Pieniny Klippen Belt have the west inclination now. The evidence of normal faulting is supported by westward dipping of bedding, anomalous landscape along the fault and generally straight fault boundary between the Pieniny Klippen Belt and Biele Karpaty Unit. Along this contact zone, the footwall sediments were probably exposed by drag along the normal fault. These are represented by the Upper Cretaceous – Palaeocene Gregorianka breccia, which is composed of clasts of light-grey calpionella limestones of the Pieniny Formation (Biancone facies). The Gregorianka breccia was also found on other places in the study area. However, the breccia from the contact zone was affected by Cenozoic deformation. (Acknowledgements: This study was supported by the Slovak Scientific Agency VEGA under the project No. 1/0388/10.)

The integration of the brittle structures analysis, river terraces asymmetry and travitonics – an approach to detect the Quaternary tectonics (Liptov region, Western Carpathians)

Ivana Pešková[1,2], Jozef Hók[2], Alexandra Sklenková – Hlavnová[3]

[1]Dionyz Stur Institute of Geology, Mlynská dolina 1, 817 04 Bratislava, Slovakia (ivana.peskova@geology.sk)
[2]Faculty of Natural Sciences, Comenius University in Bratislava, Mlynská dolina, pavilion–G, 842 15 Bratislava 4, (peskova@fns.uniba.sk, hok@fns.uniba.sk)
[3]Slovak Museum of Nature Protection and Speleology, Ul. 1.mája, 031 01 Liptovský Mikuláš

The integration of miscellaneous methods such as brittle structure analysis, travitonics and tectonic geomorphology indicate a new approach how to detect the Quaternary dynamics. The term of travitonics implies investigating of the systematic joints or tension fissures in the travertine deposits to determine the active tectonic processes. Travertine and/or tufa deposits are preferentially located along fracture traces, either immediately above extensional fissures or in the hanging walls of normal faults (Hancock et al., 1999).

The travertine occurrences in the Liptov region are situated in the westernmost part of the Liptovská kotlina basin. They overlay the Paleogene sediments as well as fluvial terraces. The age of travertine deposits is Pleistocene and Holocene (Ivan, 1941; Vaškovský and Ložek, 1972). The structural research reveals, that fractures affected the travertines, are oriented generally in NW–SE to NNW–SSE and NE–SW to ENE–WSW direction. The NW–SE to NNW–SSE oriented fractures have been observed in the Pleistocene as well as in the Holocene travertine deposits, while NE–SW to ENE–WSW oriented fractures have been observed only in the Pleistocene travertine. Therefore the NW–SE to NNW–SSE oriented fractures are considered to be the younger then the other one. The both type of fractures must have been originated under the different oriented extension.

The notable feature of the Liptov region is the asymmetric evolution of the fluvial terraces. They are well developed on the southern side of the river Váh valley, on the north there are placed only remnants of the terraces. The fluvial terraces were divided into four groups, the uppermost terrace is considered to be a pre-Quaternary. The asymmetric fluvial terraces are also developed along the southern tributaries. It implies the tectonic activity of faults generally oriented in the E–W and N–S direction during the Quaternary period.

The systematic joints were investigated in the Demänová cave system and its surroundings in the carbonate sediments in the northern slopes of Nízke Tatry Mts. The two directions of joints oriented generally in the NE–SW and NW–SE direction, were measured. The orientation of the cave corridors are conformed to the orientations of joints as well as they are conformed to the travertine fractures.

According to mentioned arguments it is possible to assume the Liptov region was formed under the changing extension stress regime in Quaternary. During the Pleistocene period operated the extension stress axis in N–S direction and during the Pleistocene / Holocene time boundary extension stress axis changed to generally W–E direction. These conclusions are in a good accordance with the preliminary results of orientation of Quaternary extension inferred from travitonics and brittle structure analysis in western part of Slovakia.

This work was supported by the Slovak Research and Development Agency under the contract No. APVV-0158-06.

Hancock P.L., Chalmers R.M.L., Altunel L. and Çakir Z., 1999: Travitonics: using travertines in active faults studies. Journal of structural geology, 21, 903-916.

Ivan Ľ., 1941: Výskyty travertínov na Slovensku. Práce štatneho geologického ústavu, zošit 9, 2□65.

Vaškovský I. and Ložek V., 1972: To the quaternary stratigraphy in the western part of the basin Liptovská kotlina. Geologické práce, Správy 59, 101-140.

Dating of major tectonic events in a complex upper crustal suture/wrench zone (Pieniny Klippen Belt, Western Carpathians)

Dušan Plašienka

Department of Geology and Palaeontology, Faculty of Natural Sciences, Comenius University, Mlynská dolina, 842 15 Bratislava, Slovakia (plasienka@fns.uniba.sk)

The Pieniny Klippen Belt (PKB) separates the External (EWC, Flysch Belt) and Central Western Carpathians (CWC) and forms a narrow, but lengthy suture zone that experienced an extraordinary shortening. Relics of older, latest Cretaceous to Middle Eocene, structures record décollement of post-Triassic PKB units from their fully subducted substratum, thrust-related folding and nappe stacking. Younger, dominantly dextral transpression was associated with the Early Miocene CCW rotation of the CWC block as the eastern part of the ALCAPA megaunit. In general, the tectonic scenario includes a transfer of the PKB units from an accretionary wedge toe to its top-rear, governed by the footwall-propagated thrusting style. In its final position, the original fold-and-thrust belt was subsequently horizontally narrowed and stretched, vertically lengthened, and ultimately brittle bended and disintegrated. The final deformation occurred along a deep-seated boundary between the buttressing ALCAPA block and the foreland European margin loaded by the EWC accretionary wedge, after their soft collision and cessation of convergence. As a result, the near-surface PKB remained fixed to this weak crustal boundary and its intricate internal edifice combines both the early shallow nappe structures and the late, orogen-parallel wrench movements.

In this contribution, an attempt is made at dating of the major PKB tectonic stages by various methods, namely by correlation of existing geochronologic (GC), sedimentary/stratigraphic (SS), burial diagenetic to low-grade metamorphic (MB) and structural/tectonic (ST) data. The following main stages of the post-Lower Cretaceous contractional tectonic evolution are defined: (i) Upper Turonian (ca 90 Ma) emplacement of the frontal Fatric nappe units to the environs of the Vahic and Oravic domains (SS, MB and ST data) followed by oroclinal arching of the outer CWC zones and likely also by large-scale block rotation of the entire CWC orogenic system by some 80° CW due to Adria indentation at ca 90–85 Ma b.p. (ST data, mainly palaeomagnetic); (ii) beginning of subduction of the Vahic Ocean below the CWC orogenic wedge at ca 88–87 Ma (SS, MB data); (iii) synorogenic, piggy-back, Gosau-type growth basins on the leading upper-plate margin (88–45 Ma, SS) sealing the 90 Ma structures; (iv) renewed thrusting of the Fatric and higher complexes over the inner Oravic zones (Kysuca-Pieniny Basin) during 85–80 Ma (SS data); (v) cessation of the Vahic subduction around 70 Ma ago (SS, ST and GC data) due to collision of the CWC wedge with the Oravic ribbon continent; (vi) first thrust event in the Oravic domain (later PKB) – the Pieniny Nappe overrode the foreland Jarmuta Basin of the submerged Czorsztyn Ridge some 70–65 Ma ago (SS); (vii) underthrusting of the Oravic basement below the CWC thrust stack, detachment of the Subpieniny Unit and its thrusting-sliding over the synorogenic Biele Karpaty and Proč Basin (Šariš Unit) along the inner margins of the Magura Ocean (65–45 Ma, SS data); (viii) individualization of the PKB Oravic units, development of the PKB curvature by adjustment to the outer CWC arc with frontal contraction in the western and dextral slicing and lateral translations in the eastern PKB segment, 65–45 Ma, ST palaeostress and palaeomagnetic data; (ix) out-of-sequence thrusting and folding along the CWC/PKB boundary, 50–45 Ma (SS, ST); (x) extensional collapse of the overthickened rear parts of the developing EWC accretionary wedge, foundation of the Central Carpathian Palaeogene Basin (CCPB) some 45–40 Ma ago (SS and ST data); (xi) subduction of the Magura Ocean approximately from 55–50 to 30 Ma, successive forelandward thrusting and stacking of the offscraped Magura units, 40–20 Ma (GC, SS, MB, ST); (xii) additional shortening, dextral transpression and uplift of the PKB, incipient development of the structural flower at the CWC/EWC boundary usually centred by the PKB, inward and outward out-of-sequence oblique reverse faulting along the PKB boundaries – 30–20 Ma, later forced compressional subsidence of the Periklippen part of the CCPB – 20 to 15 Ma (GC, SS, MB, ST); (xiii) a major CCW rotation of the eastern ALCAPA megaunit (CWC+PKB+EWC) by the northward decreasing amount from 80 to 50°, constrained to two phases 18–17 (50°) and 16–15.5 Ma (30°) in the southern CWC zones (GC and ST palaeomagnetic data); (xiv) strong backthrusting south of the northern and eastern segment of the PKB, exhumation and uplift of the Tatra Mts 15–10 Ma ago (GC, ST); (xv) gradual eastward rotation of the stress field related to the eastward shift of the subduction process in the EWC, sinistral transtension in the western PKB, 17–5 Ma (ST); (xvi) NE-ward out-of-sequence thrusting of the Magura Unit, ca 14–12 Ma (SS, MB, ST); (xvii) uplift and erosion of the eastern Periklippen CCPC zone, 12–5 Ma (GC, MB); (xviii) general extensional stress regime, 8–3 Ma. (This work was supported by the Slovak Research and Development Agency under the contracts APVV-0465-06 and APVV-0279-07.)

Shortening features in the late Miocene-Pliocene sediments along the central part of the Mid-Hungarian Mobile Belt

György Pogácsás[1], Györgyi Juhász[2], Norbert Németh[3] Árpád Dudás[1], János Csizmeg[1]

[1]Department of Physical and Applied Geology, Eotvos Lorand University, Pázmány Péter sétány 1/c, Budapest, 1117 Hungary (pogacsasgy@t-online.hu)
[2]MOL Plc, Budapest, Hungary
[3]Department for Geology and Mineral Resources, University of Miskolc, 3515 Miskolc-Egyetemváros, Hungary (foldnn@uni-miskolc.hu)

The Pannonian Basin is underlain by an orogenic collage which is built up by several tectonostratigraphic terrains. The boundary of the two main terrains, the north-western ALCAPA and the south-eastern TISZA, is the Mid-Hungarian Mobile Belt. Each terrains experienced a complex deformation because of hinterland extension spreading toward the accretionary wedge in front of the advancing orogen since the Eggenburgian. Each microplate can be characterized by frontal shortening, wrench zones along sides, and complex normal fault systems inside (Nemcok et al 2006). The faults of the Mid-Hungarian Mobile belt were active through the complete Neogene period, although with changing sense. In the recent stress field the basin shows the signs of a starting inversion (e.g. Bada et al. 2007). Shortening structures are characteristic in the Zala Basin, West Hungary (like Budafa anticline), but also occur in the Late Miocene - Pliocene sedimentary succession of the Duna Tisza Interfluve Area.

Structural analysis was carried out on historical industry seismic sections across and along the Mid-Hungarian Mobile Belt, between the Danube and the Tisza Rivers. Change of the sense of faulting is hard to determine. The structure is dominated by NE–SW or ENE–WSW striking master faults (Fig 1. and Fig 3.) with significant lateral displacements, rooted in the preneogene basement. The orientation of the conjugated faults seems to be controlled by the Preneogene – Early Neogene zones of weaknesses, therefore observed geometry (e.g. flower structure) is not necessarily indicative of the sense of the last displacements, and the direction of the slip may possibly be oblique. However, shortening features are not restricted to inverted faults. Based on seismic reflection pattern shortening related folding and uplifting was observed.

Comparing map of Late Miocen folds with Late Miocene fault map (Fig 2) three structural domains could be identified. The northern domai, situated north of the Mid Hungarian Line is characterised by dominantly ENE-WSW oriented Late Miocene faults. (Paleogene – Mid Miocene structural deformations of this domain see e.g. Csontos and Nagymarosy (1997) and Palotai and Csontos (2010). The central domain, can be found above the western continuation of the Mid Hungarian Flish Belt, is characterised by dominantly NE-SW oriented set of folds. Majority of Late Miocene anticlines have the same orientation as the Late Miocene – Pliocene faults. The southern domain seems to be only slightly folded or almost unfolded (see the southeastern part of seismic line on Fig. 1). This domain is characterised by dominantly ENE-WSW oriented faults. The central and the southern domains seems to be separated by the left lateral Paks-Kisujszállás wrench zone (Pogácsás et al 1989, Lőrincz et al 2002), being active until the Late Quaternary.The overall Late Miocene – Pliocene fault pattern is dominated by wide left lateral wrench fault zones. The main wrench faults seems to be rooted in the mesozoic-paleozoic slices of the preneogene basement. The geometry of the faults active (both in the case of major fault zones and individual faults), remained active during the several changes of the paleo stress field, and many of them were formed conjugated to these. The research work was supported by the Hungarian Scientific Research Fund (OTKA # 047159 and # 060861). Eötvös Loránd University acknowledges support of this research by IES Integrated Exploration Service, a Schlumberger Company via the PetroMod University Grant Program.

Bada G, Horváth F, Dövényi P, Szafián P, Windhoffer G, Cloetingh, S. 2007: Present-day stress field and tectonic inversion in the Pannonian basin. Global and Planetary Change, 58, pp. 165-180.

Csontos L, Nagymarosy A. 1998; The Mid-Hungarian line: a zone of repeated tectonic inversions. Tectonophysics 297. 51–71.

Juhász E, L. Ó. Kovács, P. Müller, A. Tóth-Makk, L. Phillips, M. Lantos 1997; Climatically driven sedimentary cycles in the Late Miocene sediments of the Pannonian Basin, Hungary. Tectonophysics, 282. 257-276.

Juhász Gy, Gy. Pogácsás, I. Magyar 2007; Óriáskanyon-rendszer szeli át a pannóniai üledékeket? (A giant canyon system incised into the Late Neogene (Pannonian s.l.) post-rift sediments? Földtani Közlöny 137/3, 307–326.

Lőrincz K. D, F. Horváth, G. Detzky 2002; Neotectonics and its relation to the Mid-Hungarian Mobile Belt. EGU Stephan Mueller Special Publication Series, 3, 247–266.

Nemčok M, Gy. Pogácsás, L. Pospíšil 2006; Activity timing of the main tectonic systems in the Carpathian – Pannonian Region in relation to the rollback destruction of the lithosphere, in J. Golonka and F. J. Picha, eds., The Carpathians and their foreland: Geology and hydrocarbon resources: AAPG Memoir 84, 743–766.

Palotai M. L. Csontos 2010; Strike-slip reactivation of a Paleogene to Miocene fold and thrust belt along the central part of the Mid-Hungarian Shear Zone. Geologica Carpathica. 61/6. 483-493.

Pogácsás Gy., Lakatos L., Barvitz A., Vakarcs G., Farkas Cs. 1989; Pliocene-Quaternary wrench zones in of the Great Hungarian Plain (Pliocén kvarter oldaleltolódások a Nagyalföldön). Általános Földtani Szemle, 24. 149-169.

Pogácsás Gy., R.E. Mattick, D.P. Elston, T. Hámor, Á. Jámbor, L. Lakatos, M. Lantos, E. Simon, G. Vakarcs, L.Várkonyi, P. Várnai, 1994; Correlation of Seismmo- and Magnetostratigraphy in Southern Hungary. In: Teleki P., J. Kókai, R.E. Mattick eds. Basin

analysis in petroleum exploration, a case study from the Békés basin, Hungary. Kluwer Academic Publisher, Dordrecht, Netherlands, p. 143-160.

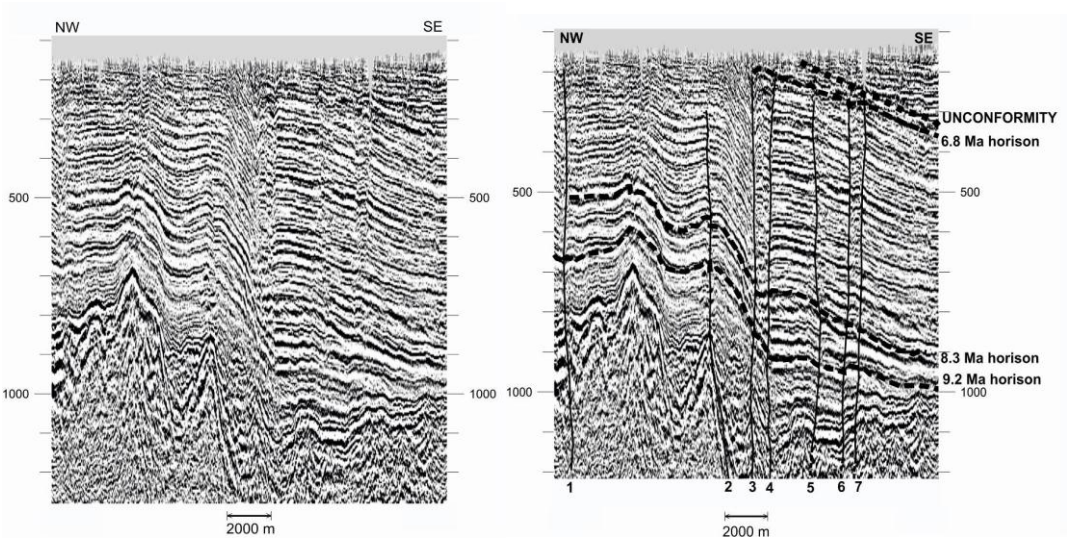

Fig 1 . NW-SE oriented seismic section. Location of the seismic line is indicated on Fig 2. Age data of correlated seismic horisons (9.2 Ma, 8.3 Ma, 6.8 Ma) were based on magnetostratigraphic and radiometric (K/Ar) data from the nearby Kaskantyú-2 and Kiskunhalas-Ny-3 wells (Pogácsás et al 1994). In the case of the Kaskantyú-2 well drilled by continous coring, the top Miocene unconformity (Juhász et. al., 1997) represents a hiatus from 6.2 Ma to 3.9 Ma. This unconformity seems to be not affected by faults of #5, #6, #7. Faults of #3, #4 are strike slip faults being active until the Late Quaternary (Pogácsás et al 1989, Juhasz et al 2007). Seismic features nearby fault #2 are indicating that faulting activity here obviously postdated the shortening related folding. Definition of key chronostratigraphic surfaces (sequence boundaries) and unconformities within the Upper Miocene – Pliocene sediments, allowed the mapping of Late Miocene anticlines (Fig 2). These folds may be connected with thrusting of the Preneogene basement (and accommodation of the unconsolidated cover), with fault ramps and with closure of pull-apart basins.

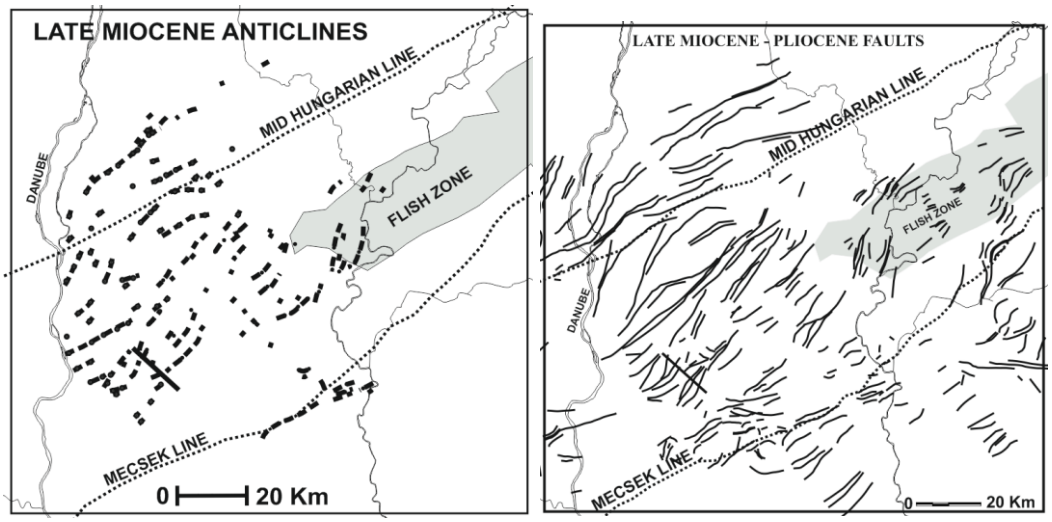

Fig. 2. Correlated Late Miocene folds (axis of anticlines) and correlated (assigned) postrift (undiferentiated Late Miocene-Pliocene) on seismic networks. ENE-WSW oriented folds have been identified on seismic network along and on both sides of the Mid Hungarian Line e.g. above the ALPACA and the TISZA terrains as well. The Mid Hungarian Flish Belt is supposed to be underlain by transitional crust and it is considered to represent a wide zone of weaknesses. Seismic section presented on Fig 1. is perpendicular to both the Mecsek line and the Mid Hungarian Line.

Slip history of the Hluboká fault derived from structural data and 3D modelling of the Budějovice Basin

Clemens Porpaczy, Dana Homolová, Kurt Decker

Department of Geodynamics and Sedimentology, Center for Earth Sciences, University of Vienna, Althanstraße 14, 1190 Vienna, Austria (clemens.porpaczy@europe.com; dana.homolova@univie.ac.at; kurt.decker@univie.ac.at)

Situated in the Bohemian Massif in southern Czech Republic, the Budějovice Basin represents a fault-bounded sedimentary basin delimited by NW-SE and NNE-SSW striking fault systems. The sedimentary basin fill consists of Upper Cretaceous (Klikov Formation) and Miocene fluvial and limnic sediments (Zliv and Mydlovary Formation). The depocenter of the Budějovice Basin is located in its south-eastern part with an overall depth of 340 m below surface. The Hluboká-Fault zone, belonging to a NW-SE striking fault system, confines the basin to the NE, partly appearing as a morphological scarp in the landscape.

The aim of this study is to get new insights into the poorly known kinematic history and the timing of fault activity of the Hluboká-Fault Zone by investigating structural features along the fault. Therefore, structural data were collected from ductile (foliation, folds and stretching lineation) and brittle structures (faults, slickensides, tension gashes etc.) in 30 outcrops situated at or in the vicinity of the Hluboká-Fault Zone. In order to obtain information on the ages of the different fault movement events, data were collected from outcrops located in crystalline basement rocks as well as in Permian, Cretaceous and Miocene sediments of the Budějovice Basin. In addition, a 3D model of the Budějovice Basin was compiled in order to assess the vertical slip history of the Hluboká Fault for the time intervals post-Cretaceous, post-Neogene and Quaternary. The assessments use the thickness and distribution of Cretaceous, Neogene and Quaternary sediments. Drilling reports from the Czech Geological Survey in Prague (Geofond), geological maps of the region (1:25 000) and a high resolution DEM were used for modeling the 3D basin geometry as well as the thickness of the Upper Cretaceous and Neogene sediments. The current basin model is based on subcrop information from 994 wells.

According to the available subcrop information the sedimentary basin fill mostly consists of Upper Cretaceous freshwater sediments of the Klikov Formation, ranging in thickness up to 320-340 m. The overlying Neogene Sediments reach an average thickness of about 20-30 m. Interpretations of the 3D basin model show that the crystalline Basement plunges towards the Hluboká Fault at eastern border of the basin with a dip of approximately 5°. There, the Hluboká Fault offsets the crystalline Basement vertically for more than about 420 m. Data show that the fault steeply dips towards SW with approximately > 65°.

Information obtained from structural field data and thin section analyses indicates that the first movement of the Hluboká-Fault System occurred at low to very low metamorphic conditions in late Variscan times. The ductile structures are overprinted by brittle faults. These include sub-vertical strike-slip faults striking parallel to the Hluboká-Fault with dextral sense of shear - found in most of the outcrops - and brittle normal faults and mineralized extension gashes striking parallel to the fault and revealing SW-directed extension. The occurrence of tension gashes in both, Variscan phyllite, Permian sediments and Cretaceous shales suggests post-Cretaceous deformation age. Normal faults striking parallel to the Hluboká Fault were observed in Permian and Cretaceous sediments at the eastern margins of the basin. Brittle strike-slip faults were recorded in Variscan basement rocks, Cretaceous and Miocene sediments.

The kinematical data obtained from the Hluboká Fault prove that the fault formed in Late Variscan times. The fault was reactivated as a dextral strike-slip fault during generally N-directed compression in the foreland of the Alpine orogen during and probably after the Neogene.

Crustal structure of mid-crustal channel flow: example from east European Variscides, the Bohemian Massif

Martin Racek[1, 2], Karel Schulmann[3], Ondrej Lexa[1, 2], Pavla Štípská[3], Michel Corsini[4], Jan Košler[5], Urs Schaltegger[6], Pavlína Hasalová[7], Alexandra Guy[3]

[1]*Institute of Petrology and Structural Geology, Charles University, Albertov 6,128 43 Praha 2, Czech Republic (racek@natur.cuni.cz)*
[2]*Czech Geological Survey, Klárov 3, Prague 1, Czech Republic*
[3]*Institute de Physique de Globe, UMR 7516, École et Observatoire de Science de la Terre, Université de Strasbourg, 1 Rue Blessig, Strasbourg 67084, France*
[4]*GéoAzur, CNRS Université de Nice Sophia Antipolis (UMR6526), 28 Av. de Valrose, BP 2135, 06103 Nice Cedex 2, France*
[5]*Centre for Geobiology and Department of Earth Science, University of Bergen, Norway*
[6]*Earth Sciences, University of Geneva, rue des Maraîchers 13, 1205 Geneva, Switzerland*
[7]*School of Geosciences, Monash University, Clayton, Victoria 3800, Australia*

Detailed structural study compares two contrasting regions along the eastern margin of the Bohemian Massif: 1) mid-crustal unit represented by Drosendorf window is surrounded by partially molten rocks of lower crustal origin and, 2) the lower crustal unit of the St. Leonhard granulite massif surrounded by migmatitic Gföhl orthogneiss and mid-crustal metasedimentary sequence of Varied group. The study reveals existence of two main metamorphic fabrics that can be distinguished in the whole studied area. Early steep foliation connected with prograde metamorphism in mid-crustal units and exhumation of the lower crustal units is reworked by flat lying amphibolite facies fabric.

In the area of Drosendorf window, the NNE-SSW trending steep fabric is best preserved in the central part of the mid-crustal domain and it is reworked by the flat foliation with increasing intensity towards margins. This later flat deformation is associated with NNE-vergent horizontal ductile flow in surrounding high grade rocks. The deformation pattern as folding at high stress side of the mid-crustal boudin and normal shearing in low stress sector are compatible with deformations originating in viscous flow around rigid inclusions.

The most important feature of the area of the St. Leonhard granulite massif is systematic variation of the steep foliation direction. This fabric is approximately NNE-SSW trending in the external part of the domain, namely in the mid-crustal units in agreement with steep fabric trend of the whole eastern margin of the Bohemian Massif. However, it progressively changes its direction to E-W in the central part (St. Leonhard granulite massif and adjacent high-grade rocks). The superposed subhorizontal NNE-verging flow results in formation of intensive E-W trending intersection lineation in the central area that is perpendicular to the main transport direction.

The gravity survey of the eastern margin of the Bohemian Massif shows an existence of gravity high corresponding to Brunovistulian domain lying underneath partially molten rocks. This indicates that these rocks occur in hangingwall of rigid basement in an area of several thousands square kilometers. The internal steep fabrics inside mid-crustal units are geometrically concordant with the NNE-SSW trending hidden basement – lower crust boundary. Nearly orthogonal direction of steep fabrics in the St. Leonhard massif can be interpreted as a consequence of N-S shortening resulting in crustal scale folding of originally NNE-SSW trending deep orogenic fabric during the highly oblique indentation of Brunovistulian promontory. The steep and flat fabrics are therefore interpreted as a result of kinematic continuum resulting from progression of rigid promontory against weak and passively folded lower and middle crust that are both thrust over the basement in form of orogenic channel-flow.

Several geochronological studies were carried out in order to constrain the timing of described processes. The U-Pb ages of zircons from intermediate granulite of St. Leonhard massif obtained by ion probe give ages with significant peak at 340 Ma. The Ar-Ar ages of hornblendes and biotites separated from samples from different crustal levels across the whole studied area give ages of 340 (hbl) and 330 (bi) Ma. U-Pb ages of monazites from the structurally underlying Gföhl orthogneiss outcropping north from the studied area give values of c. 335 Ma. These data indicate that the main metamorphic event (340 Ma, zircons in granulite) was followed by very rapid exhumation below the hornblende closing temperature resulting in attachment of this unit to upper crustal lid above the zone of active flow. However the younger monazite ages show that the underlying flowing masses were still at least next 5 Ma in the channel flow structure, providing enough of heat to keep its roof in the temperatures above the closing temperature of biotite for next 10 Ma. (The project is supported by the Czech Science Foundation (P210/10/P475)).

Analogue modelling of the tectonic evolution of Polish Outer Carpathians – influence of indenter shape

Marta Rauch

Polish Academy of Sciences, Institute of Geological Sciences, Wroclaw Research Centre, Podwale 75, 50-449 Wrocław, Poland (ndrauch@cyf-kr.edu.pl)

The analogue modelling is a tool to study the tectonic evolution of the single structure or the whole orogen by testing different hypotheses. During experiment the influence of the different primary parameteres of experiment and boundary conditions on the particular model are tested.

The object of the presented investigation is arcuate Outer Carpathian belt (Fig. 1). The influence of the different shape of the indenter/ALCAPA block for the outline and internal structure of the experimental wedge was tested. According to Marshak (2004) the indenter is a one of the parameters potentially controlling the evolution of curved fold-and-thrust belt.

The Outer Carpathians are the external pile of nappes of the Pannonian-Carpathian-Dinaric system (Fig. 1A). The most northern segment of the Outer Carpathians belongs to Poland (Fig. 1B), it is mostly the Western Outer Carpathians. Western and northern part of the Eastern Carpathians was strongly dependent on the north- and/or eastward indentation by the ALCAPA block (Kováč et al., 1994; Fodor et al., 1999; Nemčok et al., 1998). The Western Carpathians are divided into Outer and Inner Carpathians by the Pieniny Klippen Belt (Książkiewicz, 1977). The Pieniny Klippen Belt is an intensely deformed, narrow, and nearly 600 km long shear zone made up of a pile of nappes, which are composed of Mesozoic and Palaeogene sedimentary rocks (Birkenmajer, 1996). The sediments of Outer Carpathian basins were accreted gradually forming the accretionary prism, starting from the inner part (Magura nappe) towards foreland (Skole nappe and Zgłobice Unit). In the Magura nappe the deformation started in Palaeogene (Tokarski and Świerczewska, 1998). In Paleogene the northern boundary of the ALCAPA block was the Pieniny Klippen Belt (Fodor et al., 1999).

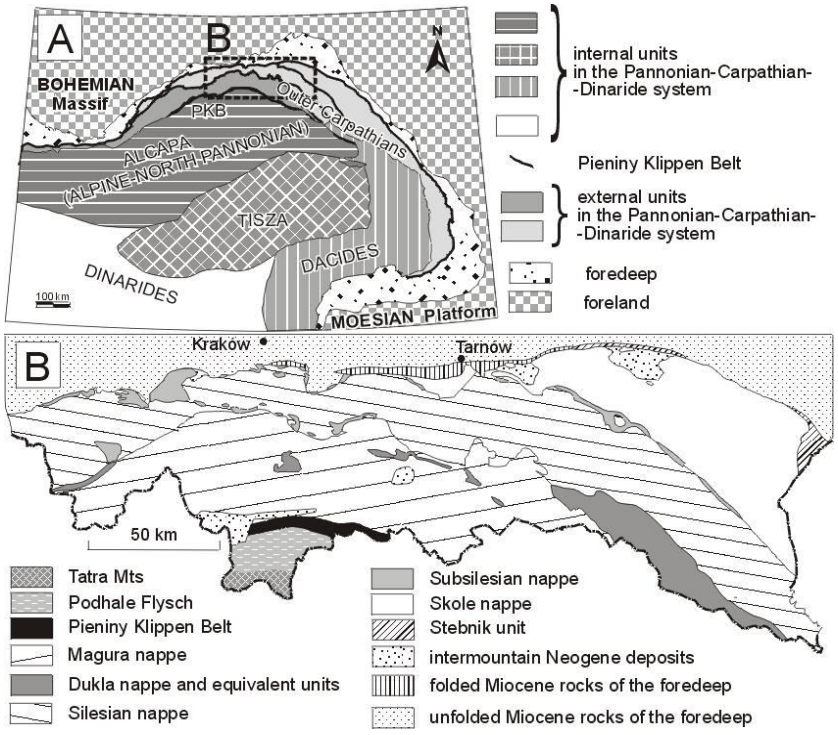

Fig. 1. Map of the Pannonian-Carpathian-Dinaride system after Csontos et al. (1992) (A) and Polish part of the Outer Carpathians (Książkiewicz, 1977) (B).

The Polish Western Outer Carpathians is a north-verging fold-and-thrust belt (Fig. 1). The main structure of this belt was formed during the Palaeogene and Neogene, when the Outer Carpathians was an accretionary wedge (Oszczypko, 2006). The belt is composed of Upper Jurassic to Lower Miocene strata and comprises several nappes (Książkiewicz, 1977). Two of these nappes, the Magura and Silesian nappes, extend along the entire belt. The other nappes are exposed mostly in the eastern part of the Polish Western Outer Carpathians.

The experiments were made in the TectoModel Lab Wroclaw, in the Institute of Geological Sciences Polish Academy of Sciences. The physical models were built using sand as analogue material to represent the brittle upper crust. The modelling was carried out using the layers about the different colour. The different shape of indenter were tested: 1) rectangular; 2) triangular (130° angle of apex); 3) triangular (90° angle of apex) and 4) quasi-triangular resembling the Palaeocene shape of the ALCAPA block in preset-day position. The material used for the modelling was quartz sand. The density of sand was 1.55 g/cm3. The cohesion of the sand was 23 kPa and the internal friction of the sand was 28º.

All experiments created the curved thrust wedges with the curved convexly thrust fronts. The curvature of the thrust wedge are imitating approximately the curvature of indenter shape. In the (1) experiment with the rectangular indenter the wedge was the least curved. The pushing of the indenter was normal to the leading margin of the indenter. The trace lines of the inner thrusts were nearly straight, parallel to the leading margin of the indenter. The thrust front was slightly convex to foreland. This experimental wedge was not enough arcuate comparing the Polish Outer Carpathians.

In the rest of the experiments, (2, 3) with the triangular or (4) with the quasi-triangular indenters, the wedges were more curved imitating approximately the curvature of the particular indenter shape. However, when the displacement of the indenter was increasing the experimental wedge was becoming progressively less curved. Namely, the thrust front was becoming less curved. Nonetheless the trace lines of the inner thrusts were still curved. Their curvature imitated more or less the curvature of indenter shape. The curvature of the indenter in the (2) experiment was almost the same as the curvature of the Polish Outer Carpathians. The (3) experiment created to much curved wedge. The (2) and (3) experimental wedges were symmetrically, what is in contradiction to the natural example. The outline of the (4) experimental wedge best reminded the outline of the Polish Outer Carpathians. This model was enough asymmetrical. However, the western part of the Polish Outer Carpathians is narrower, than the eastern one. Moreover, in the eastern part of the Polish Outer Carpathians, an additional nappe exists - the Skole nappe, which is disappearing westward.

The results of the present modelling suggest that the most proper for the experiments is an asymmetric, quasi-triangular shape of the indenter, which should be resembling to the shape of the present-day, Palaeogene margin of the ALCAPA block. However, the experimental wedge from the (4) experiment is still not enough similar to the natural example. Therefore, the modelling must be continued. The another parameters of the experiment should be tested such as the different direction of the indentation and/or the different basal friction etc. (This research was supported by Polish Ministry of Science and Higher Education Grant no. N N525 363637.)

Birkenmajer K., 1986. Stages of structural evolution of the Pieniny Klippen Belt, Carpathians. Studia Geologica Polonica 80, 7-32.

Csontos L., Nagymarosy A., Horváth F., Kováč M., 1992. Tertiary evolution of the Intra-Carpathian area: a model. Tectonophysics 208, 221-241.

Fodor L., Csontos L., Bada G., Györfi I., Benkovics L., 1999. Tertiary tectonic evolution of the Pannonian basin system and neighbouring orogens: a new synthesis of palaeostress data. In: B. Durand, L. Jolivet, F. Horvát., M. Séranne. (Eds.), The Mediterranean Basins: Tertiary Extension within the Alpine Orogen. Geological Society, London, Special Publications 156, pp. 295-334.

Marshak S., 2004. Salients, recesses, arcs, oroclines, and syntaxes – A review of ideas concerning the formation of map-view curves in fold-thrust belts. In: K. R. McClay, (Ed.) Thrust tectonics and hydrocarbon systems: AAPG Memoir 82, p. 131-156.

Nemčok M., Pospisil L., Lexa J., Donelick R.A., 1998. Tertiary subduction and slab break-off model of the Carpathian–Pannonian region. Tectonophysics, 295: 307–340.

Kováč, M., Král, J., Márton, E., Plašienka, D., Uher, P., 1994. Alpine uplift history of the Central Western Carpathians: geochronological, paleomagnetic, sedimentary and structural data. Geologica Carpathica 45, 83-96.

Książkiewicz M., 1977. The tectonics of the Carpathians. In: Geology of Poland. Volume 4: Tectonics. Geological Institute, Warszawa, 476-669.

Oszczypko N. 2006. Late Jurassic-Miocene evolution of the Outer Carpathian fold-and-thrust belt and its foredeep basin (Western Carpathians, Poland). Geological Quarterly, 2006, 50 (1): 169–194.

Tokarski A. K., Świerczewska A. 1998 – History of folding in the Magura nappe, Outer Carpathians, Poland. In: H.-P Rossmanith,. (Ed.), Mechanics of Jointed and Faulted Rocks. Balkema, Rotterdam, 125-130.

Nature and petrogenesis of topaz-bearing granites - a case study of the Krudum granite body (Slavkovský les Mts., Czech Republic)

Miloš René[1], Vojtěch Janoušek[2,3], Zuzana Kratinová[4], Matěj Machek[4], Žofie Roxerová[4]

[1]*Institute of Rock Structure and Mechanics AS CR, v.v.i, V Holešovičkách 41, 182 09 Prague 8, Czech Republic (rene@irsm.cas.cz)*
[2]*Czech Geological Survey, Klárov 3, 118 21 Prague 1, Czech Republic (vojtech.janousek@geology.cz)*
[3]*Institute of Petrology and Structural Geology, Charles University, Albertov 6, 128 43 Prague 2, Czech Republic*
[4]*Institute of Geophysics AS CR, v.v.i, Boční II/1401, 141 31 Prague 4, Czech Republic (kratinova@ig.cas.cz)*

Topaz-bearing leucogranites represent a clan of highly differentiated rocks that often contain economically significant concentrations of incompatible elements (Rb, Li, Cs, Sn, Nb, Ta, and W) but whose origin remains largely enigmatic. As a target of our complex study was chosen the Krudum granite body (KGB, c. 50 km^2), a subsidiary intrusion of the Karlovy Vary–Eibenstock Pluton. The KGB shows a markedly concentric structure; the centre is formed by Kfs-phyric Třídomí (Mu–) Bt granite, surrounded to the NW by younger, Tpz-bearing, two-mica Milíře granite. The outermost shell is formed by the youngest, Tpz–Ab Čistá granite. The inner structure of the SE edge of the KGB, partly overlain by the Slavkov Crystalline Unit, is well stratified, comprising variably greisenized Čistá granites occurring also in the Hub and Schnöd granite stocks hosting a world-famous Sn–W mineralization.

Two distinct AMS planar fabrics have been recognized. The main, subhorizontal one with a tendency to dip to SE and NW, is of magmatic origin and present in all granite types. Locally developed second fabric dipping steeply towards NE and SW is geometrically related to the late regional faults. The magnetic susceptibility in all granite types falls into the range $30–130\times10^{-6}$ (SI). In highly altered zones the susceptibility drops to negative values, while the magnetic fabric maintains its orientation. The measured thermomagnetic curves imply paramagnetic minerals as the main magnetic fabric carriers.

From geochemical point of view, the non-mineralized Třídomí, Milíře and Čistá types are subaluminous to strongly peraluminous (A/CNK = 1.03–1.52) (leuco-) granites (SiO_2 = 71.2–75.7 wt. %) which form, to a large extent, a compositional continuum. The degree of fractionation increases in this sequence, i.e. outwards. Therefore, the KGB is reversely zoned. Going from Milíře to Čistá granites, the A/CNK values increase, while the K, Ba, Sr and Zr contents as well as K/Rb, Ba/Sr and Zr/Hf ratios drop dramatically. Also the chondrite-normalized patterns get flatter (LaN/YbN = 4.0–8.1 vs. 1.1–3.8), total REE contents sharply decrease (53.4–271.1 to 6.4–64.5 ppm) and Eu anomaly deepens (Eu/Eu* = 0.41–0.21 to 0.71–0.03). The trace-element modelling indicates that the observed trends can be explained by extensive (at least 40–60 %) fractionation driven mainly by K-feldspar. Important role of accessory phases, most importantly Zrn and Mnz, are clear in view of the sharp decrease of Zr, LREE and HREE contents with fractionation. The fractional crystallization had to have been accompanied by variable degrees of country-rock assimilation and perhaps also alkalis loss to account for the sharp increase in the A/CNK values.

The inner structure of the south-eastern edge of the KGB is well stratified; the Čistá granite occurs in its upper, and leucocratic Tpz–Ab granite with subhorizontal layers of alkali-feldspar syenite in its lower parts. Both rock types form also the Vysoký Kámen stock. The uppermost part of the Hub stock is built by a pipe of gneissic breccia cemented by Tpz–Ab microgranite, which is, compared with the Čistá granite, enriched in Al (A/CNK = 1.1–1.6), F (0.3–2.0 wt. %), Na (1.1–7.4 wt. % Na_2O), Rb (91–3500 ppm) and Li (237–1130 ppm). Leucocratic Tpz–Ab granite is, on the other hand, depleted in Y (4–6 ppm), Zr (20–26 ppm) and ΣREE (7–13 ppm). The alkali-feldspar syenite was described as feldspathite in some papers (e.g., Jarchovský 2006), but this name does not agree with the magmatic nature of this rock. Compared to the Čistá granite it is considerably enriched in Na (4.6–9.3 wt. % Na_2O) and K (6.5–7.8 wt. % K_2O), but depleted in Si (64.0–66.5 wt. % SiO_2) and has a distinctly lower A/CNK value (1.0–1.2). The residual origin of the alkali-feldspar syenite is reflected in its low K/Rb ratio (32–36).

The KGB represents a reversely zoned body with the oldest, least fractionated types in the centre. The zoning is not decipherable from the structural and magnetic record, which are both uniform throughout the body. On the SE edge of KGB, within the Hub and Vysoký Kámen stocks, the geochemical and magnetic properties of the most fractionated, mineralized leucogranites were strongly modified by late- and post-magmatic fluid-related processes (feldspathization and fluoritization).

Acknowledgements: This project was funded by the Czech Science Foundation (Project No. 205/09/0540).

Jarchovský T. 2006. The nature and genesis of greisen stocks at Krásno, Slavkovský les area – western Bohemia, Czech Republic. J. Czech Geol. Soc. 51, 201–216.

Geophysical pattern of the Rožná – Olší Uranium ore district and its surroundings

Jiří Sedlák[1], Ivan Gnojek[1], Stanislav Zabadal[1], Jiří Slovák[2]

[1]*Miligal, s.r.o., Axmanova 531/13, 623 00 Brno, Czech Republic (miligal@miligal.cz)*
[2]*Správa úložišť radioaktivních odpadů, Dlážděná 6, 110 00 Praha 1, Czech Republic (slovak@rawra.cz)*

The Rožná - Olší uranium ore district is situated in the easternmost part of the Moldanubian Zone near the tectonic boundary between the Strážek (Moldanubian) Unit and the Svratka Crystalline Unit. Generally, the district comprises several nearly tectonically predisposed parallel mineralized zones up to 12 km long elongated in the NNW-SSE direction. The district is composed by two deposits (sub-districts, see Fig. 1): 1. NW Rožná deposit and 2. SE Olší deposit.

Ore bodies of economic value have been proved to the depth of 1200 m. Approximately 7 km long and 1,5 km wide NNW-SSE oriented granulite body plays the role of a wedge which unclinches the NW Rožná deposit from the SE Olší deposit. Predominant host rocks of mineralized zones are paragneisses, migmatized paragneisses and amphibolites; the surrounding Strážek (Moldanubian) Unit more embraces migmatites, orthogneisses, intercalations of marmors and erlanes and small bodies of peridotites to serpentinites. The Svratka Crystalline Unit - eastwards of the district - is composed by mica schists, paragneisses, migmatites, orthogneisses, intercalations of marmors, erlanes and quartzites and small skarn and serpentinite bodies. The tectonic contact of the Svratka and the Strážek Units plunges steeply westwards.

Eight geophysical maps result from a detailed ground gravity survey (based on 4-5 gravity stations per 1 km^2) and from a detailed airborne magnetic and gamma-ray spectrometric survey (parallel flight lines of mutual distance 250 m).

The Uranium concentration map mostly reflects man-made distribution of uranium, e.g. radioactive pollution caused by mining and processing of the U-ores. The main natural U distribution effects are: a) local U-lows on basic bodies (amphibolite, peridotite, serpentinite), b) more extent U-low on granulite body and c) U-high pertaining to a durbachite body in the S.

The map of Potassium concentraration shows a monotonous K-distribution in the prevailing part of the Strážek Unit. The rather more varied K-distribution is in the Svratka Unit where migmatites and orthogneisses create K-high while mica schists, amphibolites and serpentinites produce K-lows. A striking K-high (3 - 4.5 per cent K) follows the granulite body.

The Thorium concentration map mostly demonstrates a monotonous Th-distribution on majority of both Strážek and Svratka Units. Notable Th-lows follow basic bodies but the extreme Th-low (< 2 ppm Th) is produced by the granulite body. The most remarlable Th-high pertains to the durbachitic body (in the S). Moderately increased Th concentrations in the SW corner of the map belong to migmatites and orthogneisses.

Results of the airborne magnetic survey are presented on two maps: *a*) ΔT magnetic anomalies in the level of 80 m above the ground and *b*) horizontal gradient of the ΔT magnetic anomalies. Majority of the magnetic anomalous rocks was found within the Strážek Unit. Large amphibolite to granitized amphibolite bodies as well as sets of amphibolite intercalations inside the paragneiss and migmatite sequences prevail among them. Peridotite bodies are rare. Local magnetic anomalies sticking out in the presented segment of the Svratka Unit belong to small skarn and serpentinite bodies. Marginal parts of the magnetic source bodies are emphasized by horizontal gradients of magnetic anomalies.

Gravity survey results: Predominant feature of the Bouguer anomalies is a regional W-E decrease of the Bouguer values from the gravity high of the Strážek Unit to the gravity low of Svratka Unit and finally to the Moravian Unit (Moravicum) low being outside of the map in the E. The map of residual gravity anomalies - obtained by removal of the regional trend from Bouguer anomaly values - distinguishes individual gravity structures both in the Strážek and in the Svratka Units. The most remarkable gravity highs reflect extent amphibolite bodies, next mostly elongated gravity elevations pay attention to accumulations of amphibolite intercalations inside the paragneisses and migmatites in the Strážek Unit or within mica schist sequences in the Svratka Unit. Shallow gravity minima ~ -1 mGal reflect pearl gneisses, migmatites and orthogneisses, the most striking gravity low exceeding -1.5 mGal pertains to the granulite body W-wards of the Olší deposit. The most distinct Linsser density indications follow both tectonic and lithologic boundaries and they delimit amphibolites

Gnojek I., Sedlák J., Zabadal S., 2010. Strukturně geologická interpretace geofyzikálních měření 1:25 000 v nejbližším okolí lokality Skalka. Závěrečná zpráva. – MS SÚRAO, Praha.

Ondřík J., Hlisnikovský K., Hájek A,, Nohál M., Souček K., Staš L., Martinec P., Mazuch J., Fiala I., 2010. Skalka – digitální geologické mapy. – MS SÚRAO, Praha.

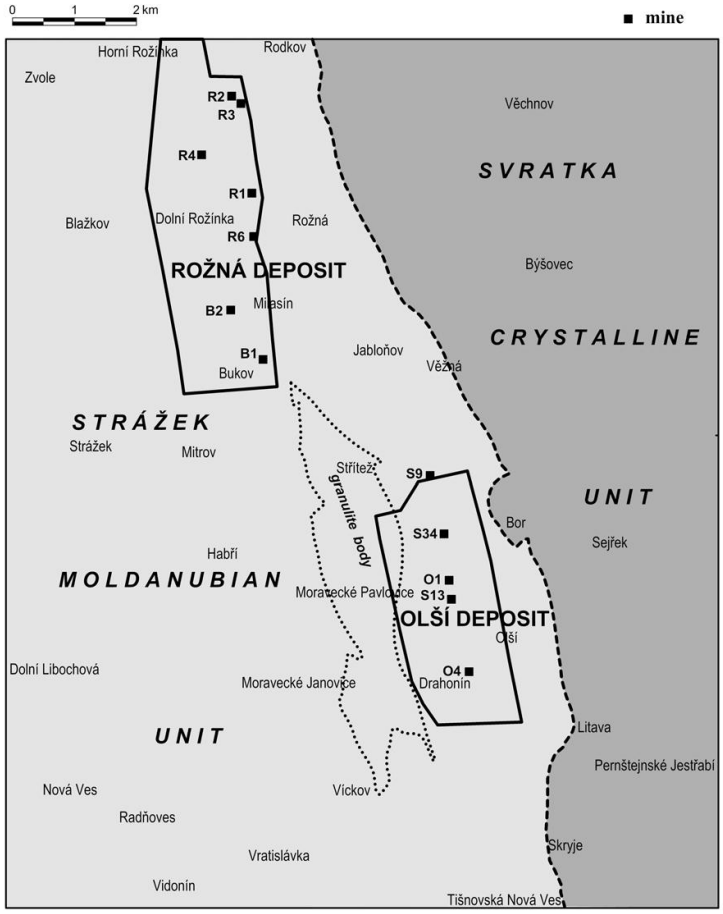

Fig. 1. Rožná - Olší uranium ore district location.

Reverse structures inferred from the geological and structural mapping (western part of the Krivánska Fatra Mts., Slovakia)

Michal Sentpetery

Comenius University in Bratislava, Faculty of Natural Sciences, Department of Geology and Palaeontology, Mlynská dolina 842 15, Bratislava, Slovakia (sentpetery@fns.uniba.sk)

Krivánska Fatra Mts. is situated in the northern part of the Central Western Carpathians within the Tatra-Fatra mountain belt. Position of the Krivánska Fatra Mts. is attractive due to immediate tectonic contact with the Pieniny Klippen Belt – an extremely complicated tectonic zone at the boundary of the Externides and the Internides of the Western Carpathians. The geological and tectonic setting of the Krivánska Fatra Mts. is composed by the several superposed Paleo-Alpine (Cretaceous) tectonic units – the lowermost Tatricum basement/cover unit, which is overthrusted by the nappes of the Fatricum and Hronicum tectonic units. This paleoalpine structure is typical top to the north-northwest tectonic displacement. It was documented in the eastern part of the Krivánska Fatra Mts., where so called "Lysica duplex" occurred in Mesozoic sequences of the Fatricum unit (Matějka, 1931; Haško & Polák, 1978; 1979). However, another dominant structure of the Krivánska Fatra Mts., "Medzirozsutce overthrust", shows the opposite – southward vergency (e.g Matějka, 1931; Haško & Polák, 1978; 1979; Marko et al., 2005). Along this structure with the generally W-E direction, the Hronicum dolomites of the northern block of the Malý Rozsutec and the Neocomian of the Fatricum overthrusted the Palaeogene sediments and the block of the Veľký Rozsutec. In the western part of the mountain range is located an immediate tectonic contact between the Jurassic and Cretaceous of the Kysuca group of the Pieniny Klippen Belt and the dolomites of the Hronicum unit. Other south-vergent structures are documented within the Central Carpathian Palaeogene sediments and the lithotectonic units of the Pieniny Klippen Belt as well as tectonic units of the Externides in northern surrounding of the studied area. The age of the south-vergent structures is considered as Early Miocene (e.g. Potfaj et al., 1993; Marko et al., 2005; Pešková et al., 2009). Despite all this, since 1979, a minimum attention was pay to this territory. For the tectonic interpretation of this area without drilling, not many previous geophysical survey and quarries, revision of a geological map was necessary. The approach based on detail geological and structural mapping, kinematic analysis and constructing a series of cross-sections reveal top to the south structures also in western part of the Krivánska Fatra Mts. (Acknowledgement: I would like to thank to the Grant UK no. UK/19/2010 for the financial support.)

Haško J. & Polák M. 1978: Geological map of the Kysucké vrchy and the Krivánska Malá Fatra Mts., 1: 50 000. Geologický ústav Dionýza Štúra, Bratislava.

Haško J. & Polák M., 1979: Explanations to the geological map of the Kysucké vrchy hills and Kriváň part of the Malá Fatra Mts., 1:50 000. Geologický ústav Dionýza Štúra, Bratislava, 145 p. (in Slovak, English summary)

Marko F., Vojtko R., Plašienka D., Sliva Ľ., Jablonský J., Reichwalder P., Starek D., 2005: A contribution to the tectonics of the Periklipen zone near Zázrivá (Western Carpathians). Slovak Geol. Mag., 11, 37 – 43.

Matějka A., 1931: La partie orientale de la Malá Fatra. in: Matějka, A., Andrusov, D. (Eds), Guide des excursions dans les Carpathes occidentales. Knih. St. geol. ústavu Čs. rep., 13A, 303–316. (In France)

Pešková I., Vojtko R., Starek D., Sliva Ľ., 2009: Late Eocene to Quaternary deformation and stress field evolution of the Orava region (Western Carpathians). Acta Geologica Polonica, 59, 1, 73 – 91.

Potfaj M., Novák J., Káňová M., Kolman L., Vomáčková R., 1993: Geologický projekt vrtu „Vadičov". Čiastková záverečná správa. Manuskript – Archív Štátneho Geologického ústavu Dionýza Štúra, Bratislava, 27 strán, 2 prílohy. (In Slovak)

Linking Rheno-Hercynian ocean and Variscan root processes in the Bohemian Massif

Karel Schulmann[1], Jean-Bernard Edel[1], Ondrej Lexa[2], Vojtěch Janoušek[3,2], Robin Shail[4], Brian Leveridge[5], Richard Scrivener[5]

[1]*Université de Strasbourg, EOST, Institute de Physique de Globe 7516, 1 Rue Blessig, 67 000 Strasbourg, France (schulman@unistra.fr)*
[2]*IPSG, Faculty of Science, Charles University in Prague, Albertov 6, 120 00 Prague 2, Czech Republic*
[3]*Czech Geological Survey, Klárov 3, 118 21 Prague 1, Czech Republic*
[4]*Camborne School of Mines, School of Geography, Archaeology and Earth Resources, University of Exeter, Cornwall Campus, Penryn, TR10 9EZ United Kingdom*
[5]*British Geological Survey, Keyworth, Nottingham NG12 5GG United Kingdom*

The formation of the Rhenohercynian oceanic crust, initiated with late Lochkovian rift-related terrestrial sedimentation and bimodal magmatism and followed by continued lithospheric extension, resulted eventually in the exhumation of mantle peridotites and limited Emsian–Eifelian seafloor spreading marked by deep marine sedimentation. Sedimentological and provenance data from the Gramscatho Group, and the geochronology of Lizard Complex magmatism and metamorphism, are consistent with the progressive, predominantly frontal, accretion of the distal passive margin during the Givetian to Famennian. Continental collision stage is marked by emergence of nappes comprising, upwards, deep marine sedimentary and volcanic rocks, oceanic lithosphere and pre-rift basement (Lizard and Giessen nappes) and upper plate high-grade gneisses (Normannian High and Mid-German Crystalline Rise) onto the northern passive margin by the earliest Carboniferous. Final "docking" event resulted in late Westphalian D2 deformation across SW England and Rhine Massif as well as contemporaneous inversion of the Culm and North Devon basins at about 320–310 Ma.

How can be these events related to what happened in a remote Bohemian Massif orogenic domain located east of Saxothuringian continent and easterly dipping Teplá subduction zone? We suggest that the exhumation of Münchberg and Mariánské Lázně ophiolites along Teplá suture coincided with above-mentioned acceleration of extension in the Rhenohercynian Basin hinterland in Emsian and Eifelian times. The transition of passive margin formation to oceanic break up is related to extreme increase in spreading velocities (from several millimeters up to 5 or 10 centimeters in case of slow or rapid rifts, respectively). This event must have been related to increase in horizontal push force in the Saxothuringian continent and transmission of horizontal stress to subducting Saxothuringian passive margin far in the east. Resulting increase in the subduction rate should have not only brought large amounts of fertile, fluid-rich oceanic material into the subduction zone, but also meant acceleration of sub-'Barrandian/Moldanubian" mantle wedge movements transporting eventually fresh and hot asthenospheric material into higher lithospheric levels of the backarc. Collectively these processes would trigger extensive igneous activity in the newly formed Central Bohemian magmatic arc and its back arc region. The rapid opening of Rhenohercynian Ocean during Early and Middle Devonian seems to have had indeed a profound impact on the formation and stability of the arc and back-arc domains above the Teplá subduction system. The first signs of intraoceanic thrusting in the Rhenohercynian realm (Lizard region) was associated with initiation of the subduction on the eastern edge of Rhenohercynian Ocean and further compression of the more easterly arc and back-arc system located above Teplá subduction zone. We suggest that, during this event, the whole Rhenohercynian and Barrandian–Moldanubian systems were in active compression leading to progressive thickening of the Bohemian root and formation of deep Moldanubian lower crust. This event is most likely related to entry of Saxothuringian continental crust into Teplá subduction zone leading to transfer of horizontal stress to the west. In that way the Saxothuringian subduction could have influenced processes in the Rhenohercynian system, which was just passing from spreading to closure mode. It was the interplay between the closure of the Rhenohercynian oceanic system in mid-Visean and weakening of orogenic lower crust in the Moldanubian region which probably triggered exhumation of orogenic lower crust in the Variscan root. Final D2 deformation at 320–310 Ma affected the whole European Variscan system together with dextral movements along lithospheric transform boundaries of Rhenohercynian origin (Paye de Bray Fault, Bavarian, Elbe and Sudetic fault zones). It is suggested that the Variscan belt was shortened between relatively stagnant Laurussia and westerly rotating Gondwana, which generated southeast directed underthrusting of Avalonian margin, external and anticlockwise rotation of transform faults and N-S pure shear shortening of lithospheric segments located in crustal lithons across the whole belt. The most conspicuous event was southward movement of the foreland Brunia Continent from north to the south, massive N–S shortening along Bavarian Zone and in the whole Saxothuringian Domain.

Sedimentation regime on a coarse-grained delta front in a tidal strait: Lower to Middle Turonian, Bohemian Cretaceous Basin

Monika Skopcová, David Uličný

Institute of Geophysics Acad. Sci. Czech Republic, Boční II/1401, 141 31 Prague 4, Czech Republic (skopcova@ig.cas.cz, ulicny@ig.cas.cz)

Sandstone bodies of the Lower and Middle Turonian, well exposed in the northwestern part of the Bohemian Cretaceous Basin, represent deposits of coarse grained deltas. Deltas prograded from elevated source areas into a narrow and shallow strait oriented in NW – SE direction (Uličný 2001). Two parallel tectonic zones delimit the main depocentre – Lužice Fault Zone in the NE and Labe – Železné Hory Fault Zone in the SW. Strong axial currents affected by the shape of the strait caused reworking and transport of the sediment along the delta front.

Clinoforms, the main architectural elements of deltas, show an intermediate dip of the delta slope ranging from 4° to 5° and the direction of the delta progradation to the W – SW. Moderate dispersion of the clinoform orientation, resulting from the field measurements, show a lobate shape of the delta body. In the field, clinoforms were found in sandstone bodies in two levels separated by a major transgressive surface. A minimum water depth of 35m during deposition is estimated from the thickness of these sandstone bodies, but an unknown thickness of the sedimentary record, estimated at a few meters, was probably destroyed by erosion during transgression. Abundant cross bedding superimposed on the clinoforms is a result of migration of 3D dunes and indicate activity of currents capable to transport coarse-grained sand. Valečka (1979) found two main current directions in the cross-strata: dominant current towards NW and subordinate current towards SSE – SE, and interpreted their tidal origin. On the basis of analysis of facies and architectures of these strata (Skopcová 2010), a more detailed description and interpretation of the palaeocurrent regime, its forcing, and relationship to the general sedimentation regime of the deltaic clinoforms, is presented here.

Compound cross-bedding, resulting from asymmetric bi-directional currents, is the predominating type of bedding. Reactivation surfaces, created by the subordinate current, are prominent in most exposures. The difference in strength of subordinate vs. dominant currents was medium to high. Couplets of mud drapes originating in slack water stages between flood and ebb are well preserved locally. Tidal bundles show lateral variation of thickness which could result from cyclic alternation of spring and neap tide.

Analysis of the thickness and geometry of compound cross-strata across the depth range of the clinoform revealed a distinct trend. The thickest cross-sets, reaching 60 – 70cm, occur in central parts of the clinoform. Smaller structures of 10 – 15cm thickness are present in both the upper and lower parts, showing a coarse grain size and less palaeocurrent asymmetry in the upper part, and a finer grain size in the lower. This is explained as a result of an interplay of two variables – sediment input that decreased downward from the delta edge combined with high sediment dispersal by the alongshore tidal (and potentially wave-induced) currents. The high rate of sediment reworking in the shallowest water was the most likely reason for the transport of a significant volume of the material down along the clinoform, where the abundance of material and still high energy of the currents in central parts of delta slope made formation of bigger dunes possible. Smaller bedforms in the deepest water reflected a decreased clastic supply rate, but two main directions of palaeocurrents remain uniform. This shows that the tidal currents affected the entire water mass in the tidal strait and brings further support to the recent numerical modeling results by Mitchell et al. (2010) that emphasized the role of the tectonic palaeotopography in inducing powerful tide-driven circulation in an otherwise microtidal Cretaceous epeiric sea of Central Europe.

Mitchell, A., Uličný, D., Hampson, G.J., Allison, P.A., Gorman, G.J., Piggott, M.D., Wells, M.R., Pain, C.C. 2010. Modelling tidal current-induced bed shear stress and palaeocirculation in an epicontinental seaway: the Bohemian Cretaceous Basin, Central Europe. Sedimentology, 57, 359-388.

Skopcová, M. 2010. Depositional architectures, stratigraphy, and depositional regime of Lower – Middle Turonian sandstone bodies, northwestern part of the Bohemian Cretaceous Basin. Diploma thesis, Charles University in Prague. (in czech)

Uličný, D. 2001. Depositional systems and sequence stratigraphy of coarse-grained deltas in a shallow-marine, strikeslip setting: the Bohemian Cretaceous Basin, Czech Republic. Sedimentology, 48, 599–628.

Valečka, J. 1979. Paleogeografie a litofaciální vývoj severozápadní části české křídové pánve. Sborník geologických věd, G 33, 47–81.

The origin of Late Devonian oceanic basins in the Variscan Belt of Europe: a record from the Vosges Klippen Belt

Etienne Skrzypek[1], Anne-Sophie Tabaud[1], Jean-Bernard Edel[1], Karel Schulmann[1], Alain Cocherie[2], Catherine Guerrot[2], Philippe Rossi[2]

[1]Ecole et Observatoire des Sciences de la Terre - UMR 7516, Université de Strasbourg, 1, rue Blessig, 67084 Strasbourg, France (etienne.skrzypek@eost.u-strasbg.fr)
[2]BRGM, BP 36009, Orléans cedex 02, France

We examined the lithological, structural, geochemical and geochronological records from the Klippen Belt located in the southern Vosges Mountains (NE France). The Klippen Belt is represented by discontinuous exposures of serpentinized harzburgite, ophicalcite, gabbro, gneiss and polymictic conglomerate overlain by deep marine pelitic sediments. Structural and gravity anomaly maps reveal that the Klippen Belt coincides with a significant discontinuity possibly occupied by a "calc-alkaline" granitic ridge. Gabbro geochemistry indicates a MOR-type affinity similar to recent slow-spreading ridges, but positive Ba, Sr, Th or U anomalies suggest the influence of fluids expelled from a subduction zone. A Sm−Nd isochron age of 372 ± 18 Ma is thought to reflect gabbro emplacement from a highly depleted mantle source (ε_{Nd}=+11.3), and U−Pb zircon ages from a gneiss sample indicate that the basement found in the klippen was most likely formed at ca. 575 Ma. Combined data indicate the formation of a passive margin during Late Devonian rifting. The klippen lithologies could testify for the presence of an ocean-continent transition environment subsequently inverted during the Early Carboniferous. Middle Visean folding and thrusting in the surrounding sediments and tectonic inversion of rift-related structures was probably responsible for final exhumation of deep parts of the basin represented by the Klippen Belt. Based on correlations with the neighbouring Variscan massifs, it is proposed that the Vosges rift sequences represent a back-arc basin related to the north-directed subduction of the southerly Paleotethys Ocean. This geodynamic reconstruction is tentatively correlated with similar ophiolotic remnants in the French Massif Central (Brévenne) and in Moravia (Horní Benešov), and the origin of Late Devonian oceanic basins in the Variscan Belt of Europe is discussed.

Impermeability of overthrusts in Eastern part of Polish Outer Carpathians

Marek Solecki, Marek Dzieniewicz, Henryk Sechman

Faculty of Geology, Geophysics and Environmental Protection, Department of Fossil Fuels, AGH University of Science and Technology, al. Mickiewicza 30, 30-059 Kraków

The poster discusses role of overthrusts in hydrocarbon migration in the eastern part of Polish Outer Carpathians. In this region, the Outer Carpathians are subdivided into four nappes (from south to north): Dukla, Silesian, Sub-Silesian and Skole. The discussed data arise from surface geochemical surveys carried out in the years 2007 and 2008. The data were obtained from analyses of 889 soil-gas samples (for details see Sechman and Dzieniewicz 2009a, 2009b). The contents of methane and sum of alkanes (C2-C5: ethane, propane, i-butane, n-butane, neo-pentane, i-pentane and n-pentane) were analysed across major overthrusts using statistical methods (Solecki 2011).

The results are presented on Figs 1 and 2. Seven profiles show changes in contents of methane and alkane's sum in relation to average methane and average sum of alkanes across major overthrusts. In the studied part of the Outer Carpathians the average concentration of methane is 3746.37 ppm, and average concentration of alkane's sum is 5.34 ppm. Median value for methan is 3.5 ppm, whereas median value for alkane's sum is 0.037 ppm. Three of the profiles (1-3) show the changes across the basal overthrust of the Dukla Nappe, whereas, four profiles (4-7) display these changes across the basal overthrust of the Silesian Nappe.

Discussed profiles show different shapes. Profiles 3 and 6 are flat for both components. Whereas, the other profiles (1, 2, 4, 5, 7) show either ascending or descending features. In profiles 1, 2, 5, 7 increase of methane concentrations match increase of alkane's sum concentrations and decrease of methane concentrations match decrease of alkane's sum concentrations. The strongest fluctuation across overthrust occurs in profiles 1 and 2. In profile 4 concentration of alkane's sum is almost constant, whereas the concentration of methane shows very strong fluctuation.

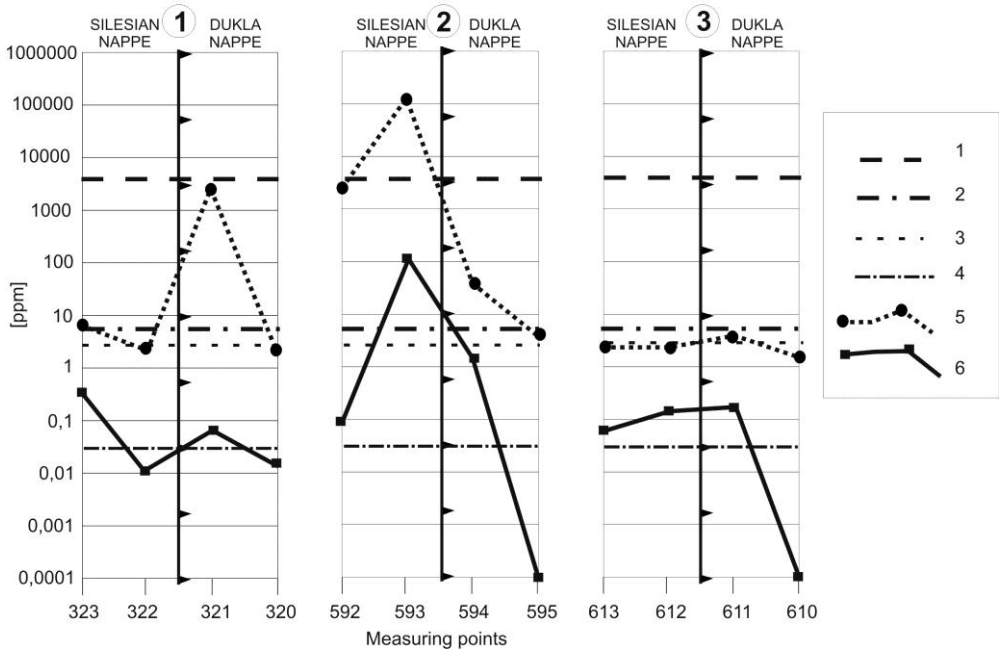

Fig. 1. Comparative graph of methane and sum of alkanes along the contact zone of theSilesian and Dukla Nappe (1 – average methane, 2 – average sum of alkanes, 3 – median value for methane, 4 – median value for sum of alkanes, 5 – methane, 6 – sum of alkanes).

The different shapes of discussed profiles suggest that influence of an overthrust on hydrocarbon flux varies along the overthrust. Flat shape of profiles 3 and 6 and low concentration of hydrocarbon suggest sealing of the overthrusts at the relevant places. Concurrently, high concentrations of methane and alkane's sum, as well as positive correlation of both suggests that the basal overthrust of the Dukla Nappe at profiles 1 and 2, as well as the basal overthrust of the Silesian at profiles 5 and 7 present pathways for hydrocarbon migration. The more intensive migration occurs along the basal overthrust of the Dukla nappe. Relationship between methane and

alkane's sum concentrations as well as high concentration of both is interpreted as an indicator of hydrocarbon source (comp. Sechman and Dzieniewicz 2009a). In profiles 1, 2, 5 and 7 source of hydrocarbon is related to deep accumulation of oil and gas. Extremely high concentration of methane without higher alkanes indicates on contemporary biochemical processes as source of it (comp. Sechman and Dzieniewicz 2009b).

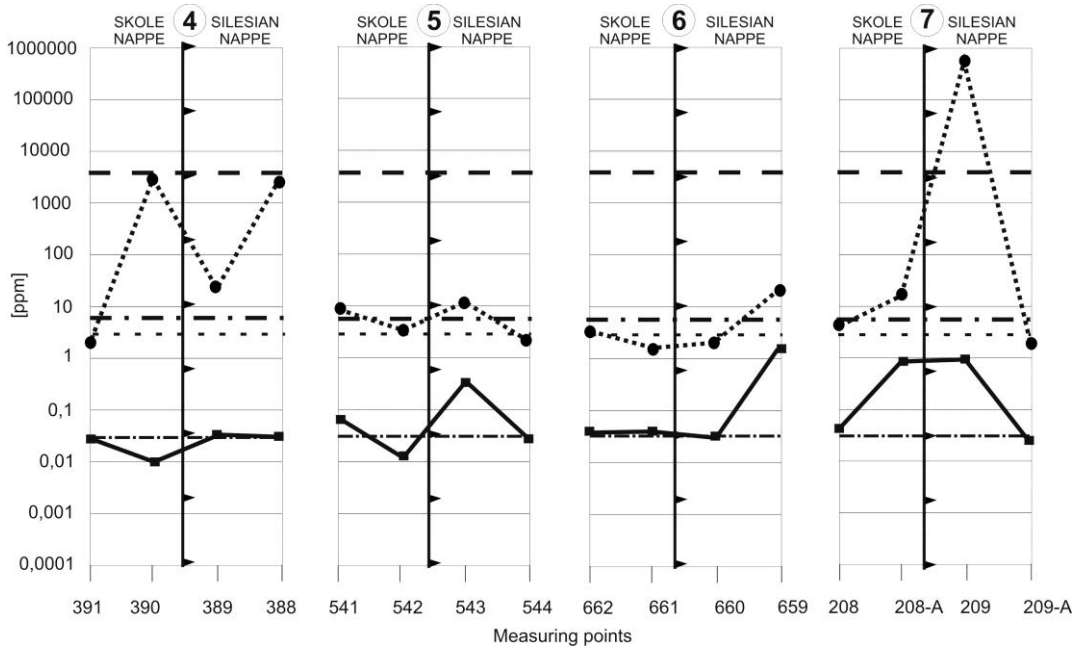

Fig. 2. Comparative graph of methane and sum of alkanes along the contact zone of the Skole and Silesian Nappe (expl. see Fig. 1).

Acknowledgements. Surface geochemical surveys carried out as the part of special research project PBS/PUPW/6/2005, realized by the Faculty of Geology, Geophysics and Environmental Protection, AGH University of Science and Technology in Kraków.

Sechman H. and Dzieniewicz M., 2009a. Analysis of results of surface geochemical surveys in the transfrontier zone of the Polish and Ukrainian Carpathians. Geologia (kwartalnik AGH) 35, 4/1, 109-127 (in Polish).

Sechman H. and Dzieniewicz M., 2009b. Methane emission measurements in selected areas of the Polish Outer Carpathians. Geologia (kwartalnik AGH) 35, 4/1, 129-153 (in Polish).

Solecki M., 2011. Statistical characteristics of hydrocarbon concentrations measured in soil air in the Carpathian Region. B.Sc. Project, Department of Fossil Fuels, Faculty of Geology, Geophysics and Environmental Protection, AGH University of Science and Technology, Kraków (in Polish).

Fracturing and alteration effects on petrophysical properties of granite. Case study in the Melechov Massif, Czech Republic.

Martin Staněk[1,2], Stanislav Ulrich[1], Yves Geraud[2]

[1]*Institut de Physique du Globe de Strasbourg, University of Strasbourg, 1 rue Blessig, 67084, Strasbourg (m4rtin.stanek@gmail.com)*
[2]*Institute of Petrology and Structural Geology, Charles University in Prague, Albertov 6, 12843, Prague (stano@ig.cas.cz)*

Fluid flow in rock is a matter of high importance in stocking of nuclear waste or in exploitation of hydrocarbon or geothermic reservoirs. In low porosity and low permeability rocks (such as granite) joints, faults and alteration zones are the main pathways for fluid migration. Propagation or reactivation of fracture as well as alteration related to eventual fluid circulation may induce fundamental changes in microporosity of rock adjacent to the fracture. In this presentation we characterise various deformation and alteration facies of a granitic rock by means of petrophysical analyses. On the basis of graphical inspection of two-dimensional plots we describe and interpret general correlation trends between measured quantities. Mercury porosimetry, nitrogen permeametry, optical scanning thermal conductivity measurements and two ultrasonic testing methods were executed on dried samples of Lipnice-type granite from the Melechov massif. Seven samples from quarries and twelve samples from a 140 m subvertical borehole have been analysed. The borehole core was sampled according to macroscopically evident along-core variations in character of deformation and alteration. Quarry samples come from granite adjacent to joints and faults belonging to different orientation sets of the studied area. The processes of fracturing and alteration are reflected by all the applied methods. Fractured parts of samples exhibit higher porosity than the less deformed ones. This is the case for penetrative type of fracturing leading to friable tectonic gouge as well as for discretely but densely fractured cohesive products. Porosimetric curves reveal that rock adjacent to a fracture contains pores with throat diameters down to, and perhaps beyond, the smallest measurable ones (5 nm), whereas rock several centimetres away from the fracture typically posses no pores with throat diameter below 30 - 40 nm. Distinct fractures in otherwise cohesive rock induce decrease of thermal conductivity of up to 20 % at places featuring the discontinuity. Ultrasonic testing methods suggest that the microporosity orientation anisotropy is strongly influenced by the granite primary structure in case that the latter is clearly present (i.e. in form of schlier bands). In this case the slowest P-wave propagation direction is perpendicular to the schlier bands with a girdle of fast directions parallel to them. In case of faults the P-waves propagate the fastest in the direction parallel to the mirror striae, suggesting either elongation of grains or planar discontinuities parallel to the striae. Compared to fresh rock, altered granite always feature shift in the pore space distribution towards small throat diameters and a decrease of the total porosity, suggesting the alteration process(-es) filled pores of intermediate diameter. Further, the altered granite gives higher values of P-wave velocity as well as of thermal conductivity suggesting diminution of pore space by alteration. The effect of alteration on the rock permeability is not clear since only one of five analysed couples of altered and fresh rock shows evidence for a decrease of one order of magnitude for the altered part, whereas the other four couples show no systematic variation. With few exceptions, thermal conductivity as well as P-wave velocity tends to be lower for higher porous sample as could be expected in regard of the much lower thermal conductivity and P-wave propagation velocity in air than in granite. P-wave velocities correlate positively with proportion of trapped porosity suggesting that the latter is represented by ink-bottle type pores rather than by thin flat cracks taking into account that for a given pore volume both thermal and mechanic energy can bypass more easily an isometric pore rather than a flat one. Fraction of trapped porosity correlates very strongly with total porosity suggesting that the ink-bottle pores represent a primary as well as a latterly developed porosity. Among samples with relatively high proportion (20 – 30%) of free porosity we find also the most porous, deformed and altered ones implying that secondary processes favour creation of crack pores. The permeability decreases with rising fraction of trapped porosity suggesting that crack-made porosity is more interconnected and therefore more permeable than ink-bottle type porosity. Permeability rises with porosity by exponential law with probable fade out or inversion of the effect for the highest porosity samples, which implies a complex evolution of pore space interconnectivity from the less to the most porous samples. Observed permeability decrease with P-wave velocities and thermal conductivity rise may be explained by reduction in porosity. We interpret in a similar manner the thermal conductivity rise towards higher P-wave velocities. Anisotropy of measured quantities is the most evident in cases of permeability and P-wave velocity, whereas the thermal conductivity shows no striking intra-sample differences between values measured in three orthogonal directions. Interpreted as a whole, the obtained petrophysical data exhibit good correlation between most of the measured quantities and represent an important database for a numerical modelling. This in turn points to some samples that deviate remarkably from the general behaviour and that were therefore examined in a more detailed manner. Intra-sample comparisons of fractured and/or altered parts with the intact ones show distinct effects of the two phenomena on the rock petrophysical properties.

The role of large-scale folding and erosion on juxtaposition of eclogite and mid-crustal rocks (Orlica-Śnieżnik dome, Bohemian Massif)

Pavla Štípská[1], Francis Chopin[1], Etienne Skrzypek[1], Karel Schulmann[1], Ondrej Lexa[2,3], Pavel Pitra[4], Jean-Emmanuel Martelat[5], C. Bollinger[6]

[1]*Ecole et Observatoire des Sciences de la Terre, Institut de Physique du Globe – CNRS UMR 7516, Université de Strasbourg, 1 rue Blessig, F-67084 Strasbourg Cedex, France*
[2]*Institute of Petrology and Structural Geology, Charles University, Albertov 6, CZ-12843 Praha, Czech Republic*
[3]*Czech Geological Survey, Klárov 3, 110 00, Praha, Czech Republic*
[4]*Geosciences Rennes – CNRS UMR6118, Université Rennes 1, Campus de Beaulieu, F-35042 Rennes Cedex, France*
[5]*Laboratoire des Sciences de la Terre – CNRS UMR5570, Université de Lyon 1, F-69622, Villeurbanne, France*
[6]*Unité Matériaux et Transformations – CNRS UMR8207, Université Lille 1, Bât. C6, F-59655 Villeneuve d'Ascq, France*

Eclogite, felsic orthogneiss and garnet-staurolite metapelite with intercalations of amphibolite, quartzite and marble occur in a 5 km long profile in the area of Międzygórze in the Orlica-Śnieżnik dome (Bohemian Massif). A structural study combined with petrographic observations and mineral equilibria modelling is used to understand the mechanism of such close juxtaposition of high pressure and medium pressure rocks in the crust. The structural succession in all lithologies shows an early shallow-dipping fabric S1 that is folded by upright folds and overprinted by a heterogeneously developed subvertical foliation S2. Late recumbent folds associated with a weak shallow-dipping axial plane cleavage S3 occur locally. The S1 fabric in the eclogite is defined by alternation of garnet-rich (grs = 22−29 mol.%) and omphacite-rich (jd = 33−36 mol.%) layers with oriented muscovite (Si = 3.26−3.31 p.f.u.) and accessory kyanite, epidote, rutile and quartz. The assemblage and garnet zoning (grscore = 29, grsrim = 22 mol.%) are compatible with a prograde P–T path from ~20 kbar and ~640 °C to ~22 kbar and ~720 °C. The assemblage in the localized retrograde foliation S2 is formed by amphibole, plagioclase, biotite and relict rutile surrounded by ilmenite and sphene that is compatible with decompression and cooling from ~9 kbar and ~730 °C to 5−6 kbar and 600−650 °C. The S3 fabric contains amphibole, plagioclase, biotite, ilmenite surrounded by sphene, and domains with albite, chlorite, K-feldspar and magnetite indicating cooling to greenschist facies conditions. The metapelites are composed of garnet, staurolite, muscovite, biotite, quartz, ilmenite and chlorite. Chemical zoning of garnet core that contains straight ilmenite and staurolite inclusion trails oriented perpendicular to the external S2 fabric indicates prograde growth from ~5 kbar and ~520 °C to ~7 kbar and ~610 °C during or after the formation of the S1 fabric. Inclusion trails parallel with the S2 fabric at garnet and staurolite rims are interpreted as continuation of the prograde path to ~7.5 and ~630 °C in the S2 fabric. Matrix chlorite parallel to the S2 foliation indicates that the subvertical fabric was still active below 550 °C. The prograde evolution of the eclogite and metapelite during/after the development of the early shallow-dipping fabric is interpreted as simultaneous burial of the lower and upper-middle orogenic crust along shallow-dipping surfaces within a continental accretionary wedge. Axial planar fabrics developed during upright folding and are associated with retrogression under amphibolite-facies conditions in the eclogite, and firstly with prograde and later with retrograde evolution in the metapelites. The shared part of the eclogite and metapelite P−T paths was achieved in the subvertical fabric and points to their common exhumation during fold amplification, which is only possible when erosion, ductile thinning or tectonic unroofing efficiently reduce the upper part of the thickened crust.

Cenozoic palaeostress reconstruction in the Western part of Hornád Depression (Western Carpathians)

Ľubica Súkalová, Rastislav Vojtko

Department of Geology and Palaeontology, Faculty of Natural Sciences, Comenius University, Mlynská dolina G, 842 15 Bratislava; (sukalova@fns.uniba.sk; vojtko@fns.uniba.sk)

The western part of Hornád Depression and Kozie chrbty Mts. are located in the northern part of the Central Western Carpathians in the Poprad and Spišská Nová Ves districts. The Hornád Depression is composed of the sedimentary sequences of the Palaeogene Subtatric Group and the Kozie Chrbty Mts. are built up by the Upper Palaeozoic Ipoltica Group and Triassic succession of the Hronic Unit. The main goal of this research was a reconstruction of the Cenozoic palaeostress fields, based on fault slips, vein and joint systems analysis. The deformation structures were measured in rocks of the Ipoltica Group, Subtatric Group, and the Lower Pleistocene travertines (Hranovnické pleso). Kinematic analysis proved a strong dominance of slickenside lineations with strike-slip movement. An observed chronology of deformation phases can be divided into seven different palaeostress fields (Fig. 1). The oldest tectonic stage (D1) was characterized by strike-slip tectonic regime with W–E compression and N–S tension. Deformation structures of this stage were recorded only in the Permian Malužiná Formation, along with the second deformation stage (D2). The D2 phase operated in strike-slip tectonic regime with WNW–ESE compression and NNE–SSW tension. Both aforementioned deformations were conditionally dated at the Lower Palaeocene to Oligocene. The next, very distinct deformation (D3) is represented by the NW–SE oriented compression and NE–SW oriented tension in the strike-slip tectonic regime. This stage includes the substage, which is characterized by the pure NE–SW tension (D3a). The age of D3 was tenuously dated at the Early–Middle Miocene, because this phase already affected the Palaeogene sediments, as well. The fourth fault generation (D4) was activated during the Middle Miocene under strike-slip tectonic regime with roughly the N–S compression and perpendicular tension. The age of the D4 deformation was determined relatively, based on the crosscutting relations between the deformation structures D4 and D5 stages. The tectonic phase D5 originated in strike-slip tectonic regime with the NE–SW direction of compression and the NW–SE direction of tension. The age of this deformation is considered to be the Late Miocene. The deformation stage D6 is characterized by a pure W–E extension. The deformation stage was dated at the Quaternary in age, as it was identified only in the Lower Pleistocene travertines. The age of last tectonic phase (D7), which consists of the NNW–SSE tension, is the Quaternary but younger than the previous one. (Acknowledgement: This work was supported by the Slovak Research and Development Agency under Contract No. APVV-0158-06.)

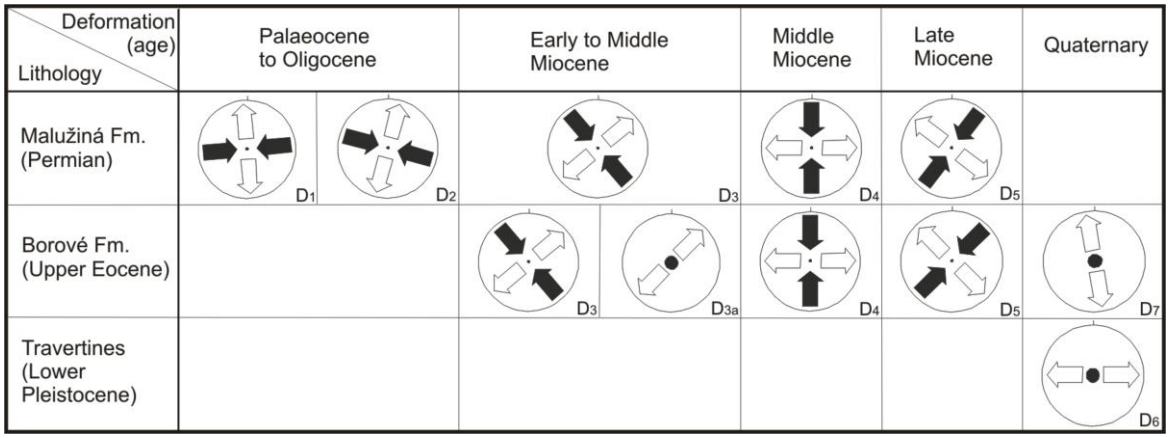

Fig. 1 Synthetic table of chronology for Cenozoic regional palaeostress fields in the Hornád Depression.

Geophysical research of Clay Fault in the vicinity of village Pičín (Barrandian, Bohemian Massif)

Vojtěch Šešulka[1], Martin Knížek[1,2], Rostislav Melichar[1]

[1]*Department of Geological Sciences, Faculty of Science, Masaryk University Brno, Kotlářská 2, 611 37 Brno, Czech Republic (siesa@mail.muni.cz, kniza@mail.muni.cz, melda@sci.muni.cz)*
[2]*ARCADIS Geotechnika a.s., Geologická 988/4, 152 00 Praha 5, Czech Republic*

Diabase dikes in the vicinity of the Clay Fault near Pičín village (Příbram district, Czech Republic) have been geophysically prospected in autumn 2009. The Clay Fault is a significant tectonic structure striking in NE-SW direction with verified length of 30 km. This fault separates Cambrian sediments in SE and Neoproterozoic sediments in NW (Fig. 1). The structure has been recognized several hundreds years ago thanks to base-metal mining in the Březové Hory district. The dip varies between app. 70° NW in the southern part (Bambas 1990) and nearly sub-vertical in the northern part (Havlíček, 1973). Although Kettner (1918) interpreted the Clay Fault as a reverse fault, Havlíček (1971, 1981) classified the structure as an overturned synsedimentary normal fault. Havlíček supported Cambrian age of the Fault by cross-cutting diabase dike (Havlíček in Mašek, red. 1986).

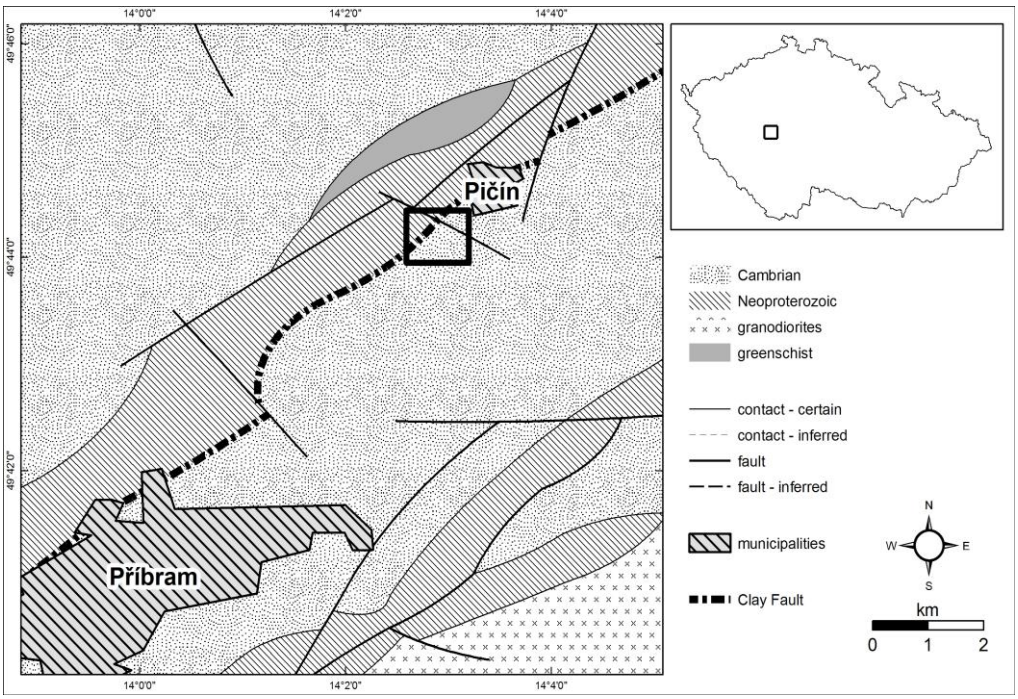

Fig. 1: General map of explored area (black rectangle)

To confirm Havlíček's idea, we used a cesium magnetometer SM-5 NAVMAG (Scintrex, Canada). It enables us to measure the Earth's magnetic field anomalies caused by various magnetized buried entities (e.g. supposed diabase dike). For our purposes we took advantage of a magnetic susceptibility contrast between Neoproterozoic rocks (0.12×10^{-3} SI), Cambrian rocks (0.032×10^{-3} SI) and diabase (0.218×10^{-3} SI). Some man-made object (tarmac road and high-pressure long distance pipeline) slightly disturb our data.

Considered locality is situated on a small hill app. 1 km southern of the Pičín village. We have measured several magnetic profiles mostly parallel to the road Pičín–Příbram (NE-SW direction) and more than 200 m in length. In spite of herein-before man-made disturbing objects, the records of absolute magnetic field δT [nT] brought relevant observatories. The most significant result is age relation opposite to Halíček's idea: diabase dike is cut by the Clay Fault, which is in opposition to *Mašek's (1986)* detail geological map (Fig. 2). This fact excludes synsedimentary age of tectonic movement along the fault.

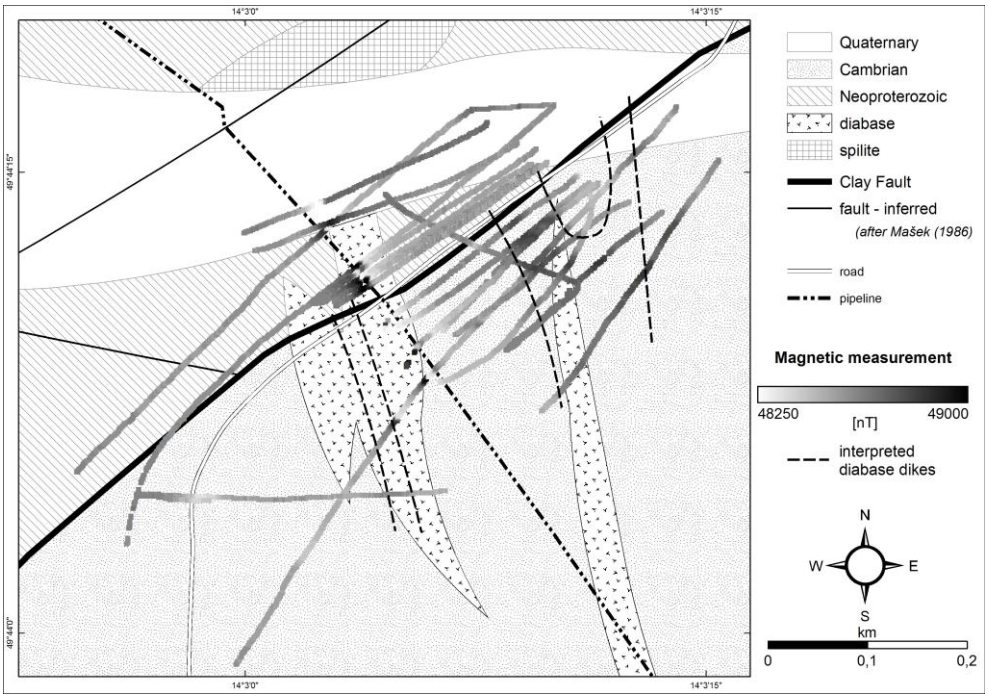

Fig. 2: Interpretation of magnetic data confronting Mašek's (1986) detail geological map.

Bambas J. 1990. Březohorský rudní revír. Komitét sympozia HPVT. Příbram.
Havlíček V. 1971. Stratigraphy of the Cambriam of Central Bohemia. Journal of Geological Sciences, Geology. 20. 7-52. Praha.
Havlíček V. 1973. Horizontální posuny na Příbramsku. Věstník ÚÚG. 48. 225-228. Praha.
Havlíček V. 1981. Development of a linear sedimentary depression exemplified by the Prague Basin (Ordovician-Middle Devonian; Barrandian area – central Bohemia). Journal of Geological Sciences, Geology. 35. 7-43. Praha.
Kettner R. 1918. Nový geologický profil příbramskými doly a příbramským okolím. Sborník České společnosti zeměvědné. 24. 28-37. Praha.
Mašek J. 1986. Základní geologická mapa ČSSR 1:25 000. List 12-433 Rosovice. ÚÚG. Praha.

Olivine microstructures related to interactions between peridotite and melts/fluids: xenoliths from the sub-volcanic uppermost mantle of the Bohemian Massif

Petr Špaček[1], Lukáš Ackerman[2,3], Jaromír Ulrych[2]

[1]*Institute of Geophysics, Acad. Sci. Czech Rep., Boční II/1401, 14131 Prague, Czech Rep.; also at Institute of Earth Physics, Masaryk University, Tvrdého 12, 60200 Brno, Czech Republic (spacek@ipe.muni.cz)*
[2]*Institute of Geology, Acad. Sci. Czech Rep., Rozvojová 269, 16500 Prague, Czech Republic*
[3]*Czech Geological Survey, Geologická 6, 15000 Praha, Czech Republic*

It is widely accepted that large parts of the Earth's upper mantle contain significant amount of volatile fluids and melts which can migrate over long distances. Since the fluid phase has a first order effect on rheology and transport properties of grain boundaries, it might play a very important role during the deformation of the mantle. Our study of the mantle xenoliths in basalts shows that the metasomatic transformations of the uppermost mantle are omnipresent in the sub-volcanic parts of the Bohemian Massif, and locally they dominate the deformation-related structures. In addition to older, penetrative modal or cryptic chemical metasomatic reactions we often observe intergranular crystallized melts of various compositions, which resided in the mantle shortly before the eruption. Inclusions of volatile fluids are extremely abundant in some of these samples, too. Microstructures related to these late phases of metasomatism are well preserved and they allow a deeper study of the mechanisms operative during the complicated interactions between peridotite and melts/fluids.

One of the most important observations is the fluid- or melt-assisted recrystallization of olivine which leaves no significant compositional fingerprints and can be easily misinterpreted as due to the dynamic recrystallization of a dry rock. In the xenolith suite from Lutynia (Klodsko region) we observe strong microstructural indications of fluid-assisted recrystallization with both old and new generation of olivine grains (olivine I and II) having identical chemical compositions within the detection limits of microprobe analysis (only the olivine grains of the latest generation related to pockets of crystallized melt have significantly higher Ca content). In these cases it is only the specific microstructure which indicates the presence of fluids during the crystal growth, such as the formation of nearly perfect sub-idiomorphic strain-free olivine II grains ("tablet olivine") growing at the expense of olivine I grains. In some samples, strong intracrystalline strain of olivine I (local dislocation densities up to 6×10^{12} m^{-2}) and its incipient subgrain rotation recrystallization indicates small but relatively high-stress deformation taking place shortly before or concurrently with the infiltration of fluids and melts. The preferred orientation of olivine II tablet grains is often observed at local scale or in the whole sample. The microfabric analyses indicate the potentially important role of preferrential development of (010) crystal faces in olivine with fluid-wetted grain boundaries. The microstructural observations allow several mechanisms of lattice- and shape-preferred orientation development in the olivine II grains: a/ selective exaggerated growth of some small grains with orientations inherited from the dynamically recrystallized host grains, b/ tendency of recrystallized grains to align their larger crystal faces by passive rotation into orientations suitable for grain boundary sliding, and c/ oriented growth of recrystallized grains along systems of preferred microfractures.

Although in Lutynia the fluid-assisted recrystallization is usually constrained to grain boundary regions of olivine I and enstatite, in some samples olivine II represents >50% of the rock volume. Xenolith samples from other localities sometimes display similar structural features and we suggest that fluid- or melt-assisted dynamic recrystalization of olivine might be rather common phenomenon, which has to be taken into account in the interpretation of olivine microfabric.

Magnetic fabric of clay gouges as a potential indicator of fault slip kinematics

Petr Špaček[1,2], Lukáš Komárek[1], Petra Štěpančíková[3], Martin Chadima[4]

[1]*Institute of Earth Physics, Masaryk University, Tvrdého 12, 60200 Brno, Czech Republic (spacek@ipe.muni.cz)*
[2]*Institute of Geophysics, Acad. Sci. Czech Rep., Boční II/1401, 14131 Prague 4, Czech Republic*
[3]*Institute of Rock Structure and Mechanics, Acad. Sci. Czech Rep., V Holešovičkách 41, 18209 Prague, Czech Rep.*
[4]*AGICO Inc., Ječná 29a, 62100 Brno, Czech Republic*

We analysed the internal magnetic fabric of clay gouges from five major faults in the Bohemian Massif and associated deformed sediments, to understand its relations to fault kinematics and to assess its possible use as a kinematic indicator. The faults studied were Hluboká Fault and Drahotěšice Fault (NW-SE and NNE-SSW strikes, both at locality Úsilné), Sudetic Marginal Fault (NW-SE strike, locality Bílá Voda), Mariánské Lázně Fault (NW-SE strike, locality Kopanina), and Jablunkov Fault (NW-SE strike, locality Milíkov). The fault rocks and associated deformed sediments (both clay rich) were sampled in 2-5m deep trenches which were made to assess the Quaternary activity of the faults. Anisotropy of magnetic susceptibility (AMS) was measured at 6.7 cm^3 cubic samples using MFK1 Kappabridge. Multiple samples were taken from each gouge (when possible) to test the directional stability of the measured AMS tensor.

The results show strikingly well developed distribution maxima of magnetic lineations (K_{max}) oriented sub-parallelly to the strike of the fault, with subhorizontal to moderate dips. The opening angles of these maxima are reasonably small and similar to those of macroscopic slickenlines (when observed). The poles to magnetic foliations (K_{min}) are often close to the fault normal, but generally free to rotate around the axis of K_{max} distribution maximum. All deflections from this rule are satisfactorily explained by cryptic shear due to the gravity-driven slope movements. AMS tensor is usually oblate, anisotropies ranging from <1 to 12.5%. All these observations are similar for fault gouges and deformed sediments adjacent to the fault. The mean susceptibility (30 to 100 × 10^{-6} SI) and its thermal dependence, indicate that paramagnetic phyllosilicates are dominant magnetic carriers.

Taking into account the rotational pseudosymmetry of AMS tensor along c-axis in phyllosilicates, the orientation of K_{max} should be due to the intersection of planar fabrics of the clay minerals. In deformed sediments our observations can be explained as due to the intersection of rotated bedding planes with secondary shear planes. In gouges, however, the magnetic fabric should be solely the result of tectonic deformation. As the faults studied were evidently re-activated with contrasting slip directions in post-Variscan history (dip-slips vs. strike-slips), one could expect complex, or at least variable fabrics, since there are always several possibilities to combine planar fabrics related to different periods of slip. From this perspective the observed uniformity of magnetic fabrics at the given locality and in the whole region studied is rather surprising. Assuming a simple structural model of a fault gouge with P-foliation and Riedel shears as the main planar features re-orienting the phyllosilicates, we should observe K_{max} in a position sub-perpendicular to the fault slip. However, this is in contradiction with identical orientations of K_{max} and slickenlines which were locally observed on the faults. In this respect, the observed relations between slickenlines and K_{max} would rather indicate some flow-folding mechanism (slackening and surging flow; sheath folding) which would re-orient the phyllosilicates along the slip-parallel axes to produce slickenline-parallel K_{max}. Possibly, the „survivor grains“, or generally domains with contrasting compatibilities, can cause flow perturbations which might produce similar ridge-like structures as slickenlines and thus produce slip-parallel K_{max}, too.

We conclude that in spite of the locally observed conformity between the magnetic lineation and macroscopic kinematic indicators, interpretations must be made with caution, since the complex and often largely unknown long-term slip history of the faults studied can result in unexpected relations of the latest fault slip direction and the fabric of the fault gouge. Although the method seems to be promising, it is first necessary to carry out a thorough study on faults with well known and long-term uniform kinematics which would allow unequivocal interpretation of the observed fabrics.

Hluboká fault: repeatedly degraded fault scarp rather than active tectonic slip

Petr Špaček[1,4], Ivan Prachař[2], Jan Valenta[3], Petra Štěpančíková[3], Jan Piskač[2], Jan Švancara[1]

[1]*Institute of Earth Physics, Masaryk University, Tvrdého 12, 60200 Brno, Czech Republic (spacek@ipe.muni.cz)*
[2]*Energoprůzkum Praha Ltd., Pod svahem 757/11, 14700 Praha, Czech Republic*
[3]*Institute of Rock Structure and Mechanics, Acad. Sci. Czech Rep., V Holešovičkách 41, 18209 Prague, Czech Rep.*
[4]*Institute of Geophysics, Acad. Sci. Czech Rep., Boční II/1401, 14131 Prague, Czech Republic*

The Hluboká fault is a steep, NW-SE striking, marginal fault of the Late Cretaceous Budějovice Basin with cumulative vertical throw of >400 m. Having conspicious morphology of the fault scarp with features characteristic of extremely rapid erosion, the fault has been repeatedly pointed out at IAEA missions as a potentially active fault, which should be included in the re-evaluation of seismic hazard at Temelín Nuclear Power Plant. For this reason we carried out a two-year research aimed at the assessment of Quaternary activity of the Hluboká fault (between the villages of Munice and Vráto), using geophysical and shallow borehole survey along individual fault segments, trenches across the fault, and dating of sediments by OSL method.

In the marginal, SE part of the fault scarp (Úsilné village) two trenches exposed the fault zone with strongly deformed, vertical to overturned Cretaceous sands and clays in contact with sheared and cataclastic Permian sediments. The observed structures indicate multiple reactivation and interference with fault system of the Blanice graben (NNE-SSW strike). All tectonic structures are uniformly affected by slope movements with gelifluction whose age was dated at 21 ka - this is the upper age limit of the latest tectonic slip on this fault segment. Similar minimum age of tectonic quiescence is indicated in the floodplain of local creeks farther to the NW (Hrdějovice) where intact fluvial sediments cover the fault with undisturbed thickness.

In the segments with high fault scarp (between Hluboká n. Vlt. and Hrdějovice) trenching was not possible and instead the continuity of Tertiary and Quaternary sedimentary bodies was studied in places where they cover the fault. In the area of Vltava floodplain the fault is buried below Quaternary and probably older (Tertiary?) sediments while the prominent morphological scarp is situated 200 m farther to the NE. This misalignment might be explained by recession of the scarp due to long-term erosion at the level close to the present-day surface. The OSL dating of the terraces on both wings of the fault proved vertically undisturbed sequence of the last 14 ka. Samples which are currently being dated will clarify the relative positions in deeper levels below the floodplain as well as in relics of higher terraces. In spite of two samples with controversial ages, similar thickness of the lower terraces on both wings of the fault suggests that the whole sequence of *Würmian* age (11-80 ka), is continuous and undisturbed by vertical tectonic movements.

In the NW segment (between Munice and Hluboká n. Vlt.), the transverse channel filled with Tertiary sediments (Mydlovary Fm., Langhian/Badenian) crosses the fault. The continuity of these sediments indicated by geophysical profiles, boreholes and trench survey, suggests that in this segment the cumulative slip on Hluboká fault in the last 15 Ma is less than few tens of meters. This is in accord with the observation that the relics of the Zliv Fm. (Burdigalian/Ottnangian) found on both wings of the fault always have similar base elevations.

Altogether, the direct observations of the structures in the trenches, the continuity of Tertiary and Quaternary sediments above the fault, and also the segmentation of the Hluboká Fault by the faults of N-S and NNE-SSW strike suggest that the fault has not been active in Quaternary. Other features, like the absence of a fault scarp in places where thick non-consolidated sediments extend over the fault clearly indicate the dominant role of lithological contrasts and differential erosion during the formation of the present-day morphological scarp. Low base elevations of Tertiary sedimentary formations together with relatively high elevations of some river terraces strongly suggest that the main fault scarp was repeatedly exhumed and covered with sediments again. The complex, generally concave-up shape of the fault scarp with several steps is probably a result of multiphase degradation in periods of low-stand erosional base levels at least during the last 15 Ma.

Intracrystal microtextures in alkali feldspars from fluid deficient felsic granulites: a chemical and TEM study

Lucie Tajčmanová[1], Rainer Abart[2], Richard Wirth[3], Dieter Rhede[3]

[1]*Institute of Geological Sciences, Freie Universität, Malteserstr. 74-100, 12249 Berlin, Germany*
[2]*Department of Lithosphere Research, University of Vienna, Althanstrasse 14, 1090 Wien, Austria*
[3]*Helmholtzzentrum Potsdam, Deutsches GFZ, Telegrafenberg, 14473 Potsdam, Germany*

Samples of essentially "dry" high-pressure felsic granulites from the Bohemian Massif (Variscan belt of Central Europe) contain large perthites with several generations of exsolution features. A first generation of albite-rich plagioclase precipitates takes the form of spindles or lenses up to 30 micrometers long with an aspect ratio of 12 to 6. The precipitates show strong shape preferred orientation. A second generation of albite-rich precipitates takes the form of thin (around 30 nanometers wide) up to several 10's of micrometers long lamellae or spindles. In the vicinity of large kyanite, garnet or quartz inclusions, the orthoclase-rich host shows diffuse exsolution features taking the shape of short and narrow spindles (tails) aligned in two directions at an angle of about 45°. The contacts between the orthoclase-rich host and the plagioclase precipitates of the first generation and the contact between the orthoclase-rich host and large kyanite, quartz and garnet inclusions is lined with a thin rim of albite. This albite was formed at a late stage of the petrogenetic history probably related to fluid infiltration and associated albitization. In the vicinity of the large inclusions the plagioclase precipitates of the first perthtite generation become significantly depleted and the perthite microstructure coarsens composed dominantly of tweed orthoclase. The integrated composition corresponds to $Or_{59}Ab_{36}An_5$ in the inclusion free domains and slightly decreases in plagioclase content ($Or_{63}Ab_{33}An_4$) towards the kyanite or quartz inclusion. This chemical change is very gentle.

The primary exsolutions probably formed by spinodal decomposition at around 850-900°C during the high pressure stage (16-18 kbar). The primary exsolution was followed by primary coarsening and albite twinning of the plagioclase precipitates. The second generation of albite-rich precipitates was formed at around 650-700 °C. TEM investigations revealed that the interfaces between the second generation plagioclase lamellae and the orthoclase rich host are coherent or semi coherent. The formation of albite linings at phase boundaries and of patch perthite produced incoherent interfaces. The patch perthites, albitization and secondary coarsening in the vicinity of large inclusions developed below 400°C contemporaneously with fluid infiltration in the course of deuteric alteration.

Hercynian dioritic rocks of the Western Carpathians: tracers of crustal – mantle interactions

Pavel Uher[1], Milan Kohút[2], Marián Putiš[1]

[1]*Department of Mineralogy and Petrology, Comenius University, Mlynská dolina G, 842 15 Bratislava, Slovakia (puher@fns.uniba.sk; putis@fns.uniba.sk)*
[2]*Dionýz Štúr State Institute of Geology, Mlynská dolina 1, 817 04 Bratislava, Slovakia (milan.kohut@geology.sk)*

Dioritic rocks (amphibole±biotite quartz diorites to melatonalites) form small (up to 1 km^2 in size) but widespread intrusive bodies within Hercynian S- and I-type granitic plutons in the Tatric and Veporic Superunit of the Central Western Carpathians, Slovakia. The diorites are equigranular to porphyric, medium- to coarse-grained mafic rocks, locally with dikes of dioritic porphyries and dioritic pegmatites. Plagioclase (An_{19-47}), amphiboles (mainly magnesiohornblend and actinolite), quartz and biotite (phlogopite to annite) form main rock-forming minerals, locally pyroxene (diopside) and K-feldspar are present. Albite (An_{03-10}), epidote to clinozoisite, chlorite (clinochlore) and muscovite represent late post-magmatic mineral assemblage. Apatite, titanite, zircon, allanite-(Ce) to epidote, pyrite, ilmenite and magnetite are the most characteristic accessory minerals.

The diorites show variable Alumina saturation index (A/CNK = 0.8 ~ 1.3) and enrichments in Ti, Fe, Mg, Ca and P relative to the associated granitic rocks. Typical feature are high contents of REE (ΣREE up to 400 ppm) and slight LREE enrichments. Europium anomalies are comparable to those reported for gabbros (Eu/Eu* = 0.8 ~ 1.1). The radiogenic isotope data $^{206}Pb/^{204}Pb$ =18.63 ~ 18.77; $^{207}Pb/^{204}Pb$ = 15.67 ~ 15.74; $^{208}Pb/^{204}Pb$ = 38.43 ~ 38.68; $^{87}Sr/^{86}Sr_{(350)}$ = 0.702 ~ 0.708; $\varepsilon Nd_{(350)}$ = -1.0 ~ +5.8; zircon $\varepsilon Hf_{(350)}$ 2.6 ~ 9.4, together with their stable isotopic characteristics ($\delta^{18}O_{SMOW}$ = 6.6 ~ 8.4 ‰; $\delta^{34}S_{CDT}$ = +0.3 ~ +0.8 ‰ and $\delta^{7}Li$ = -0.5 ~ -2.9) correspond to a lower crustal mafic (basic meta-igneous) source with limited mantle-derived contribution. Our new U-Th-Pb zircon SHRIMP dating from VSEGEI St.-Petersburg laboratory proved their Early Carboniferous magmatic origin with concordia ages ~340 to 355 Ma. Majority of studied zircon crystals exhibit standard internal texture typical for magmatic growth, usually with oscillatory and sector zoning. The ages are nearly identical or slightly younger in comparison to adjacent Hercynian granitic rocks.

Noteworthy, the mantle contribution to petrogenesis of the diorites has rather character of re-melted mantle derived mafic lower crust than fresh input of juvenile mantle melt to the Devonian/Carboniferous subduction zone what suggest the Hf model ages of zircons from these dioritic rocks. The Hf DM crustal residence model ages vary in age interval 1040 ~ 670 Ma for the Western Carpathian diorites. However, these zircon Hf model ages are slightly older but comparable to the WR two stages $Nd_{(DM)}$ model ages 980 ~ 620 Ma. Lead isotope characteristic ($^{207}Pb/^{204}Pb$ > 15.60), initial strontium ratios (partly over 0.707), and uniformly light Li isotope signature ($\delta^{7}Li$ <-0.5 ‰) suggest that these dioritic rocks could not be directly related to the juvenile Earth's mantle. Instead, a cumulate origin of the diorite rocks is advocated. It is plausible that kinetic effects may have operated during formation of these rocks, in particular if forming smaller bodies or even dioritic enclaves. However, there is no doubt that mantle magma played a significant role during the Devonian/Carboniferous orogenesis, e.g. it softened the lower crust and contributed to needful heat for their melting. Consequently, the dioritic rocks represent an important tool for understanding of magmatic processes and crustal to mantle interactions during Hercynian orogenesis in the Western Carpathians. (Acknowledgment: This work was supported by the Slovak Research and Development Agency under the contract No. APVV-0549-07, APVV-0557-06, APVV-0279-07 and APVV-VVCE-0033-07.)

Roles of structural inheritance and palaeostress regime in the evolution of the Cenozoic Eger Graben, Bohemia

David Uličný[1], Michal Rajchl[2], Radomír Grygar[3], Lenka Špičáková[1]

[1]*Institute of Geophysics, Acad. Sci. Czech Republic, Boční II/1401, 141 31 Prague 4, Czech Republic (ulicny@ig.cas.cz)*
[2]*Czech Geological Survey, Klárov 131/3, 118 21 Praha 1, Czech Republic*
[3]*VŠB – Technical University Ostrava, Institute of geological engineering, 17. listopadu, 708 33 Ostrava – Poruba, Czech Republic*

The formation of the European Cenozoic Rift System (ECRIS) was the most significant geodynamic process that affected the crust of Western and Central Europe north of the Alps during the Cenozoic. The causes of the rifting process as well as its temporal evolution have been intensely debated over the past decade, with competing hypotheses ranging from plume-related thermal doming as the cause of lithospheric extension to changes in asthenospheric flow caused by subducted slabs in the Alpine domain (e.g., Michon and Merle, 2005).

The Eger Graben is situated at the eastern edge of the ECRIS and follows a roughly NE to ENE trend, partly paralleling a major crustal boundary between the Saxothuringian and Teplá-Barrandian zones of the Variscan orogen (TSS) that formed as the suture of the Saxothuringian ocean about 340 Ma. It remains the least known part of the ECRIS in terms of structural and sedimentary history. The lack of relevant data from the Eger Graben so far has caused a great variation in large-scale interpretations of the kinematics of its opening – from a "typical pure-shear rift" (Wilson, 1993) to a pure sinistral strike-slip structure within the hypothetical sinistral shear zone of the ECRIS (Bourgeois et al., 2007). It is, therefore, important to evaluate the structure of the Eger Graben with regard to the fabric of the basement, in order to get a robust first-order understanding of the processes of Eger Graben opening and subsequent destruction.

The position of the Eger Graben in the Bohemian Massif has long been associated with the NE to ENE-trend of thre TSS. However, many subsequent geological events have modified the fabric of the Bohemian Massif during the 300 Myr remaining to the opening of the EG, and the relationship between deep-seated fabric and Tertiary upper-crustal extension is not straightforward. Two main phases of Eger Graben extension were recognized by studies of its basin fills (Špičáková et al., 2000; Rajchl et al., 2009): a roughly N-S – directed extensional phase commencing in Late Oligocene and a NE-SW – directed phase of localized extension during the Middle Miocene. The latter may have been associated with crestal extension of a growing lithospheric fold that eventually gave rise to the Krušné Hory uplift and started the partial deformation and erosion of most of the Eger Graben basin fills.

A comparison of fault array geometries along the entire length of the Eger Graben reveals several major differences between the Cenozoic extensional domains to the SE and NE of the Elbe Zone. The contrasts are best shown by comparing the Most Basin, recently documented by Rajchl et al. (2009), and the Středohoří Graben. The change in strike of the Eger Graben axis northeast of the Elbe Zone resulted in different degree of obliquity of the initial Oligocene extension in the two domains, with consequences for fault segment lengths and the dimensions and arrangement of individual depocentres / grabens. The change in strike of the Eger Graben axis across the Labe Fault Zone is closely related to the inherited structure of the chain of late Palaeozoic, early post-orogenic, intra-montane rift system of the Late Carboniferous "limnic basins" of the Bohemian Massif. These basins were recognized by Jindřich (1971) as a major extensional structure that formed above the TSS very soon after the climax of collision. The "bend" in strike of the Late Palaeozoic basin belt across the Labe Fault Zone was explained by Uličný et al. (2009) as a consequence of dextral shearing that occurred mainly during the Permian and, by a minor part, during the Cretaceous. It is clear that the underlying lithosphere-scale inhomogeneity of the TSS gave rise to the orientation of the Late Palaeozoic basin belt, but it probably cannot be directly linked to the Cenozoic extensional features. An open question remains of the northeastern termination of the Eger Graben, where it completely abandons the TSS trace, translated further east. The influence of the TSS on the Eger Graben geometry was rather indirect, mediated by the brittle upper-crustal structures inherited from the Late Palaeozoic rifting episode. Apart from this structural inheritance, a rheological imprint of the Late Palaeozoic, intra-orogenic rifting may be reflected in the offset between the axes of the two major extensional systems.

Bourgeois, O., Ford, M., Diraison, M., Le Carlier De Veslud, C., Gerbault, M., Pik, R., Ruby, N. & Bonnet, S., 2007. Separation of rifting and lithospheric folding signatures in the NW-Alpine foreland. Int. J. Earth. Sci., 96, 1003-1031.

Jindřich, V., 1971. New views in tectonic significance of platform sediments in the Bohemian Massif, Czechoslovakia. Geol. Soc. Am. Bull., 82, 763-768.

Michon, L. & Merle, O., 2005. Discussion on "Evolution of the European Cenozoic Rift System: interaction of the Alpine and Pyrenean orogens with their foreland lithosphere" by P. Dèzes, S.M. Schmid and P.A. Ziegler, Tectonophysics, 389 (2004), 1-33. Tectonophysics, 401, 3-4, 251-256.

Rajchl, M., Uličný, D., Grygar, R., and Mach, K. , 2009. Evolution of basin architecture in an incipient continental rift: the Cenozoic Most Basin, Eger Graben (Central Europe). Basin Research 21, 269-294.

Špičáková, L., Uličný, D. & Koudelková, G. (2000) Tectonosedimentary evolution of the Cheb Basin (NW Bohemia, Czech Republic) between Late Oligocene and Pliocene: a preliminary note. Studia Geophysica et Geodaetica, 44, 556-580.

Uličný, D., Špičáková, L., Grygar, R., Svobodová, M., Čech, S. & J. Laurin, J., 2009: Palaeodrainage systems at the basal unconformity of the Bohemian Cretaceous Basin: roles of inherited fault systems and basement lithology during the onset of basin filling. Bulletin of Geosciences, 84, 4, 577-610.

Wilson, M. , 1993. Magmatism and the Geodynamics of Basin Formation. Sedimentary Geology, 86, 5-29.

Roles of inherited fault systems and basement lithology in the formation of Mid-Cretaceous palaeodrainage of the Bohemian Massif

David Uličný[1], Lenka Špičáková[1], Radomír Grygar[2], Marcela Svobodová[3], Stanislav Čech[4], Jiří Laurin[1]

[1]*Institute of Geophysics Acad. Sci. Czech Republic, Boční II/1401, 141 31 Prague 4, Czech Republic (ulicny@ig.cas.cz)*
[2]*VŠB – Technical University Ostrava, Institute of Geological Engineering, 17. listopadu, 708 33 Ostrava – Poruba, Czech Republic (radomir.grygar@vsb.cz)*
[3]*Institute of Geology AS CR, v. v. i., Rozvojová 269, 165 00 Praha 6, Czech Republic (msvobodova@gli.cas.cz)*
[4]*Czech Geological Survey, Klárov 3, 118 21 Praha 1, Czech Republic (stanislav.cech@geology.cz)*

This study presents a synthesis of currently available data on the distribution of Cenomanian-age palaeodrainage systems in the Bohemian Cretaceous Basin, filled by fluvial and estuarine strata, and an interpretation of their relationships to the basement units and fault systems. Much of the progress, compared to previous studies, was made possible by a recent basin-scale evaluation of Cenomanian genetic sequence stratigraphy.

Several local palaeodrainage systems developed in the basin, separated by drainage divides of local importance and one major divide (the Holice–Nové Město Palaeohigh) which separated the drainage basins of the Tethyan and Boreal palaeogeographic realms (Fig. 1C). The locations and directions of palaeovalleys were strongly controlled by the positions of inherited Variscan basement fault zones (Fig. 1A), whereas the bedrock lithology had the subordinate effect of narrowing or broadening valleys on more *vs.* less resistant substratum, respectively. The intrabasinal part of the palaeodrainage network followed the slopes toward the Labe (Elbe) System faults and was strongly dominated by the conjugate, NNE-trending, Jizera System faults and fractures. Outlet streams – ultimate trunk streams that drained the basin area – are interpreted to have followed the Lužice Fault Zone toward the Boreal province to the Northwest, and the Železné Hory Fault Zone toward the Tethyan province to the southeast (Fig. 1B). At both the northwestern and southeastern ends of the Bohemian Cretaceous Basin, shallow-marine or estuarine conditions are proven to have existed during the early Cenomanian. Direct evidence for syn-depositional subsidence during the early to mid-Cenomanian, fluvial to estuarine phase is very rare, and the onset of deposition by fluvial backfilling of the palaeodrainage systems was driven mainly by the long-term rise in global sea level. Subtle surface warping, mostly without detectable discrete faulting, is inferred to have been a response to the onset of the palaeostress regime that later, with further stress accumulation, led to subsidence in fault-bounded depocentres of the Bohemian Cretaceous Basin and uplift of new source areas.

Uličný D., Špičáková L., Grygar R., Svobodová M., Čech S. and Laurin J., 2009. Palaeodrainage systems at the basal unconformity of the Bohemian Cretaceous basin: roles of inherited fault systems and basement lithology during the onset of basin fillng. Bulletin of Geosciences, 84, 4, 577-610.

Sedimentary record of increased subsidence and supply rates during the Late Turonian, Bohemian Cretaceous Basin (Czech Republic)

Lenka Vacková, David Uličný

Institute of Geophysics, Academy of Sciences of the Czech Republic, Boční II/1401, 141 31 Prague 4, Czech Republic (vackova@ig.cas.cz), (ulicny@ig.cas.cz)

The opening and filling of the Bohemian Cretaceous Basin took place during a mid-Cretaceous reactivation of basement fault systems of the Bohemian Massif. The general tectonic regime during the basin lifetime, as well as its changes through time, can be interpreted from analysis of geometry of clastic sequences and, partly, of even minor changes in lithology. This study is focused on sandstone-dominated strata of Late Turonian age (ca. between 90,4 and 88,9 +/- 0,4 – 0,7 Ma after Ogg et al., 2004) in the proximal part of the Bohemian Cretaceous Basin. During the Late Turonian, genetic sequences TUR 5 – TUR 7 were deposited in the Bohemian Cretaceous Basin (Laurin and Uličný, 2004; Uličný et al., 2009). Previous studies in the Cretaceous of Central Europe have indicated changes in the tectonic regime known as the ´subhercynian´ tectonic phases, but their exact timing has not yet been determined in detail (cf. Mortimore et al. 1998 and references therein).

The present research is based on two groups of data: (1) field macroscopic description of outcrops which was complemented by field measuring of the radioactivity and (2) correlation of geophysical well-logs in regional cross-sections (Vacková, 2010).

Upper Turonian sandstones are primarily of deltaic origin and were deposited in the proximal part of a deltaic system near the faulted northern margin of the Bohemian Cretaceous Basin. Low-angle clinoforms, of 1-5° slope, can be observed in the largest outcrops of favourable orientation. Individual stratal packages, interpreted as parasequences developed in prograding deltaic lobes or adjacent shoreface lithosomes, are bounded above and below by transgressive surfaces, commonly with conglomeratic transgressive lags. The lags contain rounded pebbles of quartz derived probably from eroded delta-top alluvial sediments. Many stratal packages show moderate coarsening upward. Clastic material derived from uplifted Western Sudetic Island and was transported towards the depocenter where was reworked by currents of tidal origin. The orientation of paleocurrents was relatively uniform through sequences TUR 5 to TUR 7. The most frequent direction of the paleocurrents was towards the south-east or east and there were slight changes in this direction.

The field data support previous suggestions by Uličný et al. (2009) that the end of the Turonian was the time of a significant increase in subsidence rate in a narrowed depocenter of the NW part of the Bohemian Cretaceous Basin. This increase started during TUR 6 (Late S. neptuni Zone) and continued by further acceleration during TUR 7. Based on total thickness and estimated duration of sequences TUR 6 and 7, up to a fourfold increase in accommodation rate (largely represented by subsidence) occurred in the main depocentre during TUR 7 deposition (for details see Laurin and Uličný, 2004 or Uličný et al., 2009). At the same time, strongly increased sediment input into the basin is indicated by a general increase in potassium, as shown by both outcrop gamma-ray spectra and macroscopic occurrence of feldspar grains. Another line of evidence for increased clastic input during TUR 7 time is the fact that this sequence, as an aggrading stack of prograding, shallow-water sandstones filled the entire accommodation space provided by the accelerated subsidence.

Laurin, J. & Uličný, D., 2004. Controls on shallow-water hemipelagic carbonate system adjacent to a siliciclastic margin: example from Late Turonian of Central Europe. Journal of Sedimentary Research, 74, 5, 697 – 717.

Mortimore, R., Wood, C., Pomerol, B. and Ernst, G., 1998. Dating the phases of the Subhercynian epoch: Late Cretaceous tectonics and eustatics in the Cretaceous basins of northern Germany compared with the Anglo-Paris Basin. Zentralblatt für Geologie und Paläontologie Teil I, 11/12, 1349–1401.

Ogg, J. G. & Agterberg, F. P. & Gradstein, F. M., 2004. The Cretaceous Period. In Gradstein, F.M. & Ogg, J. G. & Smith, A. (eds) A Geologic Time Scale 2004. Cambridge University Press, Cambridge, 344 – 383.

Uličný, D. & Laurin, J. & Čech, S., 2009. Controls on clastic sequence geometries in a shallow-marine, transtensional basin: the Bohemian Cretaceous Basin, Czech Republic. Sedimentology, 56, 1077 – 1114.

Vacková, L., 2010. Depositional architectures, stratigraphy and depositional regime of Upper Turonian sandstone bodies, northwestern part of the Bohemian Cretaceous Basin. (in Czech) Diploma thesis, Charles University, Prague, 1 – 113.

The finite strain estimation method, based on fibrous quartz orientation in pressure shadows around rigid inclusions in Upper Triassics siltstone

Vyacheslav Voitenko, Igor Khlebalin

Geological Department, Saint-Petersburg State University, Universitetskaya emb., 7/9, St.Petersburg, 199034, Russia (voitenkoslava@list.ru, hlebalin@bk.ru)

The Norians (T3n2-3) terrigenous rocks of Verkhoyansk complex (Far East, Russia) have been investigated on gold occurrence area inside of regional Adycha-Taryn Fault. The rocks consist of two proximal deposits of deep-water fan: the interchannels and interlobes stagnant areas and accumulative lobes of river mouth.

In generally, the rocks consist of dark gray coarse-grained siltstones and less sandstones and claystones. The siltstones are characterized by bioturbation, pyritization of deposit feeders traces, bivalve mollusks, foraminifers, fern-like plants (S=0.47-0.74%) and coalification of pieces of plans and algaes (C_{org}=0.5-1.28%). Sandstones contain the mudstone clasts, shell debris and characterized by ball and pillow, slump, clotted and ripple structures. Claystones are presented by thin bedded slaty with numerous bivalve mollusks.

In investigated rocks does not consist the traditional markers of deformation. There are observed numerous syn-tectonical regenerations rims («pressure shades»), overgrowing around aggregates of framboids pyrite.

These «pressure shades» meet everywhere, in all types of rocks from claystones to sandstones and shows the convenient strain-marker. Quartz, chlorite and sericite are presented by fibrous minerals in «pressure shades» and extended in plane of pressure solution surfaces.

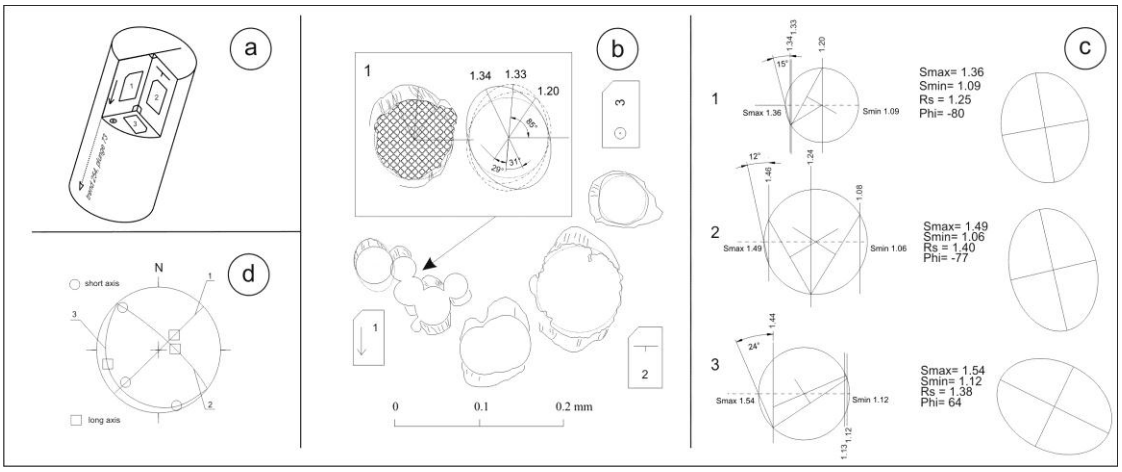

Fig. 1. The stages of finite strain estimation, based on fibrous quartz orientation in pressure shadows around rigid inclusion. a) core with orientates thin slides, b) local extensions estimation from pressure shadows with uniform fibrous quartz orientation, c) local strain-ellipses parameters calculation from Mohr circles, d) spatial orientation of short and long axes of local strain-ellipses.

Conveniently, the «pressure shades» are used for increment strain estimation (Ramsay, Huber, 1983). We used the same structures for bulk finite strain estimation. The samples were cut for strain-analysis from 16 orientates cores. Three thin slides were cut out from core, located perpendicularly to each other (Fig. 1a). An arrangement of thin slides on three planes was fixed for definition of planes attitude concerning world coordinate system.

At the following stage of research in everyone thin slide a pressure shadows around framboids pyrites were defined replaced with fibrous minerals. A main feature for investigated pressure shadows was the uniform orientation of fibrous mineral in spite of pyrite planes, unlike pressure shadows around hydrothermal euhedral pyrites.

In everyone thin slides the relative extensions ($e=l_f/l_i$, l_0= one half of pyrite grain thick, constant length following tectonics processes, $l_f= l_0$ + fibrous length in chosen direction) and its orientation were defined across pyrite planes with different orientation relative each other (Fig. 1b). The Mohr circles (Means, 1976; Rodygin, 1999) were used for calculation of the maximum extension and shortening and its orientation in thin slide planes (Fig. 1c). The next stage consists of transferring the relative strain-ellipses axes orientation to world coordinate system and strain-ellipsoid calculation. The trends, plunges and values of long and short axes of strain-ellipses are used for best-fit ellipsoid calculation from elliptical sections on arbitrarily oriented planes

(Owens, 1984) we used the software by Mark T. Brandon from Yale University (USA). The results of strain-analysis are shown on Fig. 2.

At best-fit ellipsoid calculation was accepted, that a volume was constant that won't be coordinated with the actual changes of volume, fixed by cleavage planes and «pressure shadows». However, the estimation of intensity and scales of volume change is more difficult tasks as there is no clear information on initial volume of rocks or strain indicators. Reliably it is possible to confirm about volume change only at acknowledgement of strain intensity are confirm the significant changes in a total chemical compounds of investigated rocks (Voitenko, Khudoley, Gertner, 2004). In the present research, resulting strain-ellipsoid characterizes not only anisotropy of strain inside of regional Adycha-Taryn Fault, but and spatial anisotropy of syntectonic metasomatic processes which influence to gold-bearing fluids migration.

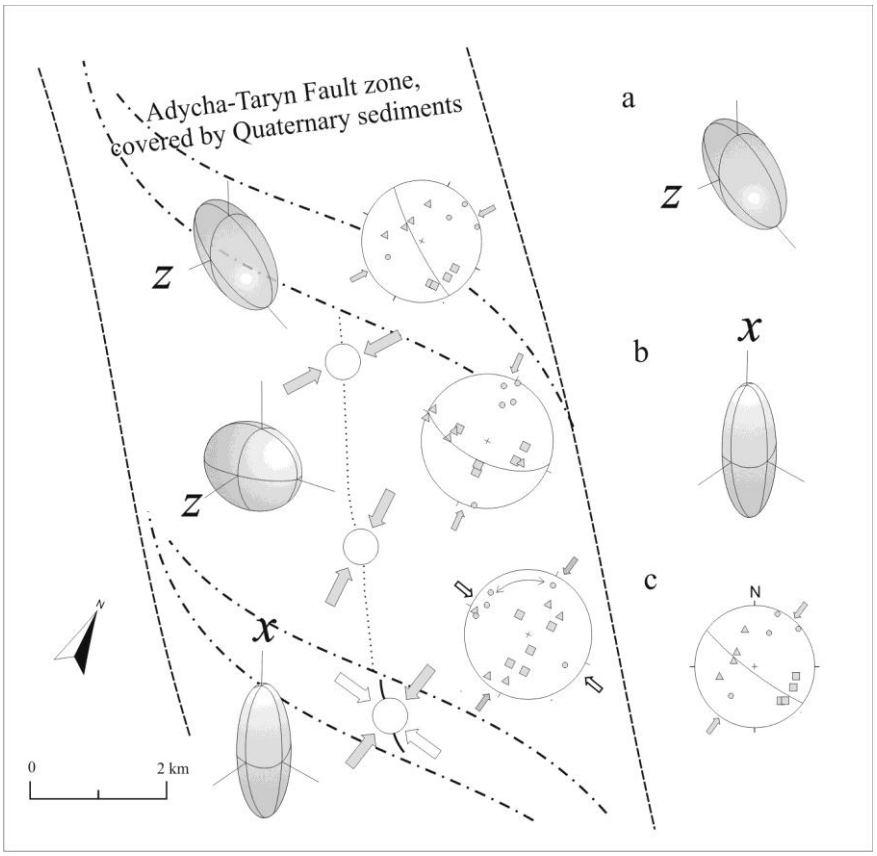

Fig. 2. The simplified scheme of central part of Adycha-Taryn Fault with stereoplots and results of strain-analysis. a) shape and orientation of oblate strain-ellipsoids, b) shape and orientation of prolate strain-ellipsoids, c) stereoplot with long (square), immediate (triangle) and short (circle) axes of strain-ellipsoids and horizontal projections of shortening axes.

Means W., 1976. Stress and Strain. Springer Verlag, New-York , U.S.A.

Owens W., 1984. The calculation of a best-fit ellipsoid from elliptical sections on arbitrarily oriented planes. Journal of Structural Geology, 5, 611 - 618.

Ramsay J. and Huber M., 1983. The Techniques of Modern Structural Geology, V.1: Strain Analysis. Academic Press, London, U.K.

Rodygin A., 1999. The methods of strain-analysis. Tomsk State University publ., Tomsk, Russia

Voitenko V., Khudoley A., Gertner I., 2004. Influence of strain on the chemical composition of low-grade metamorphic sandstones: example from Talass Ala-Tau, Kyrgyzstan. GeoLines, 17, 100–101.

Geological determinations of the Huambo River valley network (Central Andes, Peru)

Jerzy Żaba, Krzysztof Gaidzik, Justyna Ciesielczuk

Department of Fundamental Geology, University of Silesia, Będzińska 60, 41-200 Sosnowiec, Poland (jzaba@interia.pl, k.gaidzik@gmail.com, justyna.ciesielczuk@us.edu.pl)

The detailed tectono-structural studies in the area of the Huambo River, located in the vicinity of the Colca Canyon, were undertaken during the 4th, 5th and 6th Polish Scientific Expeditions, Peru 2006, 2008 & 2010. They were organized by the staff of the Department of Geology, Geophysics and Environmental Protection of AGH (University of Science and Technology) in Cracow with Professor Andrzej Paulo as the chief of this project, in collaboration with the Universidad Nacional San Augustin in Arequipa and the Sociedad Geológica del Peru in Lima.

The study area is situated in the West Cordillera in Central Andes, southern part of Peru. The ca 50 km long Huambo river starts at the elevation of about 4500 m a.s.l., and ends into the Colca River near Canco village at

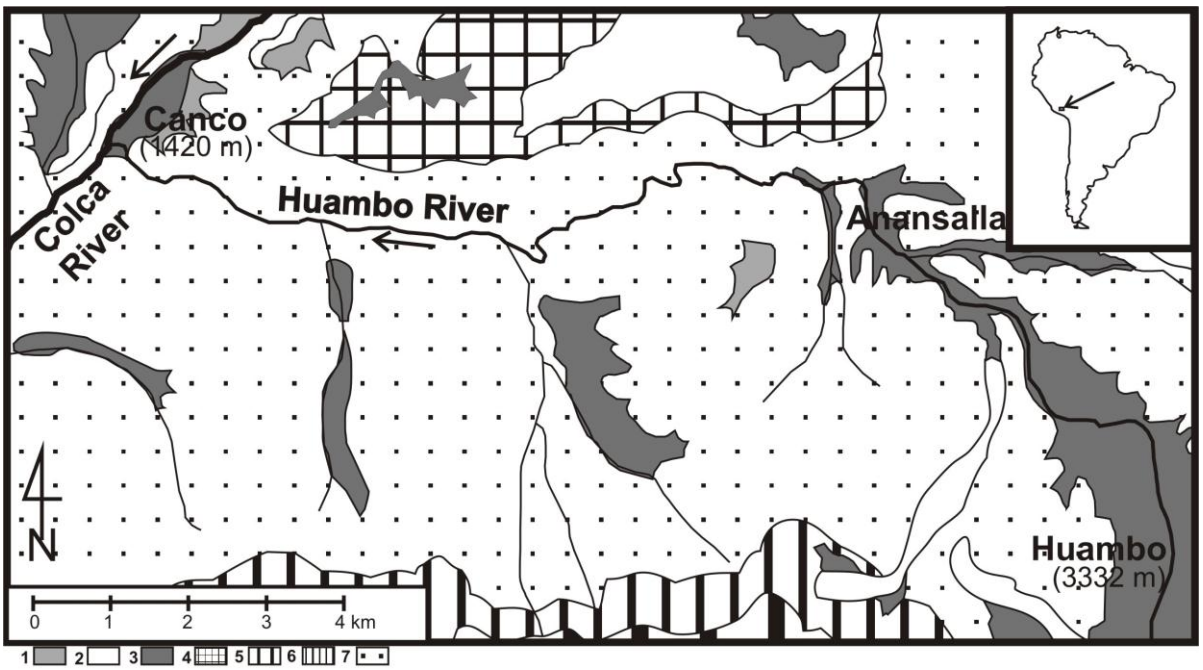

Fig. 1. Geological sketch map of the Huambo River area between Huambo and Canco (according to Caldas, 1973, simplified); 1 – colluvium and alluvium deposits (Holocene), 2 – Andahua Group (Pleistocene-Holocene), 3 – alluvium deposites and travertines (Pleistocene), 4 – Barroso Group (Pliocene-Pleistocene), 5 – Arcurquina Group (Albian), 6 – Murco Group (Berriasian – Aptian), 7 – Yura Group (Upper Jurrasic – Lower Cretaceous).

the height of about 1400 m a.s.l. (Fig. 1). The valley was cut mostly within the strongly folded and overthrusted quartz-sandstones and shales, which belong to the Yura Group of estimated Upper Jurassic-Lower Cretaceous age (Fig. 1; Caldas, 1973; Paulo, 2008).

The course and direction of the Huambo River is determined by both: continuous and discontinuous tectonic structures. The relationship between them is complicated, since rocks of the Yura Group are strongly folded and faulted (Fig. 2). The spatial orientation of bedding surfaces determine the axis position of hypothetical macrofold to be NW-SE, plunging gently towards the SE (134/19; Fig. 2C). The main joints system tends to be perpendicular to the fold structures (Fig. 2A), whereas the most common faults (mostly inverse faults and thrusts) are parallel to them (Fig. 2B).

The photolineaments representing straight segments of Huambo drainage network in the area between Huambo and Canco were drawn on the basis of satellite images (LANDSAT 7), as well as geological maps (Caldas, 1973). According to them two rose diagrams were prepared, showing the amount of photolineaments of definite strike azimuth interval (Fig. 2C), as well as the summary lengths of photolineaments of definite strike azimuth interval (Fig. 2D). They are similar to those which represent joints and faults actually stated during field studies (Fig. 2A-D). Although the detailed field studies indicated that these similarities might be confusing. It was proved that on some divisions the Huambo River uses faults system, mainly of normal sense

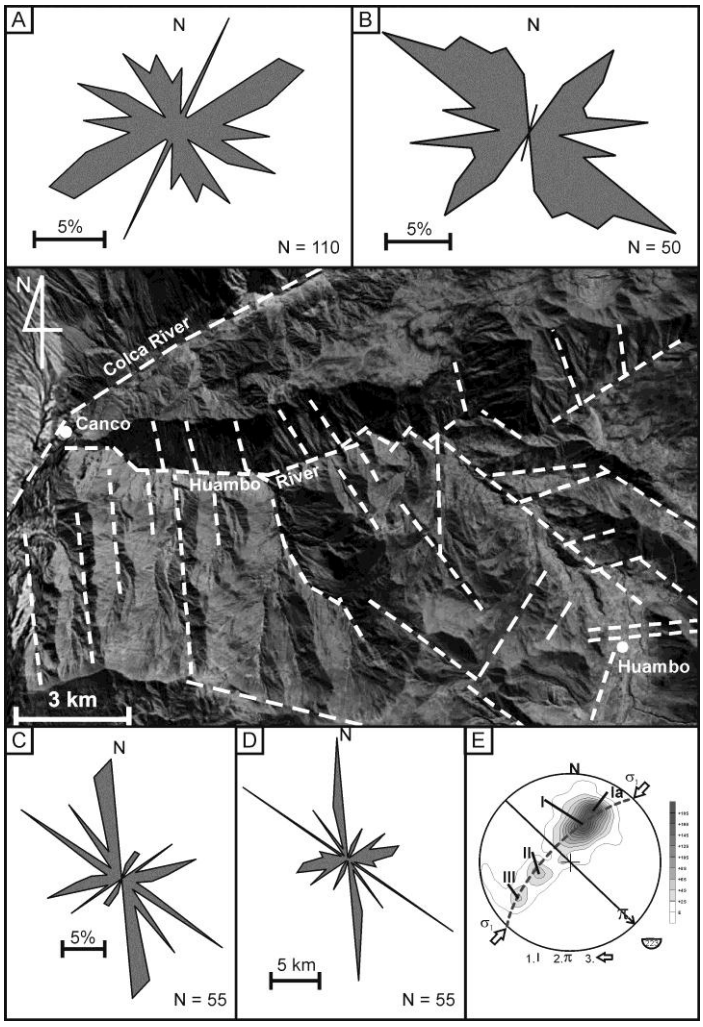

Fig. 2. Photolineaments of the River Huambo valley area (on the basis of LANDSAT 7 image). A – rose diagram of joints: max. – 10% (60-70°), B – rose diagram of faults: max. – 14% (120-130°), C – rose diagram of photolineaments: max. – 14% (120-130°), D – rose diagram of photolineaments lengths: max. – 26,4 km (120-130°), E – spatial orientation of bedding in the study area: 1 – main maxima: I – 202/37, Ia – 204/53, II – 71/30, III – 55/59, 2 – axis of hypothetical macrofold (π – 134/19), 3 – shortening direction.

of displacements (i.e.: NNW-SSE, WSW-ENE). However one of the major river directions NW-SE – which is also the main fault orientation – is determined mainly by the fold structures. In many locations the Huambo River uses them and flows parallel to the bedding strike or fold axis (Żaba et al. 2009).

Within the study area, on relatively short section of that river from Huambo to Canco (ca. 30-40 km; Fig. 1), almost every known type of river valleys according to geological structure is represented: parallel to the bedding, fold axis (anticlinal, synclinal), joint or fault, perpendicular as well as diagonal to the bedding or fold axis. All geological structures and their relation with present-day geomorphology and topography of the studied area are clearly seen because of severe and dry climate which limits any vegetation.

Caldas, J., 1973. Mapa Geologico del Cuadrangulo de Huambo. Escala 1 : 50 000. Instituto Geologico Minero y Metalurgico, Peru.

Paulo, A., 2008. Geology of the Western Cordillera in southern Peru – an outline. Kwartalnik Akademii Górniczo-Hutniczej, Geologia, 34 (2/1), 35-54 (in Polish with English summary).

Żaba J., Ciesielczuk J. & Gaidzik K., 2009. Structural position of Huambo River valley (Central Andes, Peru) and its geoeducational aspects. Studia Universitatis Babes-Bolyai, Special Issue - MAEGS-16, 72-74.

Timing of tectonothermal events in walls of the Red River Fault Zone, NW Vietnam

Andrzej Żelaźniewicz[1], Tran Trong Hoa[2], Alexander N. Larionov[3]

[1]*Institute of Geological Sciences, Polish Academy of Sciences, Podwale 75, 50-449 Wrocław, Poland (pansudet@pwr.wroc.pl)*
[2]*Institute of Geological Sciences, Vietnamese Academy of Science and Technology, Hanoi, Vietnam*
[3]*Centre of Isotopic Research, All Russian Geological Research Institute, St. Petersburg, Russia*

In northern Vietnam, there is a boundary between the South China Block (SCB) and the Indochina Block (IB) but neither its character nor position is unanimously identified. Some workers (see Roger et al., 2000) propose to locate the border along the Ailao Shan-Red River Shear Zone (ASRR) interpreted as a ca. 1500-2000 km long crustal scale, left lateral, strike-slip feature which was to be formed by the SE-ward continental extrusion of Indochina in the Tertiary. However earlier interpretations assumed that the boundary between the two blocks occurs further south at the Song Ma Zone which comprised a subduction complex of uncertain age, Siluro-Devonian or Permo-Triassic, eventually included in the Indosinian orogen (see Carter and Clift, 2008; Lepvrier et al., 2008). Recent findings of Triassic eclogites in the Song Ma Zone (Nakano et al., 2010) along with serpentinite slivers and MORB-like metabasic rocks (Tran Van Tri, 1979) support the latter option. Even if not a plate boundary, the ASRR is one of the largest fault zone in SE Asia and thus might have been affected by tectonothermal activity during the Indosinian orogeny. However, none of several (meta)igneous bodies spread along the Day Nui Con Voi Massif (DNCV) that comprises the Vietnamese sector of the ASRR, referred to as the Red River Fault Zone (RRFZ), yields Permo-Triassic ages as indicated by the results of U-Pb zircon SHRIMP dating performed in the course of our studies. Such result might suggest that the DNCV/RRFZ was not penetrated by magmatic rocks or remained inactive at that time, or it is younger than the Triassic. In the DNCV, pegmatite and granite veins dated at 77-69 Ma (U-Pb zircon, SHRIMP) cut high-grade gneisses and metabasites, which were migmatized and dextrally sheared already by Late Cretaceous times at the latest (Żelaźniewicz et al., 2005). Further deformational events occurred in the Tertiary. These data point to multi-phase tectonic history of the RRFZ which dates back at least to the Mesozoic and is evidently more complex than previously assumed.

In view of the above it is important to learn more about wall rocks to the RRFZ. For this reason, we sampled (meta)granites which occur to the SW of the DNCV/RRFZ and (meta)rhyolites and migmatites that occur to the NE of it. Our SHRIMP U-Pb zircon analyses show that in the walls of the RRFZ, in its Vietnamese sector, igneous and metamorphic rocks of Permo-Triassic age (263–248 Ma) commonly occur. The new isotopic data combined with geochemical and structural observations confirm the importance of the RRFZ as a major continental shear zone that separates units with quite different tectononothermal histories. In the Fan Si Pan complex to the SW of the RRFZ, a Neoproterozoic basement comprised of 780-740 Ma metagranites and metasediments was intruded in the Late Permian (~260 Ma) by alkaline, A-type granites. Then the crust was reactivated tectonothermally in the Eocene (50-34 Ma) by metamorphism at the NW/W-vergent oblique thrust regime with left-lateral component, which was associated with greenschist to amphibolite facies metamorphism and followed by also alkaline granite magmatism (~50-34 Ma). The Eocene batholitic intrusion partly developed at the expense of the earlier deformed Permian granites. In contrast, in the Lo Gam complex to the NE of the RRFZ, a Neoproterozoic basement (~767 Ma) was repeatedly subjected to tectonothermal activity (at ~450-420 Ma, ~350 Ma, ~265 Ma) throughout the Palaeozoic with termination in the Early Triassic (~248 Ma).

Despite the observed differences, the lithotectonic units of the two RRFZ walls belong to the SCB which acted as the upper plate during collision with the Indochina Block in the course of the Indosinian orogeny in Late Permian-Early Triassic times. The two walls of the RRFZ belong to the hinterland of the Indosinian orogen as suggested by the evidence of magmatism, metamorphism up to migmatization and ductile deformations identified by us, which concurs with observations of some earlier authors. The Red River Fault Zone is clearly a feature of long duration and probably much older then hitherto expected. The onset of complex, strike-slip dominated movement along the zone likely dates back to Permo-Triassic times and since then the shear deformations have been repeatedly occurring under different kinematic and rheologic conditions.

Carter, A. and Clift, P.D., 2008. C. R. Geoscience, 340, 83–93.
Lepvrier, C., Vuong, N.V., Maluski, H., Thi, P.T. and Vu, T.V. 2008. C. R. Geoscience, 340, 94–111.
Nakano, N. et al., 2010. Jour. Met. Geology, 28, 59–76.
Roger, F. et al., 2000. Tectonophysics, 321, 449–466.
Tran Van Tri, 1979. Geology of Vietnam (the north part). Science and Technology Publ. House, Hanoi, 78 pp.
Żelaźniewicz et al., 2005. GeoLines, 19, 121–122.

First site of Holocene faults in the outer Western Carpathians of Poland

Witold Zuchiewicz[1], Antoni K. Tokarski[2], Anna Świerczewska[1]

[1]Faculty of Geology, Geophysics and Environmental Protection, AGH University of Science and Technology, Al. Mickiewicza 30, 30-059 Kraków, Poland (witoldzuchiewicz@geol.agh.edu.pl; swiercze@agh.edu.pl)
[2]Institute of Geological Sciences, Polish Academy of Sciences, Research Center in Kraków, Senacka 1, 31-002 Kraków, Poland (ndtokars@cyf-kr.edu.pl)

We present the first example of Holocene faults in the Outer Western Carpathians in Poland. The studied locality is situated on the left-hand side of the Koninka stream valley in Koninki village, Gorce Mts., in a vertical scarp of the undermined 5.5-m-high Holocene terrace step, composed of tightly packed, subangular to subrounded gravels and cobbles, up to 25 cm in diameter. The examined straight segment of the valley trends E-W. The terrace cover, representing exclusively the bedload facies, rests on 0.4-0.5 m high strath built up of sub-horizontal, thin-bedded sandstones and shales of the Palaeocene Ropianka Formation belonging to the Konina – Lubomierz Slice of the Bystrica Subunit, Magura Nappe. Strata of the Ropianka Fm. are cut by a dozen or so high-angle small-scale normal faults and a single strike-slip fault (N60ºE). Normal faults usually trend NE-SW and NNE-SSW, subordinately NW-SE. One of the faults (165/75E) displaces the top sandstone bed, downthrowing the eastern side by 1 cm. These faults are frequently accompanied by ferrugineous efflorescences. The dominant episode of faulting was typified by extensional regime of sigma-1 oriented N300ºW.

Small-scale normal faults cutting both Palaeocene strata and the lower part of Holocene alluvium trend 35/25E and 135/45E. They die out in the medial portion of the terrace scarp by horse-tail structures and are accompanied by reorientation of clast a-b planes subparallel to the fault planes and by clast fracturing. The average number of fractured clasts per 1 m-long segment of exposure is close to 1, increasing to 3 in the nearest vicinity of young faults. Orientation of fractures cutting clasts is variable, clustering however around NE-SW. The upper part of gravel series does not reveal tectonic disturbances.

Such deformations must have been induced by relatively strong earthquakes, unknown from historical record of the Outer Carpathian seismicity. Fault attitude points to NW-oriented axis of the minimum principal stress, which is compatible with parameters of the present-day stress field in the Outer Western Carpathians of Poland.

Authors Index

bold - talk, normal - poster, *italic* - co-author